

國立交通大學

電控工程研究所

碩士論文



多通道行動與無線 EEG 系統之新式設計

A New Design of

Multi-channels Mobile and Wireless EEG System

研究生：王琬茹

指導教授：林進燈 教授

中華民國 一 百 年 七 月

多通道行動與無線 EEG 系統之新式設計

A New Design of Multi-channels Mobile and Wireless EEG System

研 究 生：王琬茹

Student：Wan-Ru Wang

指導教授：林進燈

Advisor：Chin-Teng Lin

國立交通大學

電控工程研究所



Submitted to Institute of Electrical Control Engineering
College of Electrical and Computer Engineering
National Chiao Tung University
in partial Fulfillment of the Requirements
for the Degree of
Master
in

Electrical and Computer Engineering

July 2011

Hsinchu, Taiwan, Republic of China

中華民國一百年七月

多通道行動與無線 EEG 系統之新式設計

學生：王琬茹

指導教授：林進燈 博士

國立交通大學電控工程研究所碩士班

摘要

在過去的研究中，大多數的學者使用包含強大功能的標準化量測儀器來收錄高訊號品質的腦電位(EEG)訊號；然而，由於此套腦電位系統較笨重而巨大，這也造成在日常生活當中收錄腦波變成一項困難的任務。因此我們提出一套多通道行動與無線腦電位系統足以容易應用於醫療用途、居家照護控制介面，以及科學認知實驗等等。此套系統包含三個部份：(1)乾電極、(2)多通道行動無線腦電位擷取電路裝置，和(3)腦電位展示程式。其中乾電極不需要依靠電極膠來降低皮膚與電極的阻抗值的前置準備工作，卻比起濕電極有更好的長時間偵測品質。而實作出來的電路裝置能為 16 個輸入通道提供服務，並且體積小、重量輕巧。此外，後端展示程式能透過無線通訊介面接收腦電位訊號，並且將數位資料存成檔案以利線下分析。

在本研究中，我們也設計出一套系統驗證的方法逐步為我們的系統驗證出效能。從最後的結果中，我們得知此套系統有 72-95%的程度相似於 Neuroscan 公司出產的標準化量測系統；而結合在多通道腦電位擷取電路裝置的乾電極不僅可以量測到與濕電極相似的腦電位訊號特徵，也能在 oddball 認知實驗當中量測到相當微小的事件相關電位(ERP)訊號，並與濕電極所量到的訊號有 93-95%的相似

程度。總結來說，我們宣稱此套系統量測腦電位確實有可靠的訊號品質，並且可以方便地應用於日常生活當中。

關鍵詞：腦電位系統、腦電位、行動與無線腦電位擷取電路、多通道、乾電極、系統驗證、P300、Oddball 實驗



A New Design of Multi-channels Mobile and Wireless EEG System

Student: Wan-Ru Wang

Advisor: Dr. Chin-Teng Lin

Institute of Electrical Control Engineering
College of Electrical and Computer Engineering
National Chiao Tung University



Abstract

In past study, most of researchers used standard measurement instrument which produced strong functions to monitor EEG activity with high signal quality. However, recording EEG trends to be a difficult task in dairy life during to hardly moving the heavy, huge, and wired EEG system. Hence, we mention a multi-channels mobile and wireless EEG system which can be easily used for medical application, home care control interface, cognitive experiments, and so on. The system includes three parts: (1) dry sensors, (2) multi-channels mobile and wireless EEG acquisition circuitry, and (3) EEG display program. Dry sensor needs not any skin preparation with conductive gels to maintain small skin-sensor impedance but still make the better long-term monitoring performance than wet sensor. The circuitry is implemented to serve 16-channel inputs and has a miniature area and light. In addition, back-end display program receives EEG data via wireless communication and can also save digital data as a file for off-line analysis.

In this study, we also design the method of system verification to verify the performance of our system step by step. Finally, the results show that our circuitry and program is 72-95% correlate to standard measurement instrument like Neuroscan system. Dry sensor applied in multi-channels device can not only monitor the similar EEG feature with wet sensor but also detect pretty tiny EEG signal even ERP in Oddball task with 93-95% correlation with wet sensor. In conclusion, we demonstrate our proposed system is exactly reliable and can be conveniently applied in dairy life.



KEYWORD: EEG system, electroencephalogram, mobile and wireless EEG acquisition circuit, multi-channels, dry sensor, system verification, P300, oddball task

誌謝

本論文的完成，首先要感謝指導教授林進燈博士這兩年來的悉心指導，讓我學習到許多寶貴的知識，在學業及研究方法上也受益良多。另外也要感謝口試委員們的建議與指教，使得本論文更為完整。

其次，感謝林伯昱博士、陳聖夫博士和柯立偉博士在我研究期間，不吝惜給予我指導方針。感謝實驗室學長張哲睿、劉育航教導我硬體偵錯的方法；陳世安學長和研究助理王林宇協助我完成系統認證實驗；感謝腦科學研究中心提供我完善的研究資源；感謝為我研究貢獻腦波的十名受測者，願意彈性配合我的實驗時間毫無怨言；感謝岡儒、胤宏、小昭在我熬夜做研究的日子裡，經常陪我吃宵夜為我加油打氣；感謝珍珍學姐偶然的一番話，啟發我在繁雜的數據當中找到呈現成果的核心路。



感謝我的父母親無條件支持我為研究領域的付出，在我受挫時總第一時間關心我，和你們共享天倫之樂是我的福氣，相信你們看到我的成長也會備感光榮。此外，最要感謝我的生命導師教導我如何心安心定完成研究，開啟我智慧讓我事半功倍，沒有你，將沒有本篇論文的準時完成。

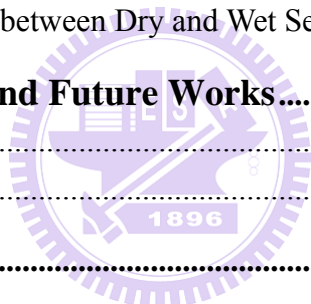
謹以本論文獻給我的家人及所有關心我的師長朋友們。

Contents

摘要.....	iii
Abstract.....	v
誌謝.....	vii
Chapter 1 Introduction.....	1
1.1 EEG system.....	1
1.2 Previous Work.....	3
1.3 Motivation.....	7
1.4 Organization of Thesis	8
Chapter 2 Material and Method	9
2.1 Biosignals.....	9
2.1.1 Electroencephalogram (EEG).....	10
2.1.2 Electrooculography (EOG).....	12
2.1.3 Electromyogram (EMG).....	13
2.2 EEG Signal Preprocessing.....	14
2.3 Method of Data Acquisition and Record	15
2.3.1 System Overview	15
2.3.2 Dry Sensor	16
2.3.3 Multi-channels Mobile and Wireless EEG Acquisition Circuitry	19
2.3.3.1 Front-End Filter and Amplification Circuit.....	20
A. Instrumentation Amplifier.....	21
B. High Pass Filter	22
2.3.3.2 Multiplexer.....	24
2.3.3.3 Analog to Digital Converter and Micro-controller	25
A. Timer Interrupt.....	26
B. Analog to Digital Converter	27
C. Moving Average	30
D. UART Interface.....	31
2.3.3.4 Wireless Transmission.....	32
2.3.3.5 Power Management	33
A. Power Supply Circuit.....	33
B. Charging Circuit.....	34

2.3.4 Implementation of the EEG Acquisition Circuitry	35
2.3.5 EEG Display Program.....	36
2.3.5.1 Receive Package and Display	37
A. Package Protocol.....	37
B. Display Digital Data to Analog Signal.....	38
2.3.5.2 Save Data as a File	38
2.3.5.3 User’s Guide	39
2.4 Experiment: P300 and Oddball task	41
2.4.1 P300	41
2.4.2 Oddball Task.....	43
Chapter 3 Experiment Results and Discussion	48
3.1 System Verification of Simulated Signals.....	49
3.1.1 Performance Test in Time Domain	49
3.1.2 Performance Test in Frequency Domain.....	50
3.2 Circuitry and Program test compared to reference system.....	52
3.2.1 Participant	53
3.2.2 Experiment Procedure and Presentation	53
3.2.3 Method of Analysis	55
3.2.4 Experiment Results	56
3.2.4.1 Blink Action Comparison Results.....	56
A. Time-Domain Correlations	56
B. Frequency-Domain Correlations	58
3.2.4.2 Tooth Action Comparison Results	59
A. Time-Domain Correlations	59
B. Frequency-Domain Correlations	61
3.2.4.3 Normal Action Comparison Results	62
A. Time-Domain Correlations	62
B. Frequency-Domain Correlations	65
3.2.5 Discussion.....	66
A. Blink Action State	66
B. Tooth Action State	67
C. Normal Action State	67
3.3 Sensor Basic Test	69
3.3.1 Participant	70
3.3.2 Experiment Procedure and Presentation	70
3.3.3 Method of Analysis	73
3.3.4 Experiment Results	75
A. Results after Averaging All Subjects and All Positions	75

B. The Best Trial Data in Blink Action.....	76
C. The Best Trial Data in Close Action.....	78
D. The Best Trial Data in Tooth Action	79
E. The Best Trial Data in Normal Action.....	81
F. The Worst Trial Data.....	82
3.3.5 Discussion.....	83
A. Sensor Test for All Subjects and All Positions.....	83
B. The Similarities between Dry Sensor and Wet Sensor.....	85
3.4 Sensor Test in Oddball Task.....	87
3.4.1 Participant	87
3.4.2 Experiment Procedure and Presentation	87
3.4.3 Method of Analysis	89
3.4.4 Experiment Results	90
3.4.5 Discussion.....	92
A. P300 of Single Stimulus.....	92
B. P300 of Oddball Task.....	92
C. Comparison between Dry and Wet Sensor.....	94
Chapter 4 Conclusions and Future Works.....	95
4.1 Conclusions.....	95
4.2 Future Works.....	96
References.....	97



List of Figures

Fig. 1- 1: the outward appearance of Quik-cap produced by Neuroscan [6].....	4
Fig. 1- 2: The outward appearance of SynAmps RT produced by Neuroscan [6].....	5
Fig. 2- 1: EEG activities in different frequency bands [5].....	11
Fig. 2- 2: Blink features	13
Fig. 2- 3: The recommended derivation of EOG	13
Fig. 2- 4: The EMG electrodes recorded pattern of chin muscle tension [12].....	14
Fig. 2- 5: The diagram of EEG preprocessing.	14
Fig. 2- 6: System overview of our proposed EEG system.	15
Fig. 2- 7: (A) Several images of the proposed dry EEG sensor are shown. (B) An exploded view of the proposed dry sensor is presented. Each probe includes a probe, plunger, spring, and barrel.[13].....	17
Fig. 2- 8: Impedance change data representing the skin-electrode interface on the (a) forehead (F10) and (b) at hairy sites [13]	18
Fig. 2- 9: Long-term impedance variation measurements on the forehead site (F10) for wet and dry electrodes [13].....	19
Fig. 2- 10: Circuitry frameworks overview	19
Fig. 2- 11: Left- the R_G decides the gain of preamplifier, and the high pass filter of preamplifier decided by R_G and C. Right- block diagram of INA2126.....	21
Fig. 2- 12: Simulation of amplifier's frequency response in stage 1	22
Fig. 2- 13: High-pass filter circuits.	23
Fig. 2- 14: Simulation of amplifier's frequency response in stage 2.	23
Fig. 2- 15: Simulation of amplifier's total frequency response.	24
Fig. 2- 16: The outer appearance and block diagram of CD74HC4067	25
Fig. 2- 17: MSP430 Architecture [14]	26
Fig. 2- 18: Operating flow chart in MSP430F1611	26
Fig. 2- 19: Timer A up mode for interrupt function of MSP430F1611	27
Fig. 2- 20: ADC12 Block Diagram [14]	28
Fig. 2- 21: Diagram of the sampling and conversion with timer A trigger	29
Fig. 2- 22: Transmission buffer.....	29
Fig. 2- 23: Result of noise cancellation by using moving average [15]	31
Fig. 2- 24: PCB Blue Tooth antenna [16]	33
Fig. 2- 25: Power supply circuit.....	33
Fig. 2- 26: LP3985 block diagram	33

Fig. 2- 27: Left- Charging circuit in our portable bio-signal acquisition system. Right- Block diagram of BQ24010DRC.....	34
Fig. 2- 28: The outward appearance of implemented circuitry.....	35
Fig. 2- 29: TXT file contexts	39
Fig. 2- 30: User interface with opening window	39
Fig. 2- 31: Appearance of display Program within receiving process.....	40
Fig. 2- 32: (a) P300 [24] (b) Context updating theory of P300 [18].....	41
Fig. 2- 33: Schematic illustration of the single-stimulus (top), oddball (middle), and three-stimulus (bottom) paradigms [20]	44
Fig. 2- 34: Experimental scene description [21].....	44
Fig. 2- 35: Grand averaged ERP from visual modalities for each task difficulty, stimulus type, and recording site (n = 16) [21].....	45
Fig. 2- 36: Relationship between P300 and target-to-target interval (TTI) [21]	46
Fig. 3- 1: System verification overview.....	48
Fig. 3- 2: Result of 5Hz simulated signal test.....	49
Fig. 3- 3: result of non-linear simulated signal test	50
Fig. 3- 4: Results of different frequency test	51
Fig. 3- 5: Diagram of circuitry and program test compared to reference system	52
Fig. 3- 6: Experiment environment and setting view.....	54
Fig. 3- 7: Experiment procedure in one trial.....	54
Fig. 3- 8: Sensor positions in this experiment, referring to 10-20 system (Guideline for Standard Electrode Position Nomenclature, 2006).....	55
Fig. 3- 9: The best performance of time domain at FP1 (up) and T3 (down) within “Blink”	56
Fig. 3- 10: The best performance of time domain at CZ (up), T4 (mid), OZ (down) within “Blink”	57
Fig. 3- 11: The best performance of frequency domain at FP1 (left), T3 (right) within “Blink”	58
Fig. 3- 12: The best performance of frequency domain at CZ (left), T4 (right) within “Blink”	58
Fig. 3- 13: The best performance of frequency domain at OZ within “Blink”	59
Fig. 3- 14: The best performance of time domain at FP1 within “Tooth”	59
Fig. 3- 15: The best performance of time domain at T3 (up), CZ (mid), T4 (down) within “Tooth”	60
Fig. 3- 16: The best performance of time domain at OZ within “Tooth”	61
Fig. 3- 17: The best performance of frequency domain at FP1 (left), T3 (right) within “Tooth”	61

Fig. 3- 18: The best performance of frequency domain at CZ (left), T4 (right) within “Tooth”	62
Fig. 3- 19: The best performance of frequency domain at OZ within “Tooth”	62
Fig. 3- 20: The best performance of frequency domain at FP1 (left), T3 (mid), CZ (down) within “Normal”	63
Fig. 3- 21: The best performance of time domain at T4 (up), OZ (down) within “Normal”	64
Fig. 3- 22: The best performance of frequency domain at FP1 (left) and T3 (right) within “Normal”	65
Fig. 3- 23: The best performance of frequency domain at CZ (left), T4 (right) within “Normal”	65
Fig. 3- 24: The best performance of frequency domain at OZ within “Normal”	65
Fig. 3- 25: overall results of circuitry and program test.	68
Fig. 3- 26: Diagram of sensor basic test	69
Fig. 3- 27: Experiment environment of sensor basic test.....	71
Fig. 3- 28: The view of sensor placement. (a) Ground, (b) Dry sensor and wet sensor, (c) Reference	71
Fig. 3- 29: The procedure of sensor basic test in one trial	72
Fig. 3- 30: Positions of dry sensor and wet sensor in sensor basic test	72
Fig. 3- 31: No-use data for floating case and saturation case	73
Fig. 3- 32: Diagram of analysis method in sensor basic test	74
Fig. 3- 33: Overall results of sensor basic test.....	75
Fig. 3- 34: The best performance of Blink at FP1	76
Fig. 3- 35: The best performance of Blink at T3 (up), CZ (mid), OZ (down).....	77
Fig. 3- 36: The best performance of Close at FP1 (up), T3 (mid), CZ (down).....	78
Fig. 3- 37: The best performance of Close at OZ	79
Fig. 3- 38: The best performance of Tooth at FP1	79
Fig. 3- 39: The best performance of Tooth at T3 (up), CZ (mid), OZ (down).....	80
Fig. 3- 40: The best performance of Normal at FP1 (up), T3 (mid), CZ (down)	81
Fig. 3- 41: The best performance of Normal at OZ	82
Fig. 3- 42: The worst performance during to 60-Hz Electromagnetic Interference	82
Fig. 3- 43: The worst performance during to motion artifact	83
Fig. 3- 44: The worst performance during to DC shifting	83
Fig. 3- 45: Procedure of oddball experiment	88
Fig. 3- 46: Positions of dry sensor and wet sensor in oddball task.....	88
Fig. 3- 47: No-use data for floating case, saturation case, and DC shifting	89
Fig. 3- 48: ERP of s01 (left-up), s02 (right-up), s03 (left-down), s04 (right-down) in oddball task	90

Fig. 3- 49: ERP of s05 (left-up), s06 (right-up), s07 (left-mid), s08 (right-mid), s09
(left-down), s10 (right-down) in oddball task..... 91

Fig. 3- 50: Sensor overall comparison in oddball task..... 94

Fig. 3- 51: Sensor comparisons for all subjects in oddball task..... 94

Fig. 4- 1: The 16-channel electrode positions..... 96

Fig. 4- 2: The mechanism example..... 96



List of Tables

Table 1: Medical and physiological parameters [29]	9
Table 2: Common band of EEG [46]	10
Table 3: Feature of blink behaviors	12
Table 4: Stage details of front-end filter and amplification circuitry	20
Table 5: Data format (channel number)	30
Table 6: Specification of implemented hardware system	36
Table 7: Header of package.....	37
Table 8: data information of package.....	37
Table 9: Channel data.....	37
Table 10: data-encoding method.....	37
Table 11: The maximum and average correlations of time domain at every position within “Blink”	58
Table 12: The maximum and average correlations of frequency domain at every position within “Blink”	59
Table 13: The maximum and average correlations of time domain at every position within “Tooth”	61
Table 14: The maximum and average correlations of frequency domain at every position within “Tooth”.....	62
Table 15: The maximum and average correlations of time domain at every position within “Normal”.....	64
Table 16: The maximum and average correlations of frequency domain at every position within “Normal”.....	66
Table 17: Analysis results of Blink in sensor basic test.....	75
Table 18: Analysis results of Close in sensor basic test.....	75
Table 19: Analysis results of Tooth in sensor basic test.....	76
Table 20: Analysis results of Normal in sensor basic test.....	76

Chapter 1 Introduction

1.1 EEG system

In conventional scalp EEG, the recording is obtained by placing electrodes on the scalp with a conductive gel or paste, usually after preparing the scalp area by light abrasion to reduce impedance due to dead skin cells. Many systems typically use electrodes, each of which is attached to an individual wire. Some systems use caps or nets into which electrodes are embedded; this is particularly common when high-density arrays of electrodes are needed.

Electrode locations and names are specified by the International 10–20 system [1] for most clinical and research applications (except when high-density arrays are used). This system ensures that the naming of electrodes is consistent across laboratories. In most clinical applications, 19 recording electrodes (plus ground and system reference) are used. [2] A smaller number of electrodes are typically used when recording EEG from neonates. Additional electrodes can be added to the standard set-up when a clinical or research application demands increased spatial resolution for a particular area of the brain. High-density arrays (typically via cap or net) can contain up to 256 electrodes more-or-less evenly spaced around the scalp.

Each electrode is connected to one input of a differential amplifier (one amplifier per pair of electrodes); a common system reference electrode is connected to the other input of each differential amplifier. These amplifiers amplify the voltage between the active electrode and the reference (typically 1,000–100,000 times, or 60–100 dB of voltage gain). In analog EEG, the signal is then filtered (next paragraph), and the EEG signal is output as the deflection of pens as paper passes underneath. Most EEG systems these days, however, are digital, and the amplified signal is digitized via

an analog-to-digital converter, after being passed through an anti-aliasing filter. Analog-to-digital sampling typically occurs at 256–512 Hz in clinical scalp EEG; sampling rates of up to 20 kHz are used in some research applications.

During the recording, a series of activation procedures may be used. These procedures may induce normal or abnormal EEG activity that might not otherwise be seen. These procedures include hyperventilation, photic stimulation (with a strobe light), eye closure, mental activity, sleep and sleep deprivation. During (inpatient) epilepsy monitoring, a patient's typical seizure medications may be withdrawn. The digital EEG signal is stored electronically and can be filtered for display. Typical settings for the high-pass filter and a low-pass filter are 0.5-1 Hz and 35–70 Hz, respectively. The high-pass filter typically filters out slow artifact, such as electrogalvanic signals and movement artifact, whereas the low-pass filter filters out high-frequency artifacts, such as electromyographic signals. An additional notch filter is typically used to remove artifact caused by electrical power lines (60 Hz in the United States and 50 Hz in many other countries). [3] As part of an evaluation for epilepsy surgery, it may be necessary to insert electrodes near the surface of the brain, under the surface of the dura mater. This is accomplished via burr hole or craniotomy. This is referred to variously as "electrocorticography (ECoG)", "intracranial EEG (I-EEG)" or "subdural EEG (SD-EEG)". Depth electrodes may also be placed into brain structures, such as the amygdala or hippocampus, structures, which are common epileptic foci and may not be "seen" clearly by scalp EEG. The electrocorticographic signal is processed in the same manner as digital scalp EEG (above), with a couple of caveats. ECoG is typically recorded at higher sampling rates than scalp EEG because of the requirements of Nyquist theorem—the subdural signal is composed of a higher

predominance of higher frequency components. Also, many of the artifacts that affect scalp EEG do not impact ECoG, and therefore display filtering is often not needed.

A typical adult human EEG signal is about 10 μ V to 100 μ V in amplitude when measured from the scalp [4] and is about 10–20 mV when measured from subdural electrodes.[5]

1.2 Previous Work

The international standard measurement instrument like Neuroscan system is used for cognitive experiments by many researchers. Neuroscan provides state of the art systems for the acquisition and analysis of EEG and ERP data. The systems are integrated platforms, designed to allow uncompromising solutions for seamless recording and analysis of EEG data across a variety of domains. Neuroscan has developed multiple hardware (Quik-Cap Electrode Placement System and SynAmps RT) and software systems (SCAN Acquisition software) that combine to build the ideal platform for a particular area of research. Because of this flexibility, the components and the platforms Neuroscan build are not limited to any specific area of research, providing flexibility to move from recordings in one area to another, often, and with the same configuration.

Quik-Cap Electrode Placement System (Quik-Caps, EEG, Fig. 1-1) – Neuroscan offers a variety of Quik-Caps to provide speedy, consistent application of up to 256 electrodes. Quick-Caps are manufactured of highly elastic breathable Lycra material with soft neoprene electrode gel reservoirs for enhanced patient comfort. All electrodes are placed according to the International 10-20 electrode placement standard. Quik-Caps are available in a variety of electrode configurations from 12 to 256 channels as well as in 5 different sizes, and with a variety of electrode materials to meet every lab requirement. Neuroscan strongly recommends the use of Ag/Ag/Cl -



Fig. 1- 1: the outward appearance of Quik-cap produced by Neuroscan [6]

sintered electrodes because of their durability and ease of cleaning and re-use. Each cap offering is designed to cover a specific range of sizes.

Using the past two decades of experience and best available technology, Neuroscan is pleased to offer the SynAmps RT (Fig. 1-2) to the Neuroscience community. Dedicated to high-density recordings, SynAmps RT is a 70 Channel amplifier system, consisting of 64 monopolar, 4 bipolar and 2 high-level channels. Each channel has a dedicated 24 bit A-to-D, to ensure the most accurate sampling available. Active Noise Cancellation is an integral feature of the SynAmps RT design, providing unparalleled noise immunity. This ensures an accurate representation of the neurophysiological activity even in the most hostile electromagnetic environments. Using the latest technology has not only allowed us to make the SynAmps RT our most capable amplifier ever, it has also allowed us to put it into a small, cost effective package.

SynAmps RT Consists of Three Components: (1) Headbox - Each Headbox consists of 70 channels, and multiple Headboxes can be linked together to build high-density systems. Our modular approach to amplifiers provides a simple and flexible upgrade path.

All of the essential electronics have been moved to the Headbox. Our low noise 24 bit A-to-D chip allows for low gain to be used while still maintaining the resolution required for the most critical researcher. Data is digitized immediately in the headbox and transmitted to the host computer via a high-speed USB-2 connection guaranteeing lossless transmission. Quality of the signal is assured by our impedance testing circuitry, which allows you to verify impedance both on the Headbox and in a software display. Touch-proof connectors are provided to allow for the greatest flexibility, while our high-density connector permits Quik-Cap™ to be easily connected. Inputs for high-level signals are also provided, allowing you to capture the time series data of other measures along with the EEG. (2) System Unit - Serving as a hub for multiple Headboxes, the system unit is the distribution center, assuring absolute synchronization of sampling and triggers between all of the Headboxes. The System Unit is also the communication center with the host computer. Using a USB2 connection, the system unit ensures accurate transmission of data and trigger timing information. (3) Power Unit - Isolation of the subject from the power mains is a critical safety aspect of a complete system. The Power Unit houses a medical grade transformer, allowing you to connect those devices that contact the subject to one reference point. This assures that leakage currents and proper grounding meet world wide certification safety requirements for patient connected devices.



Fig. 1- 2: The outward appearance of SynAmps RT produced by Neuroscan [6]

The SCAN Acquisition software serves as the interface to the SynAmps and NuAmps. SCAN Acquisition provides a multitude of recording options which are saved in unique files that can be recalled for each experiment, ensuring that each individual data set is acquired with the same parameters. Even with the numerous options for acquiring the data the software is straightforward and simple to use. The SCAN Analysis software is a comprehensive tool for processing and analyzing EEG and ERP data. With decades of combined experience and active research collaborations with major research labs world wide, the research and development team has strived to implement every major data processing and analytical tool that is typically used as a transform into the SCAN software. The latest advancements included a programming-based batch processing language, a PCA/ICA filter toolbox and EKG and Blink reduction tools. As new developments occur in the field of neuroscience, Neuroscan will continue to develop its solutions for your research.[6]



1.3 Motivation

In this study, we mention the EEG system for wireless and mobile EEG acquisition purpose. In past study, the standard EEG measurement instruments were very heavy, huge and wired to be not suitable for dairy life applications. We propose the EEG system can overcome the drawback of them, and minimize the hardware frameworks for convenience and light weight. Moreover, we also expect the EEG system monitoring multi-channels signals. In miniature area of hardware system, to implement as possible as we can most channels to simultaneously monitor EEG activities on the whole head.

Traditional wet electrode as Quick-cap produced by Neuroscan needs skin preparation of spread conductive gels between electrodes and skin sites to reduce impedance. In this study, we try to combine dry sensors in our EEG system to measure multi-channels input signals. The goal will be also achieved that this EEG system can be used in dairy life as medical application and the others. Long-term monitoring in EEG system is increasingly important for home care. In sum of the above motivation, we expect to implement miniature multi-channels mobile and wireless EEG system combining dry sensors. In addition, the system also has good reliability for long-term monitoring.

1.4 Organization of Thesis

In chapter 2, the material and method of implementing our proposed EEG system will be introduced. We will also illustrate the background knowledge of P300 and Oddball task for the following experiment. In chapter 3, we will design the method of system verification and apply it to our system for presenting the performance. There will be four verifying processes going on. We will explain the analysis results for four kinds of verification and discuss how good it can be not only in general test but in standard cognitive experiments. Finally, in chapter 4, we will summarize all consequents as overall conclusions and mention the future works for our system.



Chapter 2 Material and Method

In this chapter, we try to design an EEG system including portable, wireless, multi-channels but miniature specification. It needs not conduction gels for conveniently wearing and taking off for any user in daily life. For these purposes, we research how to establish the most complete and strongest functions using finite hardware resources. In the experimental process, we try to verify our system by going on three experiments. One is the circuitry and program test compared to reference system, one is sensor basic test, and the other is sensor test in Oddball task. Thus, in this chapter, the thesis of P300 and Oddball task is introduced to preview background knowledge of system verification experiment.

2.1 Biosignals

Biosignal is a summarizing term for all kind of signals that can be measured and monitored from biological beings. The term biosignal is often used to mean bio-electrical signals but in fact, biosignal refers to both electrical and non-electrical signals. The study only considers electrical ones. Electrical biosignals are usually taken to be electric current produced by the sum of electrical potential differences across a specialized tissue, organ or cell system like the nervous system. Thus, among the best-known bio-electrical signals are the following difference types [8]. The difference types of Electrical potentials which may be measured on the brain are listed in Table 1[9].

Table 1: Medical and physiological parameters [9]

Parameter	Principal Measurement Range of Parameter
EEG	20uV-200uV
EMG	10uV-5000uV
EOG	50uV-3500uV

2.1.1 Electroencephalogram (EEG)

Electroencephalography (EEG) is the measurement of electrical activity produced by the brain as recorded from electrodes placed on the scalp. When measuring from the scalps, recorded the EEG signal is about 20-200uV for a typical adult human. And a common system reference electrode is connected to the other input of each different amplifier. These amplifiers amplify the voltage between the active electrode and the reference (typically 1,000–100,000 times, or 60–100 dB of voltage gain). The EEG is typically described in terms of rhythmic activity and transients. The rhythmic activity is divided into bands by frequency. The common band of EEG is shown as Table 2 [5] and Fig.2-1.

Table 2: Common band of EEG [5]

Type	Frequency (Hz)
Delta	Up to 4
Theta	4 – 7
Alpha	8 – 13
Beta	13 – 30
Gamma	30-100

Delta wave tends to be the highest in amplitude and the slowest waves. It is seen normally in adults in slow wave sleep. It is also seen normally in babies.

Theta wave is seen normally in young children. It may be seen in drowsiness or arousal in older children and adults; it can also be seen in meditation. Excess theta for age represents abnormal activity. On the contrary this range has been associated with reports of relaxed, meditative, and creative states.

Alpha wave is the "posterior basic rhythm" (also called the "posterior dominant rhythm" or the "posterior alpha rhythm"), seen in the posterior regions of the head on both sides, higher in amplitude on the dominant side. It emerges with closing of the

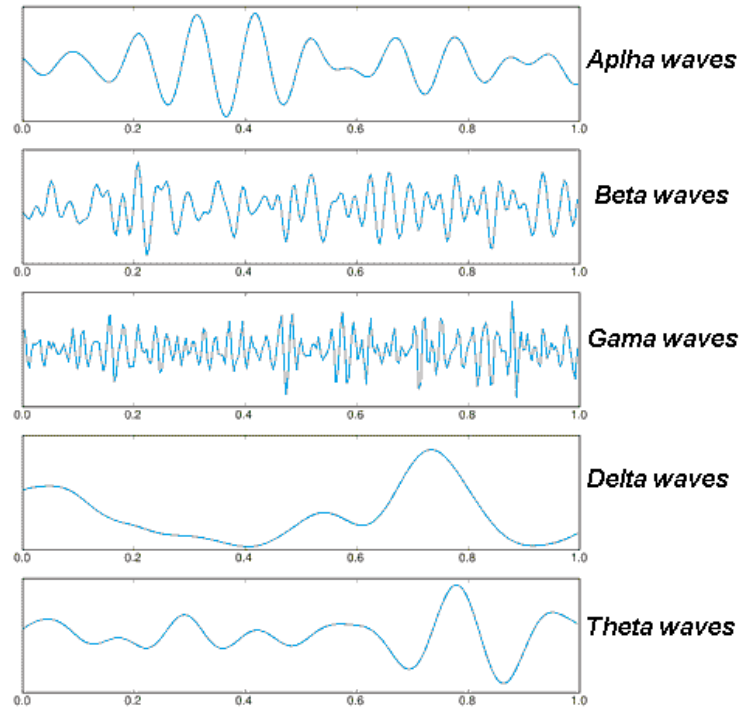


Fig. 2- 1: EEG activities in different frequency bands [5]

eyes and with relaxation, and attenuates with eye opening or mental exertion. The posterior basic rhythm is actually slower than 8 Hz in young children (therefore technically in the theta range).

Beta wave is seen usually on both sides in symmetrical distribution and is most evident frontally. Beta activity is closely linked to motor behavior and is generally attenuated during active movements. Low amplitude beta with multiple and varying frequencies is often associated with active, busy or anxious thinking and active concentration.

Gamma rhythms are thought to represent binding of different populations of neurons together into a network for the purpose of carrying out a certain cognitive or motor function.[5]

2.1.2 Electrooculography (EOG)

Electrooculography (EOG) is a technique for measuring the resting potential of the eyeball. Mostly, there are two electrodes placed above and below the eye, and the resulting signal is called vertical EOG. If the eye is moved from center position toward left or right, then one of the electrodes would see the positive side of the eyeball and the other would see the negative side. There would be a potential difference between the electrodes. If we assumed the resting potential as a constant, then the potential difference become a measure for the eye position called eye movement measurements [10].

Eye movement measurements is usually used as a reference of stages of sleep which included three main stages called: awake, REM and NREM. Eye movement is significantly difference during these three stages, so lots of research of sleep used this measurement to observe variation. In this study, the vertical EOG is derived using three electrodes: input, reference and ground. Two electrodes (FP1,FP2) are placed above the left and right eyes as the input and the other below the right ear as the reference signal. There is also an electrode as ground fixed on the center of forehead (the same as the ground signal of EEG). The feature (Fig. 2-2) of these blink behaviors is listed in Table 3. The recommended placement of EOG is shown as Fig 2-3.

Table 3: Feature of blink behaviors

Behavior	Description
Blink amplitude	A typical blink has an amplitude of 400uV
Blink duration	Nearly 200ms – 400ms for one blink
Blink frequency	About 15-20 times per minutes for a relaxed person

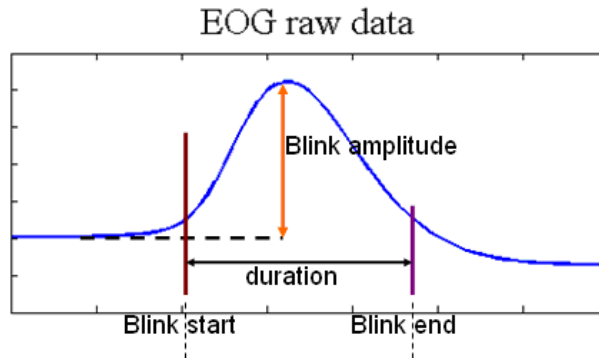


Fig. 2- 2: Blink features

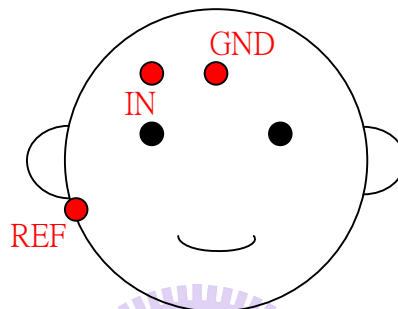


Fig. 2- 3: The recommended derivation of EOG

2.1.3 Electromyogram (EMG)

Electromyography (EMG) is a technique for evaluating and recording the electrical activity produced by skeletal muscles. EMG is performed using an instrument called an electromyograph, to produce a record called an electromyogram. An electromyograph detects the electrical potential generated by muscle cells when these cells are electrically or neurologically activated.[11]

The brainwave acquisition system not only regularly monitors EEG signal across cortex by time to time, but also may measure electrical activity produced by skeletal muscles near the chin when users grinding or gripping their teeth. This EMG signal which is transmitted along chin muscle surrounding to the skin on the brain is referred to high-frequency and high-amplitude noise of brainwave. Hence, one of goals of EEG preprocessing technique is to remove EMG noise as much as possible to enhance EEG signal-to-noise ratio.

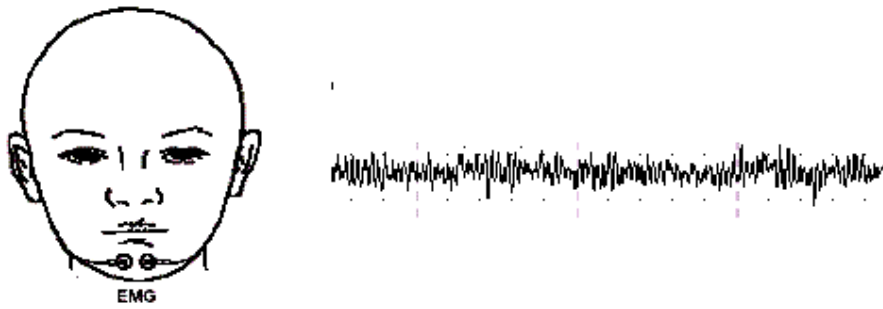


Fig. 2- 4: The EMG electrodes recorded pattern of chin muscle tension [12]

2.2 EEG Signal Preprocessing

The EEG preprocessing steps are shown in Fig. 2-5. Raw data which generated from cortex in the brain consists of whole frequency, and electrical activity in which is very tiny to be easily covered by other higher-amplitude potentials or noises produced from body. DC is one of unwelcome noises. Thus, for the microvolt-scale EEG data of interest, the input one-channel EEG signal passes a high-pass filter with a cutoff frequency of 0.1 Hz in first step. Next, the filtered data which has around 20uV-200uV of potential range is amplified to 5500 times, and then output around 110mV-11V of potential range. Before amplified data being saved to buffer, it will be down sampled to 125Hz first for the purpose of reducing data size, and be filtered 60Hz noise from the environment by moving average. Finally, the digital data saved in the buffer accomplishes EEG preprocessing.

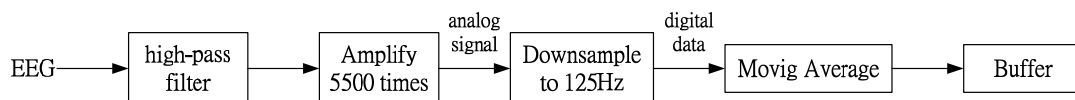


Fig. 2- 5: The diagram of EEG preprocessing.

2.3 Method of Data Acquisition and Record

In this session, we focus on this whole system hardware. Following the design flowchart, we will introduce the design methods of hardware circuits and firmware structures steps by steps.

2.3.1 System Overview

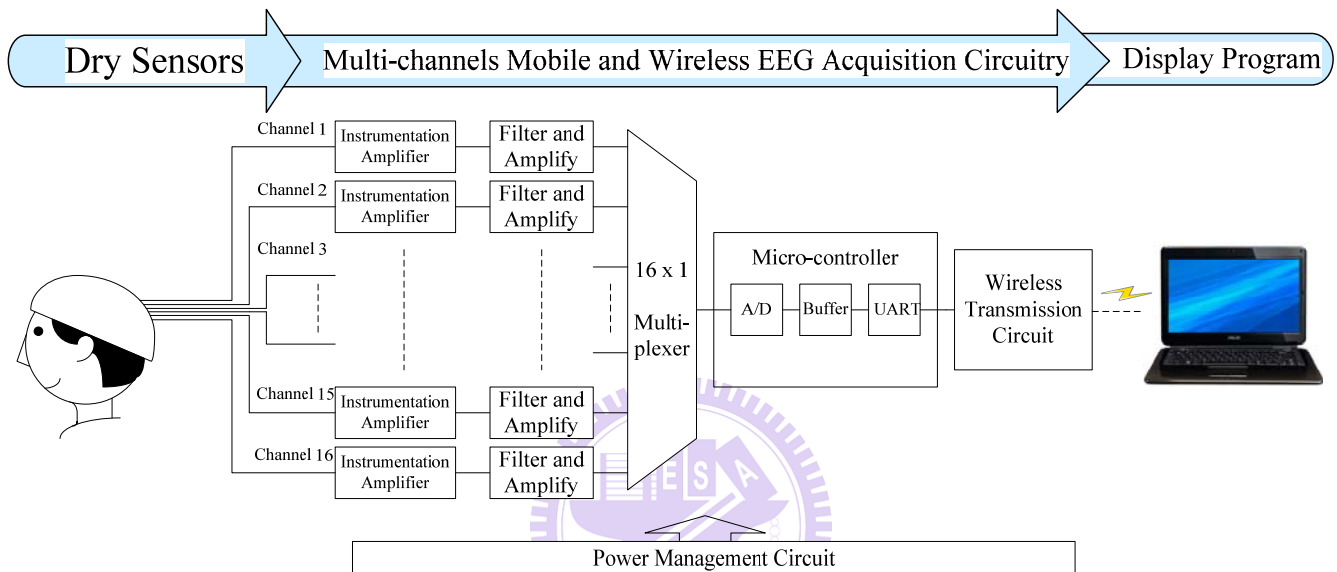


Fig. 2- 6: System overview of our proposed EEG system.

The major work in this study is to establish a hardware system which can be applied to front-end dry sensors and back-end received program to implement a multi-channels mobile and wireless EEG system. Our proposed EEG system has three parts as Fig. 2-6: (1) dry sensors, (2) a multi-channels mobile and wireless EEG acquisition circuitry, (3) an EEG display program.

Human brain is sphere-like and also has a little of resistance in hair site. One dry sensor was created to have multi-metal-columns of adjustable length, so it could perfectly fit user's curvature skin on the brain just like wet sensor, avoid hair site, and let user feel non-pricking as well as comfortable. Every dry sensor placed on the whole head continuously monitored electrical activity carried from the cortex of user's brain, and transmitted EEG signals to front-end filter and amplification circuit

via linking wires. Multi-channels front-end circuit included Instrumentation amplifiers, filters and amplifiers for upgrading Signal-to-Noise Ratio (SNR) of received raw EEG data. Moreover, the 0.1Hz high-pass filter could reduce DC shifting influence of dry sensors and exactly improve innate shortcoming of dry sensors. Then, multi-channels signals would be sequentially passed to micro-controller by a 16-to-1 multiplexer of fast switching rate. For being limited by the speed of multiplexer, the output signal was down sampled to 125Hz. Then, an Analog-to-Digital Converter (A/D) transferred analog signal to digital data. Buffer saved digital data until UART receiving request of wireless transmission circuit. If the request was accepted, UART would transmit the multi-channels digitized data to Wireless Transmission Circuit, and then Wireless Transmission Circuit carried the whole EEG data to back-end EEG display program in PC via Bluetooth. In this EEG preprocessing, Power Management Circuit always provided stable 3V to every chip of hardware system. If the power was too low, Power Management provided power until 0.8V by which micro-controller would be off.

The major work of back-end record program in PC, which simultaneously received events of experiment and EEG digital data from Bluetooth, was to show the multi-channels digital-to-analog signal on a frame in real-time and also saved all digital data as a file.

2.3.2 Dry Sensor

In the present study, novel dry-contact sensors for measuring EEG signals without any skin preparation are designed, fabricated by an injection molding manufacturing process and experimentally validated. Conventional wet electrodes are commonly used to measure EEG signals; they provide excellent EEG signals subject to proper skin preparation and conductive gel application. However, a series of skin

preparation procedures for applying the wet electrodes is always required and usually creates trouble for users. To overcome these drawbacks, novel dry-contact EEG sensors were proposed for potential operation in the presence or absence of hair and without any skin preparation or conductive gel usage. The dry EEG sensors designed to include a probe head, plunger, spring, and barrel (Fig. 2-7). The 17 probes were inserted into a flexible substrate using a one-time forming process via an established injection molding procedure. With these 17 spring contact probes, the flexible substrate allows for high geometric conformity between the sensor and the irregular scalp surface to maintain low skin-sensor interface impedance. Additionally, the flexible substrate also initiates a sensor buffer effect, eliminating pain when force is applied. The proposed dry EEG sensor was reliable in measuring EEG signals without any skin preparation or conductive gel usage, as compared with the conventional wet electrodes.[13]

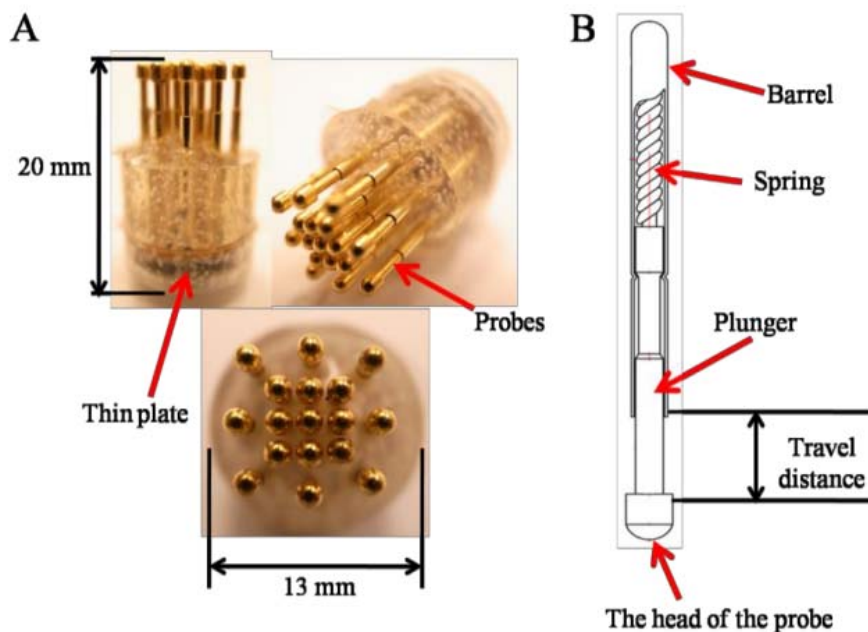


Fig. 2- 7: (A) Several images of the proposed dry EEG sensor are shown. (B) An exploded view of the proposed dry sensor is presented. Each probe includes a probe, plunger, spring, and barrel.[13]

In this study, we use dry sensors to monitor EEG activity which is distributed on the whole head because of dry sensors would be verified more suitable for hairy-site placement and long-term measurement than wet electrodes. As Fig. 2-8 shown, the results indicate that the impedance of the proposed dry EEG sensor is close to that of the wet electrode and is even lower on the hairy site. Significantly, the flexibility of the proposed dry EEG sensor is effective in tightly contacting the scalp surface and providing clear EEG signals without any skin preparation or conductive gel usage.[13] As Fig. 2-9 shown, the drawback of wet electrodes which could not maintain the same impedance in long time, but dry sensor can improve this problem to maintain the pretty tiny varies of impedance compared to wet sensor. After measuring one hour, the impedance of wet sensor eventually is larger than of dry sensor.

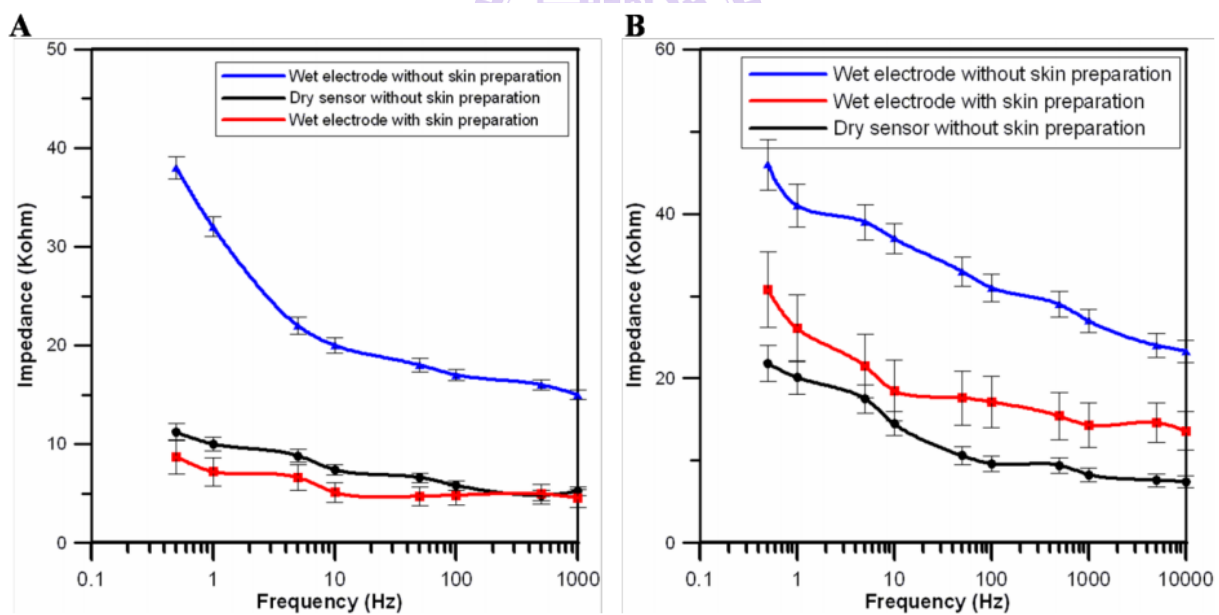


Fig. 2- 8: Impedance change data representing the skin-electrode interface on the (a) forehead (F10) and (b) at hairy sites [13]

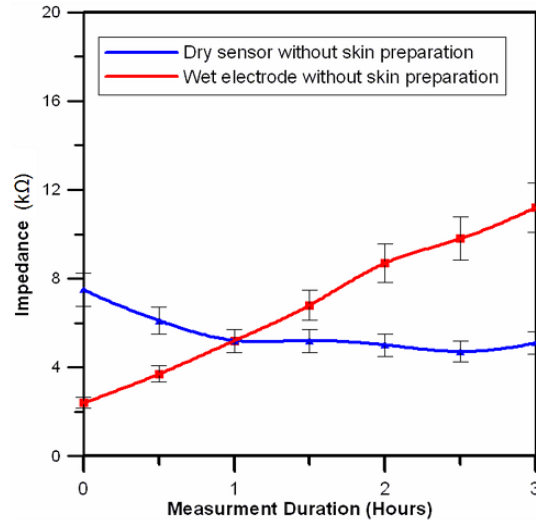


Fig. 2- 9: Long-term impedance variation measurements on the forehead site (F10) for wet and dry electrodes [13]

2.3.3 Multi-channels Mobile and Wireless EEG Acquisition Circuitry

Circuitry

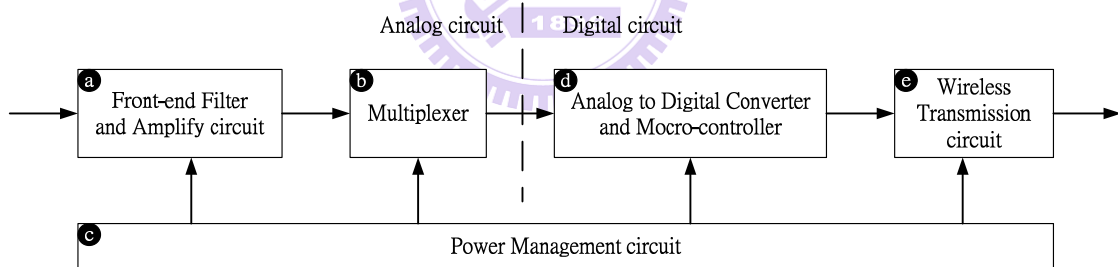


Fig. 2- 10: Circuitry frameworks overview

The multi-channels mobile and wireless EEG acquisition circuitry combines the power, amplifier, high pass filter, ADC, and wireless controller into one. It is a light weight, miniature, and wireless monitor for recording EEG signals. It owns 16-channel EEG-signal measurement. The multi-channels mobile and wireless EEG acquisition circuitry mainly contains two subsystem: (1) analog circuit: (a) front-end filter and amplification circuit, (b) multiplexer, (c) power management circuit; (2) digital circuit: (a) analog to digital converter and micro-controller, (b) wireless

transmission circuit and. The diagram of the mobile and wireless EEG acquisition circuitry is shown as Fig. 2-10.

In this study, the major work is we miniaturize the physical size of hardware as possible as we can, but do not decrease the necessary functions of EEG system. So that sometimes we have to trade of size and function to get the best performance to implement it. Finally, the EEG hardware system can amplify original signal to 5500 times, filter upper 0.1Hz frequency band, and sample to 125Hz digital data. As the following, we explain sequentially the procedure of trading of size and function in every function module.

2.3.3.1 Front-End Filter and Amplification Circuit

The front-end circuit consisted of Instrumentation amplifier and high-pass filter. In some researches, other circuit designs preferred to use unit gain filters and one variable gain amplifier. Moreover, they didn't use a high-pass filter to cut-off the noise in low frequency band. In this study, Dry sensor has an innate shortcoming because motion artifact and DC shifting. To improve them, front-end circuit needs high pass filter to maintain the typical EEG information in low power range without saturation. Besides, if the total magnification is very large about 5500 times, the filter circuit has to include "big" capacities. For miniaturization purpose, it's not an ideal design. Once technically allocating two stages for amplifying, this problem can be solved. Hence, we design two stages (Table 4) in which the first stage is Instrumentation amplifier including high pass function, and the second stage is also high pass filter amplifier.

Table 4: Stage details of front-end filter and amplification circuitry

Stage	Amplifier	Gain	High-pass cut-off frequency
1	Instrumentation amplifier	5.5	0.1
2	Operational amplifier	1000	0.1

A. Instrumentation Amplifier

Instrumental amplifier INA2126 was used as the first stage of analog amplifier. INA2126 consists of 2 channel instrumentation amplifiers into one package. INA2126 owns an ultra low input current and a high common-mode rejection ratio (CMRR) about 90dB. A high CMRR is important in applications that the signal of interest is represented by a small voltage fluctuation superimposed on a (possibly large) voltage offset, or when relevant information is contained in the voltage difference between two signals. Instrumental amplifier INA2126 provided not only the function of gain, but also that of one stage high pass filter by adding a capacitor. The output voltage of the INA2126 is referenced to the voltage on the reference terminal. INA2126EA/250G4 we selected was DBQ package drawing and about 5mm x 6mm size. The Instrumentation amplifier circuit design is shown in Fig. 2-11 and the simulation of frequency response is in Fig. 2-12.

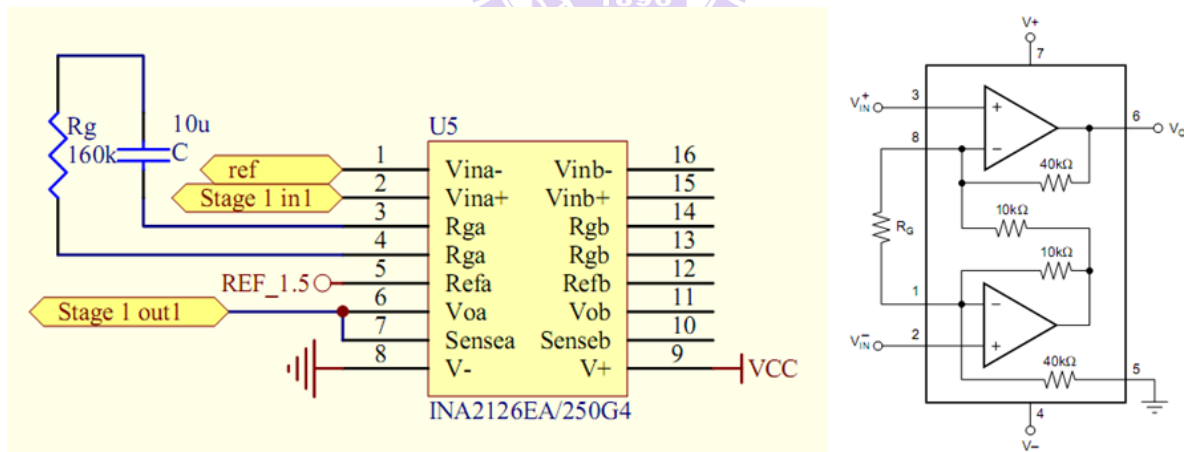


Fig. 2- 11: Left- the R_G decides the gain of preamplifier, and the high pass filter of preamplifier decided by R_G and C . Right- block diagram of INA2126

$$Gain = 5 + \frac{80k}{R_G}$$

$$f_0 = \frac{1}{2\pi \cdot R_G \cdot C}$$

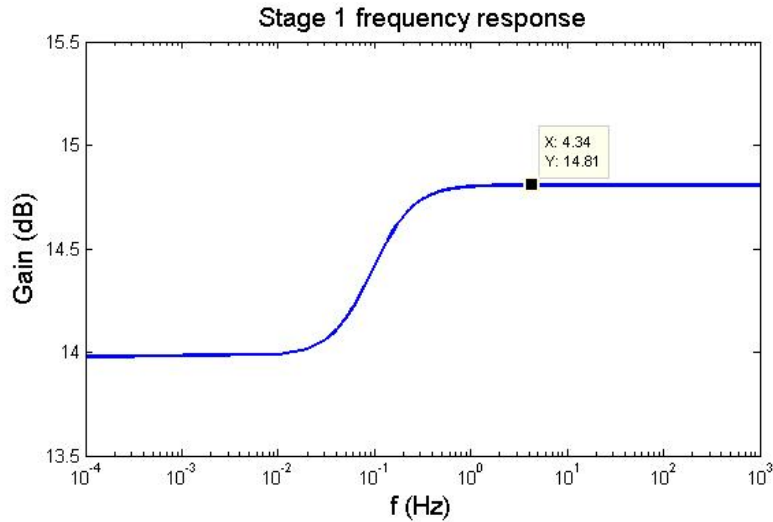


Fig. 2- 12: Simulation of amplifier’s frequency response in stage 1

B. High Pass Filter

In this thesis, operational amplifiers were used to achieve the function of band-pass filter. The AD8609 is quad micro-power rail-to-rail input and output amplifiers and low dc offset was chosen to be high pass filter. Fig. 2-13 shows one channel High-pass filter circuits. The 3dB cutoff frequency of high pass was decided by passive components R3, R4, C1 and C2; and the other component R1, and R2 are responsible for enhancing magnification. AD8609AR we selected was 14-Lead SOIC package description and about 8.5mm x 6mm size. Fig. 2-14 shows the simulation of amplifier’s frequency response (EEG) in stage 2 and Fig. 2-15 shows the simulation of amplifier’s total frequency response.

$$Gain = 1 + \frac{R_2}{R_1}$$

$$f_H = \frac{1}{2\pi\sqrt{R_3R_4C_1C_2}}$$

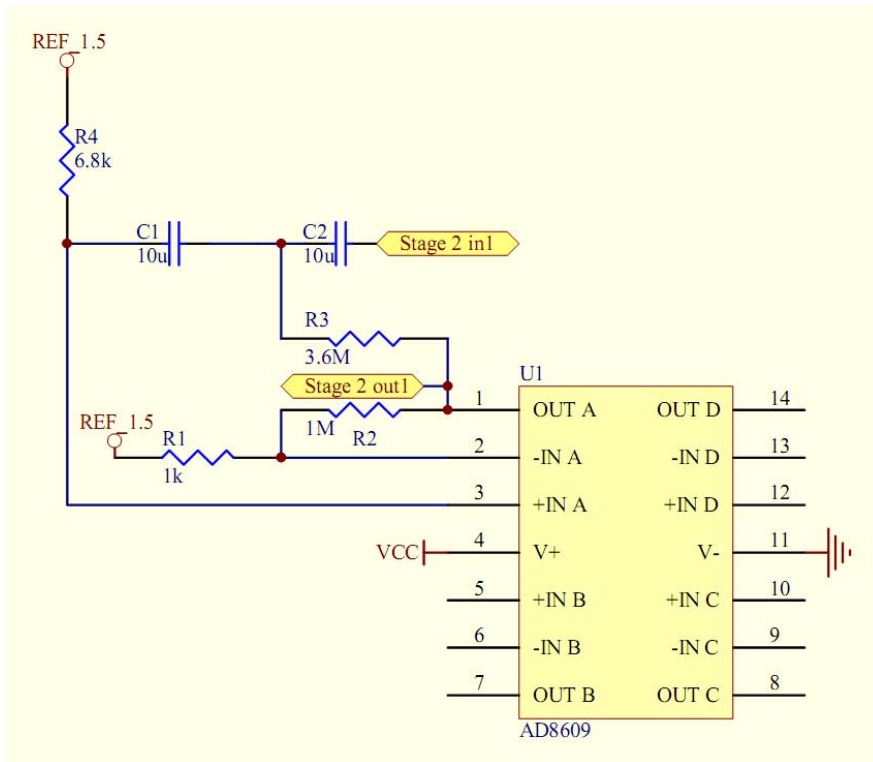


Fig. 2- 13: High-pass filter circuits.

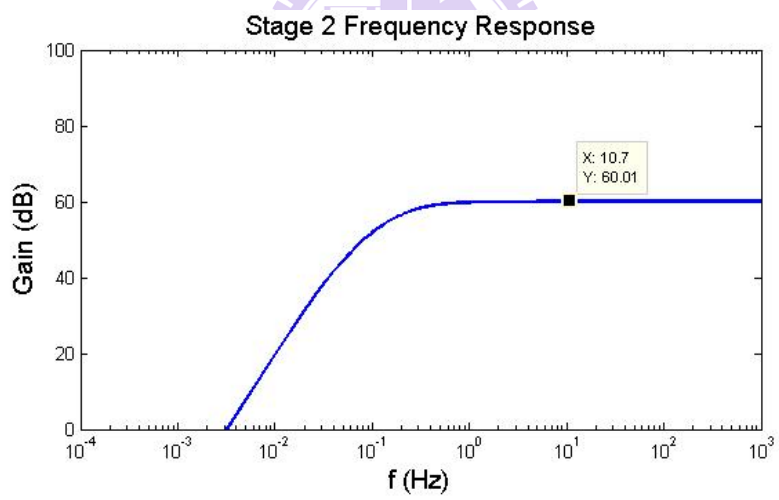


Fig. 2- 14: Simulation of amplifier's frequency response in stage 2.

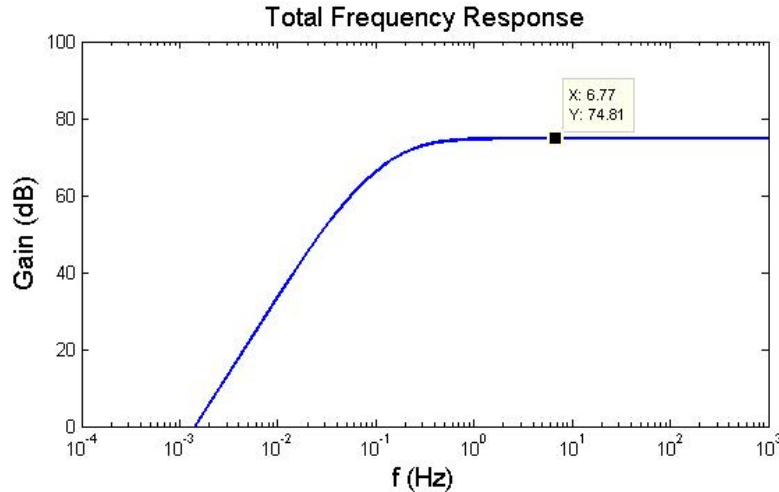


Fig. 2- 15: Simulation of amplifier’s total frequency response.

2.3.3.2 Multiplexer

As shown forward, for Multi-channels EEG system design, we select INA2126 x 8 and AD8609 x 4 to measure 16 channel bio-signals. The analog information would carry to next stage – analog-to-digital converter (A/D), but the number of A/D is finite. Hence there was need a multiplexer sequentially pass analog information to A/D. In other words, the major work of Multiplexer is Allocating finite resource to Multi-channels.

In addition, next issue is which stage multiplexer suited to serve. To consider that tiny analog signal mixing noise from environment go through multiplexer may mix other noise more, the amplified analog signal (noise is smaller than real EEG signal) fitted to be the input of multiplexer. Therefore, Multiplexer placed behind front-end circuit and forward A/D of micro-controller.

CD74HC4607 is a 16-to-1 multiplexer, and it can be fabricated to about 8mm x 8mm size (CD74HC4607SM96) by very small package SSOP. We researched the sizes of 2-to-1 multiplexer x 8, 4-to-1 multiplexer x 4, and 8-to-1 multiplexer x 2 were all not smaller than a 16-to-1 multiplexer for the smallest package in existing fabrication procedure. As shown by Fig. 2-16, select pin S0, S1, S2, and S3 and

select-valid pin Inhibit was linked to output pin of micro-controller. Output pin - out was linked to A/D of micro-controller. Multiplexer should achieve passing analog signal from input to output into 250 us in which micro-controller make select pin “On”. Because the maximum transmission time of CD74HZ4607 is about 300 ns in 25°C temperature, it made no problem for high-speed 16-to-1 Multiplexer CD74HZ4607.

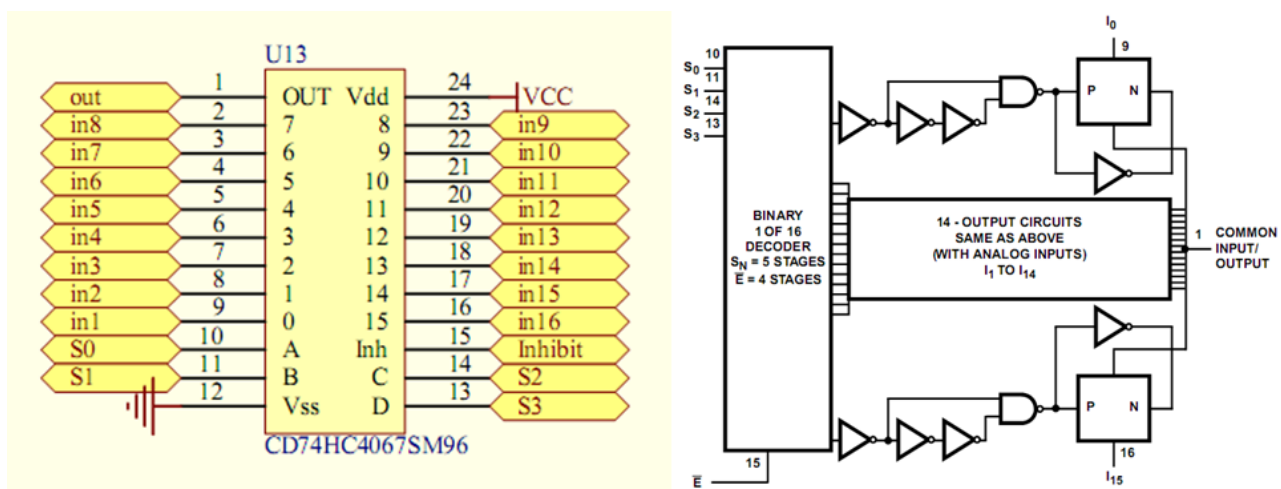


Fig. 2- 16: The outer appearance and block diagram of CD74HC4067

2.3.3.3 Analog to Digital Converter and Micro-controller

For the data acquisition system, it needs a controller to organize the working of ADC and encode the digital data to Bluetooth module by UART port. The MSP430 is particularly well suited for wireless RF or battery powered applications. The MSP430 incorporates a 16-bit RISC CPU, peripherals, and a flexible clock system that interconnect using a von-Neumann common memory address bus (MAB) and memory data bus (MDB) shown as Fig. 2-17. The clock system is designed specifically for battery-powered applications. Dedicated embedded emulation logic resides on the device itself and is accessed via JTAG using no additional system resources. We configure with built-in 16-bit Timer A, a fast 12-bit A/D converter, one

set first, as shown in Fig. 2-19. When the timer counted to the TACCR0 value, the TACCR0 CCIFG interrupt flag would be set. When the timer counted from TACCR0 to zero, the TAIIFG interrupt flag would be set. In our Mobile EEG acquisition module, 4.096MHz crystal oscillator was used as system clock of MSP430F1611, and TACCR0 is set to 1024 for making a rate 4 kHz.

$$TACCR0 = \frac{4.096M}{4k} = 1024$$

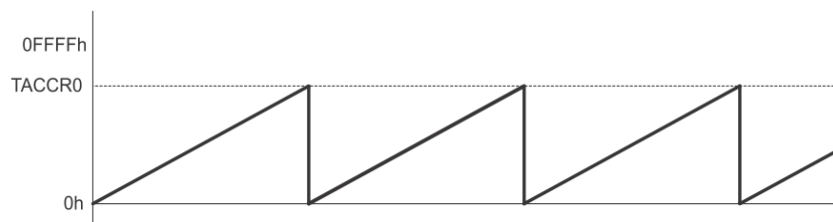


Fig. 2- 19: Timer A up mode for interrupt function of MSP430F1611

Time A uses 4 kHz to control select pin of multiplexer via output pin of MSP430, so the switching rate from one channel to the other one is 2 kHz. When finishing the sequential visit for all channels, total time is 8 ms. In this way, our propose system can implement 125Hz of sampling rate to catch analog signal.

B. Analog to Digital Converter

In this system, for passing the signal through wireless, it needs an analog to digital converter to convert the continuous signal to discrete number. To suit with the filtered and amplified signal from front-end circuit, built in ADC of MSP430 was chosen to be an analog to digital converter.

Fig. 2-20 shows ADC12 Block Diagram. The ADC12 module supports fast, 12-bit analog-to-digital conversions. The module implements a 12-bit SAR core, sample select control, reference generator and a 16 word conversion-and-control

buffer. The conversion-and-control buffer allows up to 16 independent ADC samples to be converted and stored without any CPU intervention [14]. The ADC12 inputs are multiplexed with the port P6 (A0-A7) pins, which are digital CMOS gates. An analog-to-digital conversion is initiated with a rising edge of the sample input signal SHI. The signal SHI will be set by interrupt routine of timer A at 2 kHz. The ADC12 module is configured by three control registers, ADC12CTL0, ADC12CTL1 and ADC12MCLTx. Those registers are set to enable core, select conversion clock, set conversion mode, sample and input channels define. In our system, we used the “one channel, single conversion each” mode. In this mode, the certain channel is sampled and converted once. Fig. 2-21 shows a diagram for sampling time and conversion time of ADC with trigger by timer A. Therefore, the conversion time of ADC is fast enough to fit the requirement of the sampling rate of the whole system. The ADC result of each channel will be 12 bits long in the form of an unsigned integer whose

$$\text{value is: } 4095 * \frac{A_x - V_{R-}}{V_{R+} - V_{R-}}$$

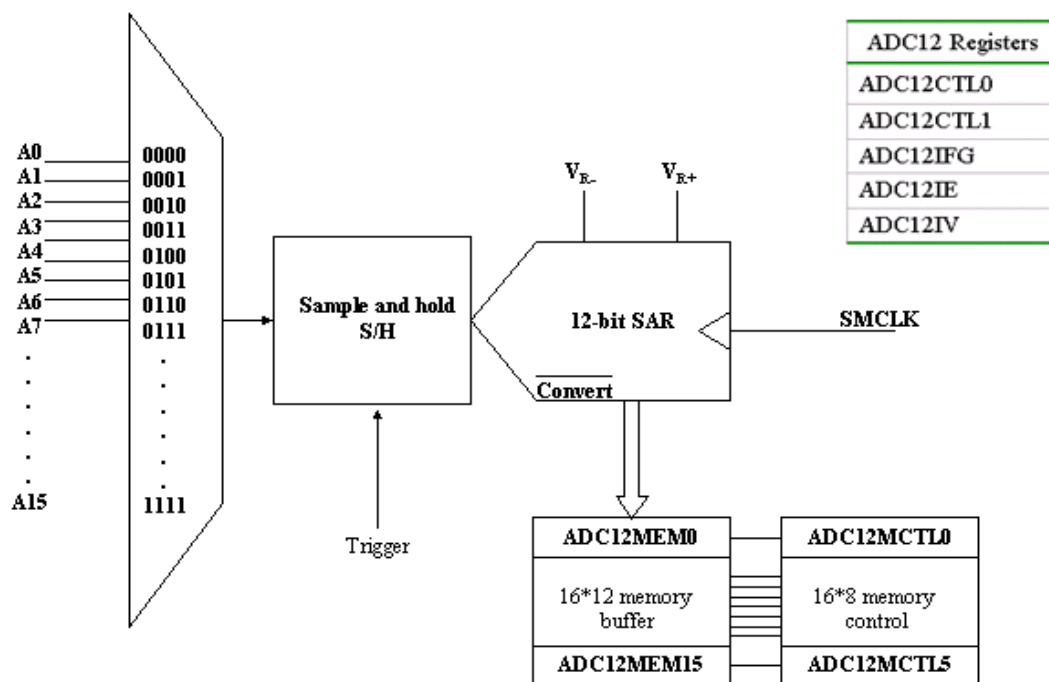


Fig. 2- 20: ADC12 Block Diagram [14]

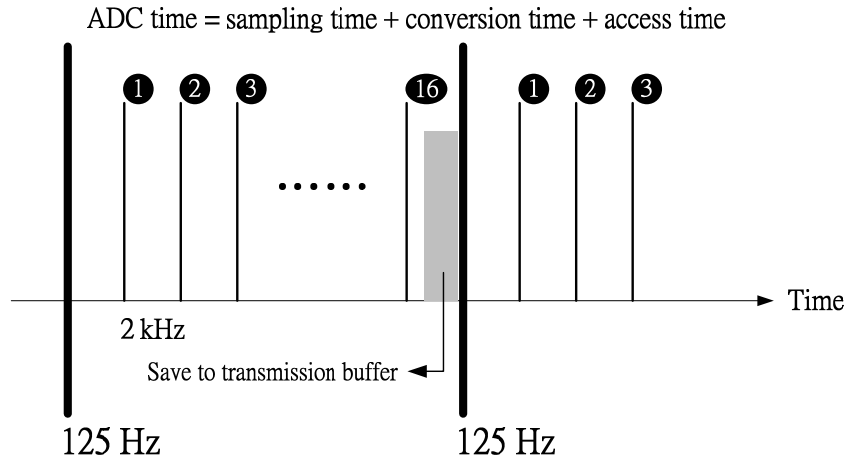


Fig. 2- 21: Diagram of the sampling and conversion with timer A trigger

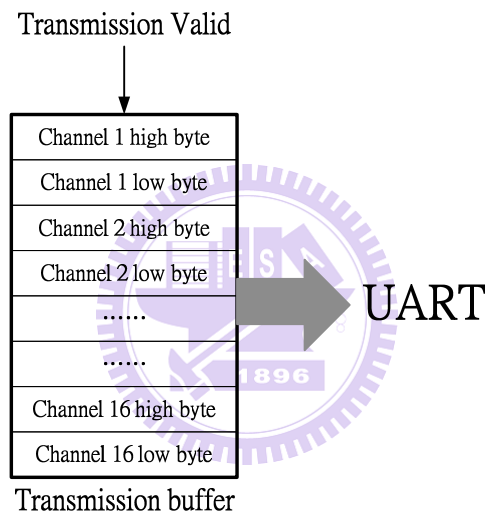


Fig. 2- 22: Transmission buffer

When conversion results are written to a selected ADC12MEMx, the corresponding flag in the ADC12IFGx register is set. An interrupt request is generated if the corresponding ADC12IEx bit and the GIE bit are set. After ADC12IFGx register set, the interrupt service routine of ADC started. In the interrupt service routine, we buffered ADC12MEMx. Next, a moving average filter was used to remove 60-Hz power interference, and then filtered signal data was encoded before wireless transmission. Fig. 2-22 shows transmission buffer, and Table 5 shows data format saved in transmission buffer.

Table 5: Data format (channel number)

Header	information	data						
ff	74	(1) high byte	(1) low byte	(2) high byte	(2) low byte	(16) high byte	(16) low byte

C. Moving Average

Moving average, also called rolling average or running average, is usually used to analyze a set of data points by creating a series of averages of different subsets of the full data set. Moving average can be applied to any data set, however, it is most commonly used with time series data to smooth out short-term fluctuations and highlight longer-term trends or cycles. The choice between short- and long- term, and the setting of moving average parameters depends on the requirement of application. Mathematically, moving average is a type of convolution and is similar to a low-pass filter used in signal processing. The moving average filter is optimal for a common task: reducing random noise while retaining a sharp step response. This makes it as the premier filter for time domain encoded signals.

Given a sequence $\{a_i\}_{i=1}^N$, the output of an n -moving average is a new sequence $\{s_i\}_{i=1}^{N-n+1}$ defined as the average of subsequences of n terms. The formula of moving averaging was shown as followings.

$$s_i = \frac{1}{n} \sum_{j=1}^{i+n-1} a_j$$

Therefore, the sequences s_n of n -moving averages when $n = 2,3$ can be expressed as

$$s_2 = \frac{1}{2} (a_1 + a_2, a_2 + a_3, \dots, a_{n-1} + a_n)$$

$$s_3 = \frac{1}{3} (a_1 + a_2 + a_3, a_2 + a_3 + a_4, \dots, a_{n-2} + a_{n-1} + a_n)$$

Fig. 2-23 shows the results of noise cancellation by using moving average. A function generator was used to generate sin wave, and our portable bio-signal acquisition system was used to record this signal. If our portable acquisition module was close to some electric instruments, the signal recorded from the acquisition module would be easily influenced by noise of 60 Hz power line. In the above figure of Fig. 2-23, it showed that the original sin wave had been contaminated by 60Hz power-line noise. After filtering by using moving average with 2-point moving window, we found moving average could effectively remove power-line noise, as shown in the below figure of Fig. 2-23.

$$Num_of_window = \frac{Sample_rate}{60} = \frac{125}{60} = 2.08$$

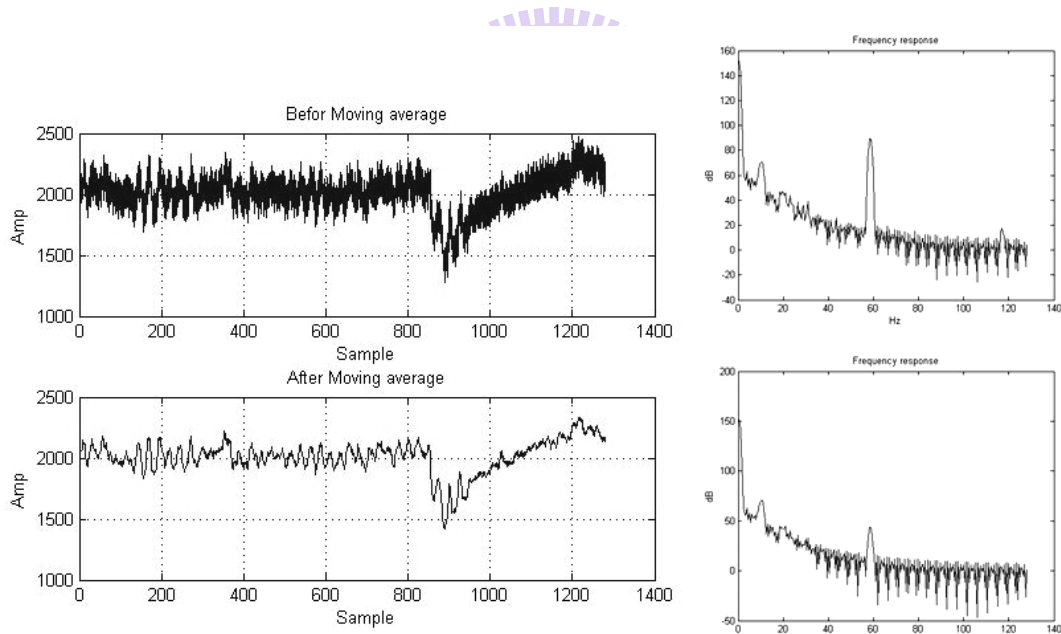


Fig. 2- 23: Result of noise cancellation by using moving average [15]

D. UART Interface

In asynchronous mode, USART connected MSP430 to external systems via two external pins, URXD and UTXD. In UART mode, USART transmitted and received characters at a bit rate asynchronously to another device. Timing for each character

was based on the selected baud rate of USART. In our study, the transmitter and receiver used the same baud rate. For initializing UART, RX and TX had to be enable first, and then decided the baud rate of UART and disable SWRST. The required division factor N for determining baud rate was listed as followings:

$$N = \frac{BRCLK}{\text{baud rate}}$$

Here, BRCLK was 4 MHz, and baud rate was 115200 bit/s. After initializing UART, the micro-controller could transmit data filtered by moving average to BLUE TOOTH module via UART.

2.3.3.4 Wireless Transmission

Bluetooth is a wireless protocol utilizing short-range communication technology to facilitate data transmission over short distances from fixed and/or mobile devices. The intent behind the development of Bluetooth was the creation of a single digital wireless protocol, capable of connecting multiple devices and overcoming issues arising from synchronization of these devices. In this study, Bluetooth module BM0203 was used. BM0203 is an integrated Bluetooth module to ease the design gap and uses CSR BlueCore4-External as the major Bluetooth chip. CSR BlueCore4-External is a single chip radio and baseband IC for Bluetooth 2.4GHz systems including enhanced data rates (EDR) to 3Mbps. It interfaces to 8Mbit of external Flash memory. When used with the CSR Bluetooth software stack, it provides a fully compliant Bluetooth system to v2.0 of the specification for data and voice communications. All hardware and device firmware of BM0203 is fully compliant with the Bluetooth v2.0 + EDR specification. Bluetooth operates at high frequency band to transmit wireless data, so it can be perfect worked by using a PCB antenna, as shown in Fig. 2-24.

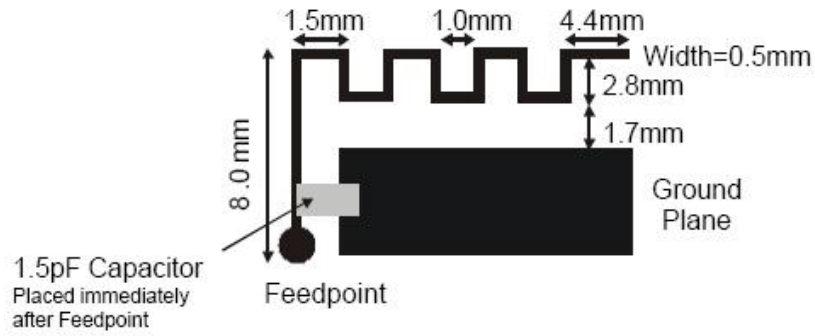


Fig. 2- 24: PCB Blue Tooth antenna [16]

2.3.3.5 Power Management

Power Management circuit in our Mobile EEG acquisition circuitry includes two parts: one is power supply circuit, and the other is charging circuit.

A. Power Supply Circuit

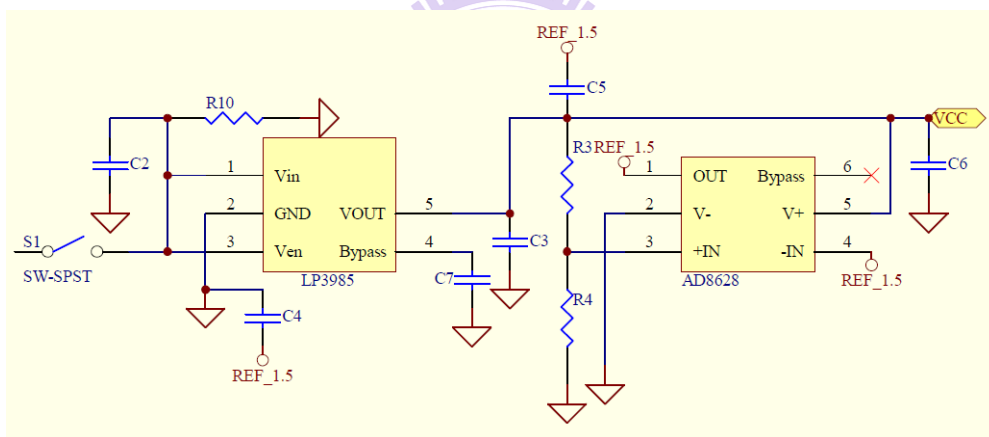


Fig. 2- 25: Power supply circuit

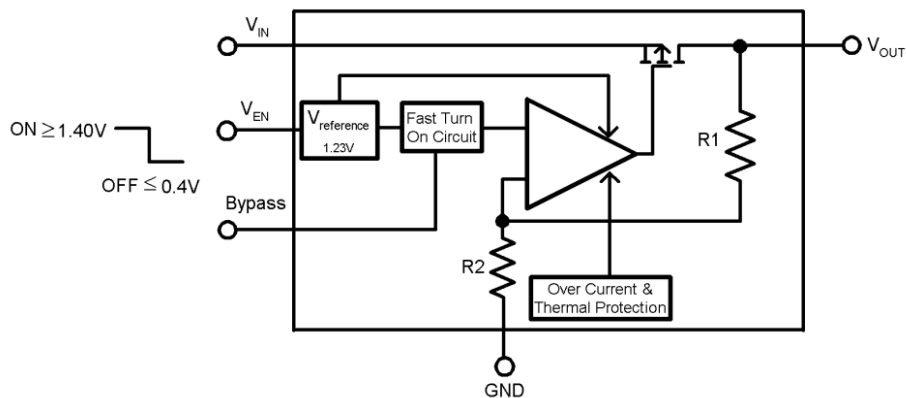


Fig. 2- 26: LP3985 block diagram

In our portable bio-signal acquisition system, the operating voltage VCC was at 3V, and the virtual ground of analog circuit was at 1.5V. In order to provide stable 1.5V and 3V voltage, a regulator LP3985 (Fig. 2-26) was used to regulate battery voltage to 3V. LP3985 is a micro-power, 150mA low noise, and ultra low dropout CMOS voltage regulator. The maximum output current can support 550mA. Furthermore, the turn-on time can reach 200 μ s. A voltage divider circuit was used to divide 3V voltage into 1.5V, and a unity amplifier constructed from AD8628 was used to provide a voltage buffer. The total power supply circuit was shown in Fig. 2-25.

B. Charging Circuit

The charging circuit BQ24010DRC had integrated power FET and current sensor for 1-A charging applications. The maximum charging current can arrive at 1A. The battery's power would be detected automatically by charging circuit and switched to charging mode when battery's power was not enough. BQ24010DRC also protected battery to avoid over charging or over driving [16]. The charging circuit was shown in Fig. 2-27.

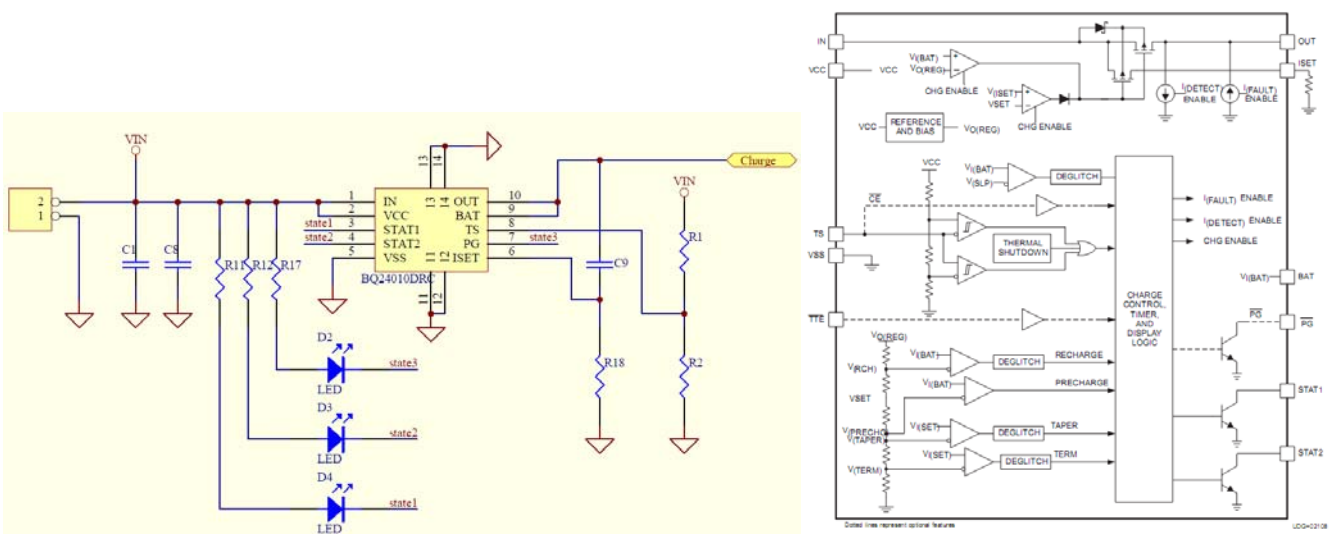


Fig. 2- 27: Left- Charging circuit in our portable bio-signal acquisition system. Right- Block diagram of BQ24010DRC

2.3.4 Implementation of the EEG Acquisition Circuitry

The demand factors of our proposed EEG acquisition circuitry are lightweight, miniature, multi-channels, portable, wireless, and long-time monitoring. All of these are indeed implemented on a board, which is called “16-channel EEG device”. This device is only 50mm x 60mm large finally. Furthermore relative standard EEG measurement system like Neuroscan system, it improves convenience, practicality, and wide application. Real-time operation test verifies this circuit can be used about 10 hours. Hence, it is suitable for general long-term monitoring in daily life for most of users, even through for medical use and for scientific experiments. The outward appearance of implemented circuitry is showed by Fig. 2-27.

In design procedure, we found out the best parameters of circuit by MATLAB simulation. Moreover, the cut-off frequency of high-pass filter is 0.2Hz for physical device different from 0.1Hz we expected. Although a little error in design, the device measures EEG activity of interest is very enough. Besides the cut-off frequency, the other specifications of device are almost same as our design. As Table shown, the specification of 16-channel EEG device is listed. Table 6 shows Specification of implemented hardware system.

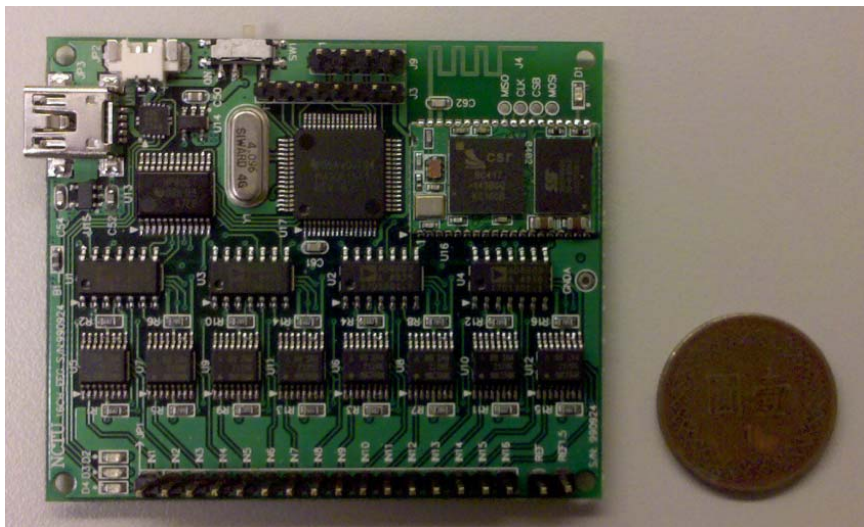


Fig. 2- 28: The outward appearance of implemented circuitry

Table 6: Specification of implemented hardware system

Type	Mobile and Wireless EEG Acquisition Circuitry
Channel Number	16
Size	50 mm × 60 mm
Weight	< 50 g
Power	3V
Power capacity	about 10 hours
Battery	rechargeable Lithium 3.7V 450mAh
Recharge port	Mini USB
Power Supply Rejection Ratio	88 dB
Input impedance	10 GΩ
Input Common Mode Rejection Ratio	90 dB
Input signal range	± 272.7 uV compared to reference potential
Gain	5500
Bandwidth	0.2 Hz ~ 62.5Hz
ADC resolution	12 bits
Sampling rate	125 Hz
Communication interface	Bluetooth 2.0
Transmission baud rate	115200 bit/s

2.3.5 EEG Display Program

EEG display program is designed for two purposes: (1) display record EEG data on the frame, (2) save record data to a file. This session explains the method of display program steps by steps.

2.3.5.1 Receive Package and Display

A. Package Protocol

For display purpose, we expected the program received transmission digital data package continuously via Bluetooth. The data package format follows MSP430 encoding which explained in Table 5 of session 2.3.3.3 B. which is including one byte of header, one byte of data information, and 16 channel data. The program recognizes out package header through checking receiving data from byte to byte. On the other words, this program owns itself communication protocol, which once finding out common header, begins to decode certain package information and the following fix length of data. Table shows package protocol and function (2-1) shows decode thesis.

$$Sampling_rate = 2^{data_value}, Channel_number = 2^{data_value} \quad (2-1)$$

Table 7: Header of package

Header		Data information	
f	f	Sampling rate	Channel number

Table 8: data information of package

data value	0	1	2	3	4	5	6	7	8	9	10
Sample Rate / Channel number	1	2	4	8	16	32	64	128	256	512	1024

Table 9: Channel data

Channel data						
(1) high byte	(1) low byte	(2) high byte	(2) low byte	(16) high byte	(16) low byte

Table 10: data-encoding method

High byte		Low byte	
01	high six bits	10	low six bits

B. Display Digital Data to Analog Signal

The actual EEG signal needs a function to convert digital data to analog data.

See the thesis:

$$\begin{aligned} Actual_EEG_signal &= \left(\frac{data_value}{2^{ADC_resolution}} \times Power \right) - Virtual_GND_potential \\ &= \left(\frac{data_value}{2^{12}} \times 3 \right) - 0.5 \end{aligned}$$

The program already defaults ADC resolution is 12 bits and isn't adapted by user interface. As for the actual potential value is not influence the method of display. After the program receive the 0-4096 range of data value, it just plots multi-channels data values in width-required frame, and shows the curve length according to sampling rate from package information and the number of display second from user interface.

2.3.5.2 Save Data as a File

Display program which was installed in the computer continuously receives digital data packages one by one via Bluetooth if it is started. In the beginning, user interface would ask user whether to save data as a file or not. If the save request is set, the program not only displays real-time converted analog signal but also saves received digital data as a TXT-format file simultaneously. In the TXT file, data package is saved as a row value once, and each channel data is saved as column value. The first column means the first channel data, and the second column means the second channel ones, and so on. From left to right put each channel data in order and the final column means the 16-th channel data or event value if user needs. Incidentally referring, the program record received event data with the rate of receiving. Program would get event file name and event input comport from user interface. So that every time the program receives one package, it synchronously checks certain input comport whether receiving event information or not. If event

value appears, the program recognizes it and save a value in final column behind 16 columns. However, if event value doesn't appears, the program just save zero value in this event column. As following, Fig. 2-29 shows data appearance in TXT file.

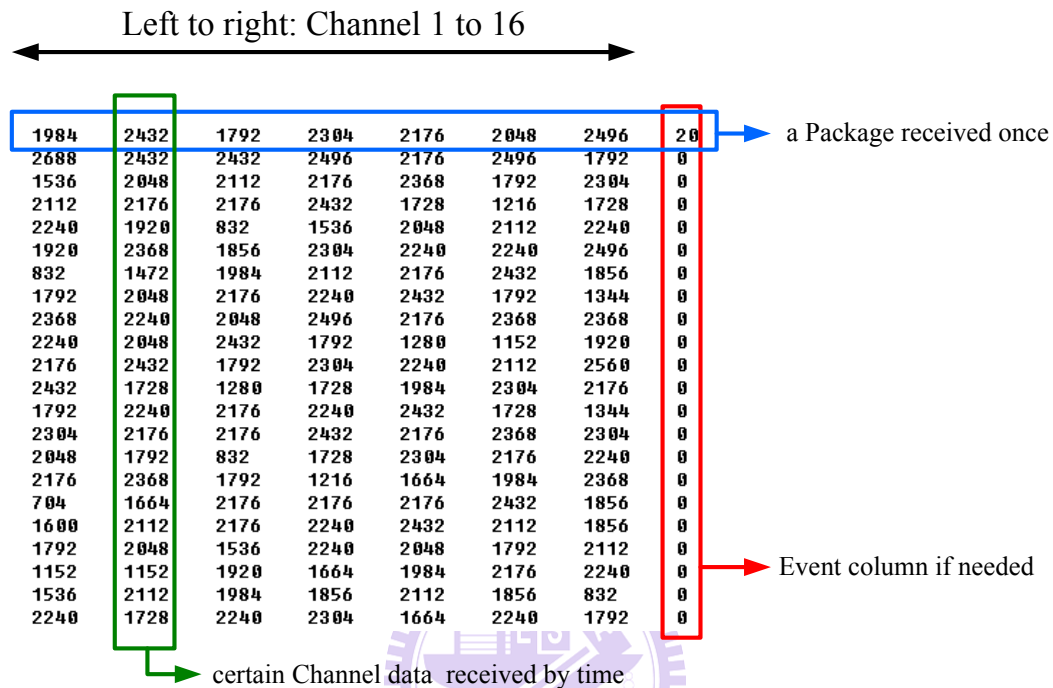


Fig. 2- 29: TXT file contexts

2.3.5.3 User's Guide



Fig. 2- 30: User interface with opening window

As Fig. 2-30 shown, the 1st row mentions certain Bluetooth module using now. After opening this program, user can click “Refresh” button to search existing Bluetooth modules in finite distance. The 2nd row asks user that this program is going to display how much time for EEG real-time signal. The 3rd row asks user whether to save receiving data as a TXT file or not. If yes, please select a new file name. The 4th row asks user whether simultaneously receiving event value via a specified comport or not. The 5th row asks user whether to let program automatic checking the synchronization between event and channel data. After finished above request menu, user can click “Beginning” button to start this program. In addition to, to click “Quit” button stops this ongoing program. Moreover, Fig. 2-31 shows the window once starting to receive EEG data.

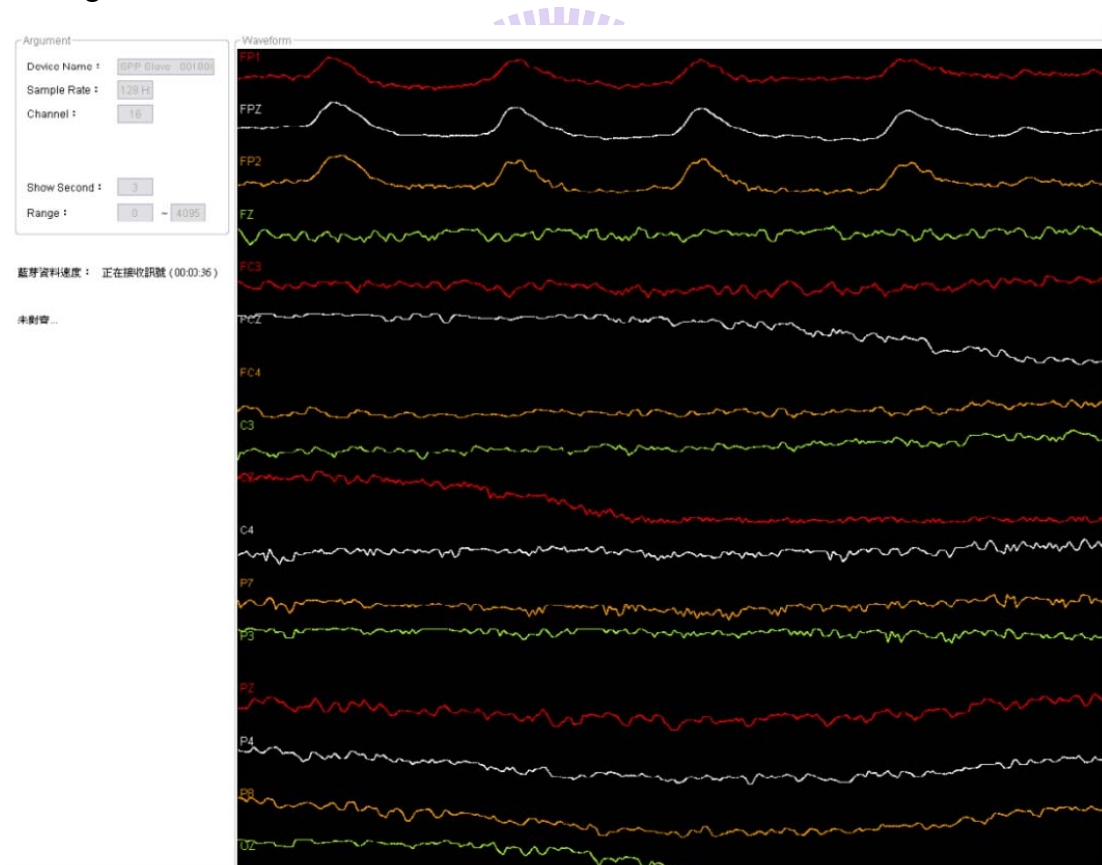


Fig. 2- 31: Appearance of display Program within receiving process

2.4 Experiment: P300 and Oddball task

For system verification purpose, we need a standard cognitive experiment to make sure our proposed mobile and wireless system can measure tiny EEG activity even though Event-Related Potential (ERP). Thus, we introduce P300 and Oddball task in this session progressively.

2.4.1 P300

Event-related potential (ERP) refer to averaged EEG responses that are time-locked to more complex processing of stimuli; this technique is used in cognitive science, cognitive psychology, and psychophysiological research. An event-related potential (ERP) is any measured brain response that is directly the result of a thought or perception. More formally, it is any stereotyped electrophysiological response to an internal or external stimulus.[24]

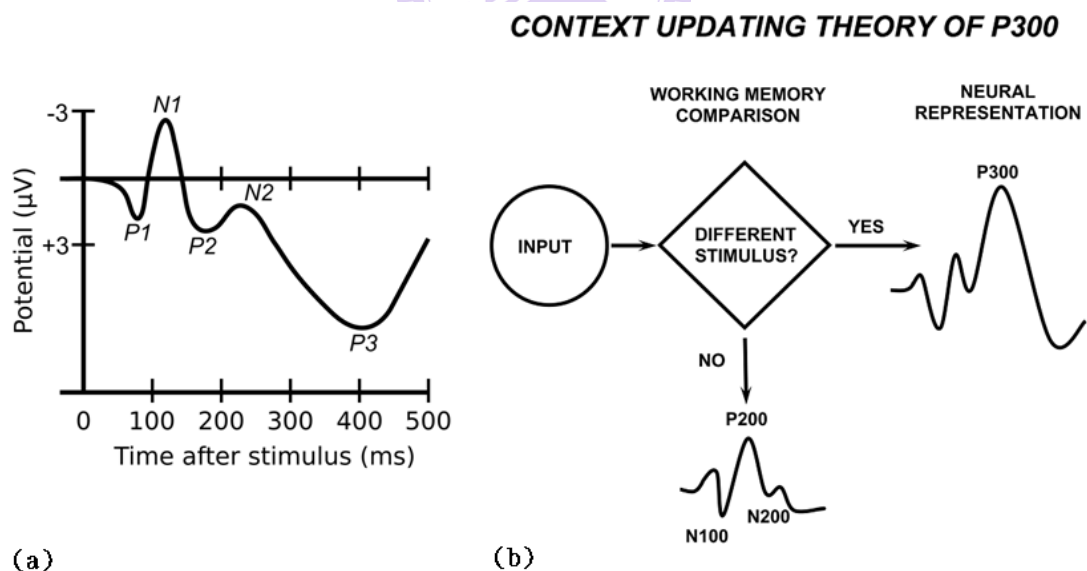


Fig. 2- 32: (a) P300 [24] (b) Context updating theory of P300 [18]

The P300 (Fig. 2-32 (a)) is a positive component of the event-related potential (ERP) that peaks 300ms or more (up to 900 ms) after a stimulus. Unlike some of the earlier evoked potentials, it is supposed to be an “endogenous” component in the

sense that it depends very much on the processing of the stimulus context and levels of attention and arousal (Polich and Kok 1995). The P300 has commonly been investigated with “oddball” paradigms, in which occasional relevant (“target”) stimuli have to be detected in a train of frequent irrelevant “non-target” or “standard” stimuli. Such oddball paradigms reliably yield P300 responses with a parietocentral scalp distribution to target compared to standard stimuli irrespective of stimulus (visual, auditory, somatosensory) or response (button press, counting) modality. Interestingly, P300 responses are also observed when trains of regular stimuli are interrupted by stimulus omissions, which underlines the endogenous nature of this component.

The amplitude of the P300 increases with lower probability and higher discrimination of targets. Its latency increases when targets are harder to discriminate from standards but not when response times increase for other reasons. P300 latency is thus an attractive tool to separate the mental chronometry of stimulus evaluation from response selection and execution (Coles and others 1995). The P300 is widely believed to be a neural signature of the mechanisms required to change the mental model of the environment to make an appropriate response (Polich 2003). In terms of classical cognitive domains, both attention (selecting the deviant stimulus from the train of irrelevant stimuli) and working memory (supporting this process by maintaining the features of the standard stimulus for comparison) seem to be involved. However, the higher amplitude of the P300 for easily discriminated targets (that is, when demand on working memory should be low) and the lower amplitude in tasks with high memory load (Kok 2001) indicate that the interplay between attention and working memory in the generation of the P300 is not straightforward and certainly not simply additive.[18]

Fig. 2-32 (b) shows schematic illustration of the P300 context-updating model (Polich, 2003). Stimuli enter the processing system and a memory comparison process is engaged that ascertains whether the current stimulus is either the same as the previous stimulus or not (e.g. in the oddball task, whether a standard or a target stimulus was presented). If the incoming stimulus is the same, the neural model of the stimulus environment is unchanged, and sensory evoked potentials (N100, P200, and N200) are obtained after signal averaging. If the incoming stimulus is not the same and the subject allocates attention resources to the target, the neural representation of the stimulus environment is changed or updated, such that a P300 (P3b) potential is generated in addition to the sensory evoked potentials. [18]

2.4.2 Oddball Task

P300 occurs when a stimulus is presented. Oddball task is just one of method to detect it. Besides, past researchers also designed single-stimulus and three-stimulus experiment to study the characteristic of P300. As following Fig. 2-33 shown, single-stimulus experiment induce single P300, oddball experiment induce a larger amplitude of P300 when stimulus discrimination occurred, and three-stimulus experiment induce P3a and P3b when distracter stimulus and difficult stimulus discrimination occurred respectively.

As Fig. 2-33, schematic illustration of the single-stimulus (top), oddball (middle), and three-stimulus (bottom) paradigms, with the elicited ERP from the stimuli of each task at the right (Polich and Criado, 2006). The single-stimulus task presents an infrequent target (T) in the absence of any other stimuli. The oddball task presents two different stimuli in a random sequence, with one occurring less frequently than the other does (target=T, standard=S). The three-stimulus task is similar to the oddball with a compelling distracter (D) stimulus that occurs infrequently. In each task, the

subject is instructed to respond only to the target and otherwise to refrain from responding. The distracter elicits a P3a, and target elicits a P3b (P300). [20]

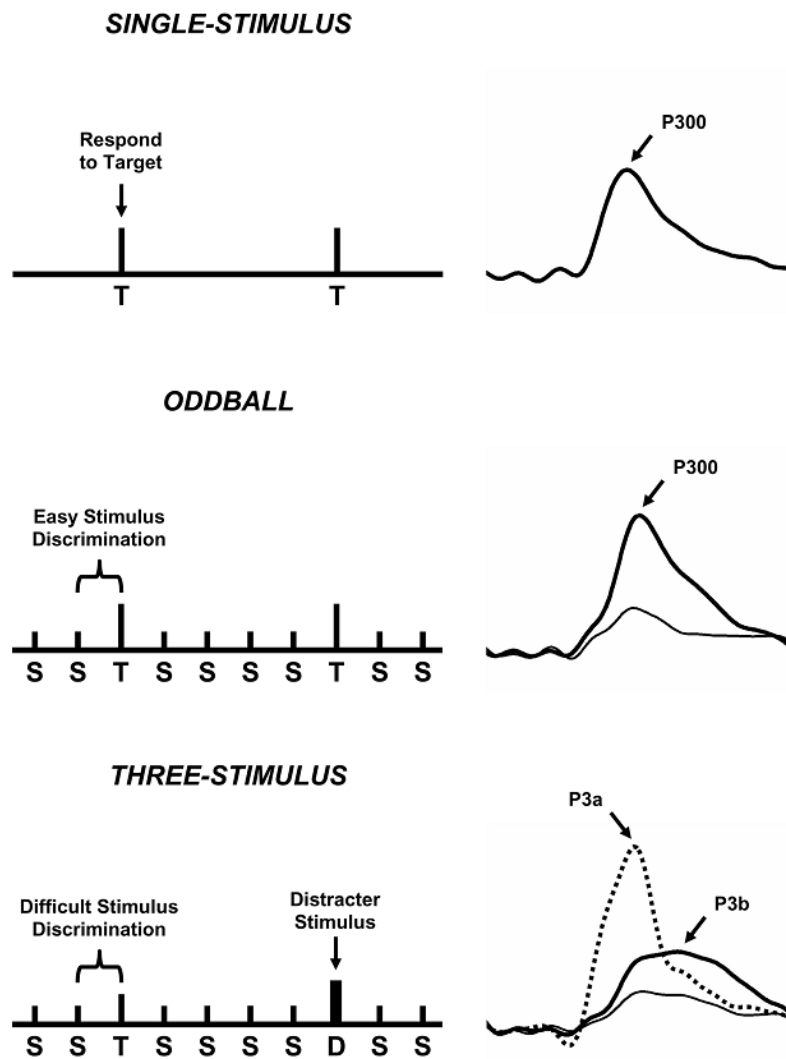


Fig. 2- 33: Schematic illustration of the single-stimulus (top), oddball (middle), and three-stimulus (bottom) paradigms [20]

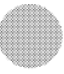
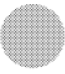

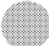
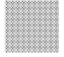
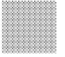
Target/standard discrimination	Visual (cm ²)	
	Easy	Difficult
Target (0.10)	12.57 	12.57 
Standard (0.80)	6.16 	10.18 
Non-target (0.10)	12.57 	12.57 

Fig. 2- 34: Experimental scene description [21]

In past study, Marco D. Comerchero and John Polich designed an oddball task and investigated P300 of different position. Fig. 2-34 summarizes the stimulus properties for the visual modalities. EEG activity was recorded during 2 blocks, each of which consisted of 350 stimulus presentations that lasted approximately 12 min. Stimuli were defined as target, non-target, and standard and presented with probabilities of 0.10, 0.10, and 0.80, respectively. Task conditions were defined according to the level of perceptual difficulty of the target/standard discrimination, such that for each modality subjects were presented with one Easy and one difficult condition. The task in all conditions was to respond to the target stimulus by pushing a mouse button with the right index finger as quickly and accurately as possible. Response time and error rates were recorded. All subjects were given a practice block consisting of 15 stimulus trials before each condition. Modality order was counterbalanced across subjects, but the Easy task was always presented first for each modality to promote successful task performance in the subsequent difficult condition.[21]

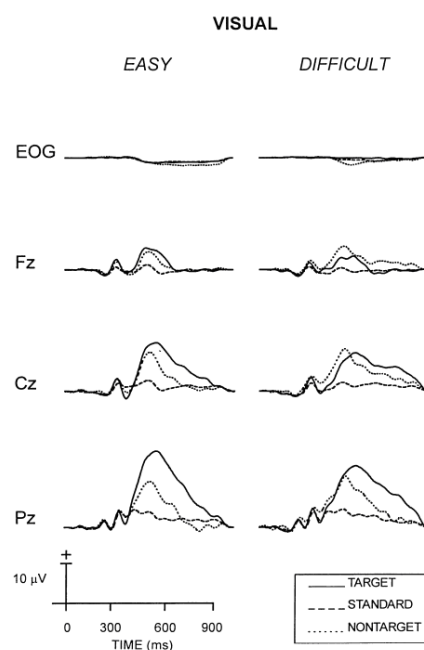


Fig. 2- 35: Grand averaged ERP from visual modalities for each task difficulty, stimulus type, and recording site (n = 16) [21]

Fig. 2-35 presents the grand average ERP from the target, standard, and non-target auditory and visual stimuli in the Easy and difficult task conditions. For the Easy tasks, target stimuli elicited P300 components that were largest at the parietal electrode. Non-target stimuli elicited P300 components that were similar in morphology to those elicited by target stimuli but with appreciably smaller amplitude across all electrode sites. For the difficult tasks, target stimuli elicited P300 components that exhibited smaller amplitudes and longer latencies than those from the Easy tasks. Non-target stimuli elicited P300 components that were larger and earlier at the frontal and central electrodes than those from the target stimuli. Target P300 amplitude was larger than the non-target amplitude at the parietal electrode.[21]

P300 scalp distribution is defined as the amplitude change over the midline electrodes (Fz, Cz, and Pz), which typically increases in magnitude from the frontal to parietal electrode sites (Johnson, 1993).[21] As Fig shown, we can get a conclusion of the amplitude of Pz is the largest, the medium amplitude is in Cz, and the smallest amplitude is in Fz.

In addition, what about the relationship between target-to-target interval and P300 amplitude? The following fig. presents the results. We can get information that no matter using TT, NT, NNT, or NNNT experiment, the major reason of deciding the P300 amplitude is target-to-target interval. And the largest amplitude detected in about 12-second target-to-target interval.

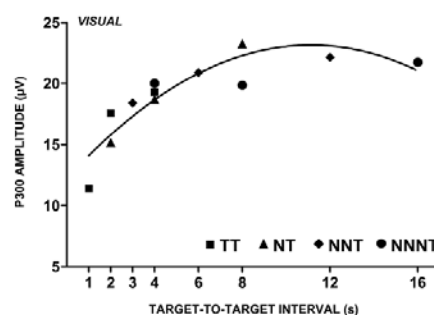


Fig. 2- 36: Relationship between P300 and target-to-target interval (TTI) [21]

As Fig. 2-36, P300 amplitude plotted as a function of target-to-target interval (TTI) for the target (T) stimulus in an oddball task across sequences of preceding non-target (N) standard stimuli. The legend defines the symbols used to depict various non-target and target sequences. The subject is instructed to respond only to the target stimulus. P300 amplitude increases independently of local sequence and global target probability. The regression lines reflect curvilinear best fit for a second order polynomial. Similar results have been found for the single-stimulus paradigm when only target stimuli are presented (Gonsalvez et al., 2007). Adapted from Gonsalvez and Polich (2002) with permission of the authors and Blackwell Publishing (Copyright 2002).[21]

To summarize the above researches, we get four important points: (1) oddball task includes standard stimulus and target stimulus, both inducing different amplitude of ERP, (2) P300 amplitude is larger in easy stimulus discrimination than difficult one, (3) the amplitude change over the midline electrodes (Fz, Cz, and Pz), which typically increases in magnitude from the frontal to parietal electrode sites, and (4) target-to-target interval also effect P300 amplitude. By referencing to these, we design an oddball experiment in this study and then also verify P300 pattern could be measured by our proposed system.

Chapter 3 Experiment Results and Discussion

In this chapter, we verify the reliability of our proposed EEG system step by step. In order to the whole multi-channels mobile and wireless EEG system is consisting of many independent modules which need to be verified respectively. The method of the whole system verification (Fig. 3-1) is mainly separated four sessions: (1) system verification of simulated signal, (2) circuitry and program test compared to reference system, (3) sensor basic test, and (4) performance test of sensors in Oddball task.

First, 16-channel EEG device is inputted simulated signals. Check the correlations in time and frequency domains from TXT file saved by back-end record program. The second, our proposed EEG acquisition circuitry and program is compared by reference system for comparison in time and frequency domains through three-action experiment. Next, dry and wet sensors would be respectively placed the surrounding positions on subjects' head to verify whether dry sensor is suitable for long-term monitoring and good convenience in our EEG system. Moreover, the four-action experiment verifies four kinds of characteristic performances in our EEG system. In this part, sensor would be verified the less difference between three subjects. Finally, two kinds of sensors are also really applied in Oddball task, and we verify the dry sensor indeed measures tiny EEG activity like Event-Related Potential (ERP) from ten subjects.

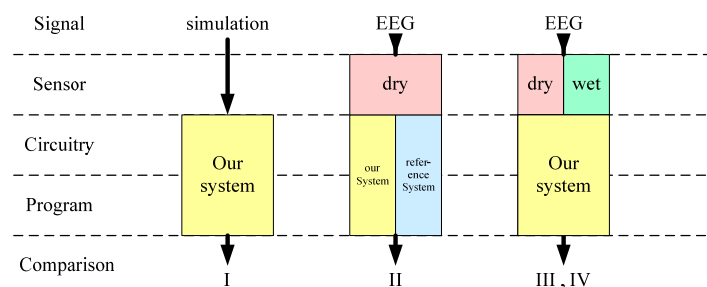


Fig. 3- 1: System verification overview

3.1 System Verification of Simulated Signals

The method for system verification of simulated signals is that our EEG acquisition circuitry catches standard simulated signals produced by function generator, and then the signals are amplified, filtered, and transmitted to back-end EEG display program via Bluetooth. We compare record data saved by program and standard simulated signals created by MATLAB. Analysis technique is computing data correlation in time and frequency domains respectively. By this way, we effectively get how good performance our EEG system can be.

3.1.1 Performance Test in Time Domain

As Fig. 3-2 shown, function generator produced 5Hz simulated signal to circuitry, and program received amplified digital data like blue curve. In addition, red curve created by MATLAB was standard 5Hz simulated signal. Fig. shows 20-second data and also masks computed time-domain correlation in each second. The results illustrate every one-second correlation is high above 99.5%.

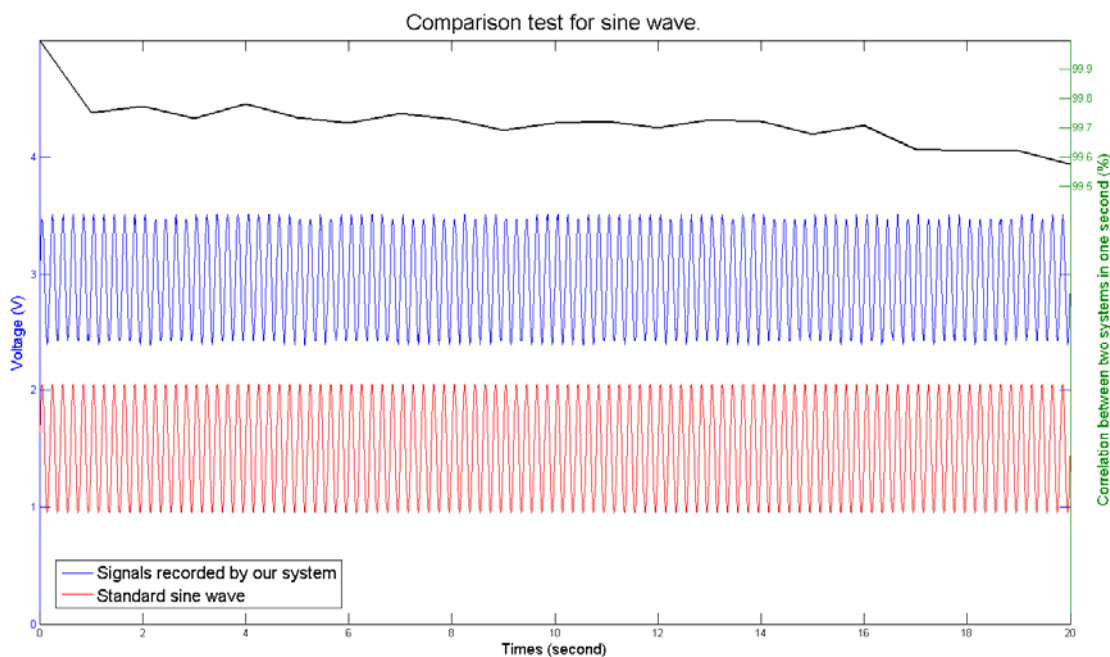


Fig. 3- 2: Result of 5Hz simulated signal test

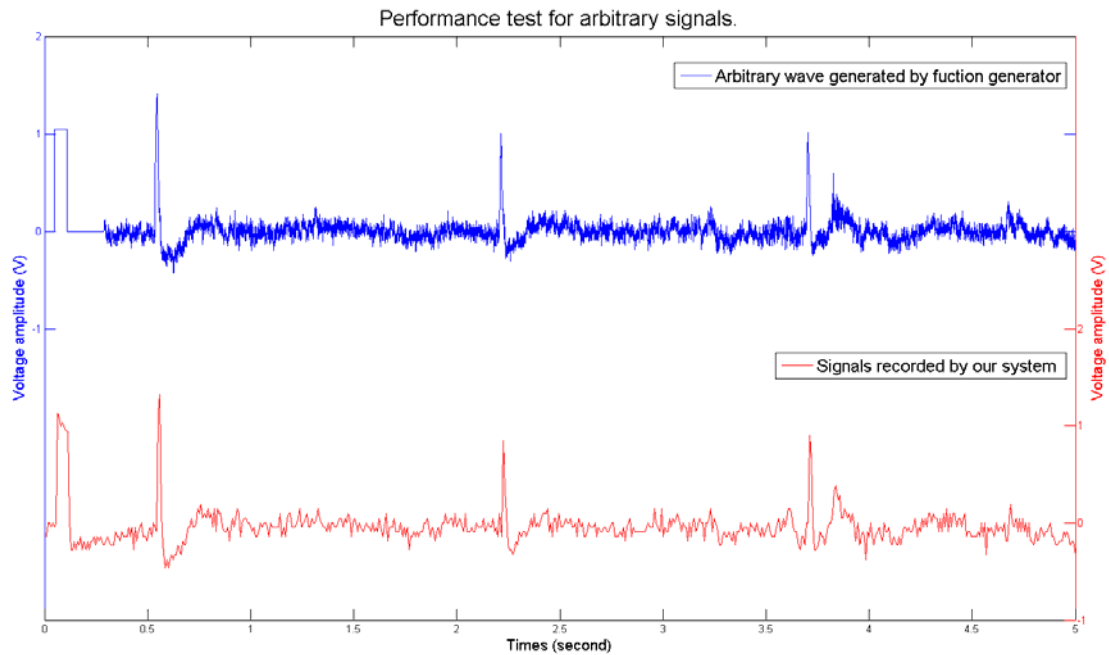


Fig. 3- 3: result of non-linear simulated signal test

Apart from the above-mentioned, we also tried to establish a non-linear simulated signal through function generator, and equally the signal was record by our program. To make a comparison between the pre-designed data and received data, we found out our proposed EEG system really record the features of certain non-linear signal in each time. Like Fig. 3-3, blue curve is pre-designed non-linear simulated signal, and red curve is record data by our system. Because of our system was created low-sampling rate of 125Hz, record data automatically filtered the noise over 125Hz. Hence, red curve is more clear than blue curve. Similarly, the result showed the best performance of simulated signal test in time domain.

3.1.2 Performance Test in Frequency Domain

We used function generator to produce 5Hz, 10Hz, 15Hz, and 20Hz simulated frequency respectively. Then FFT comparison verified the performance in frequency domain. As Fig. 3-4 shown, each specific frequency is correctly received by system.

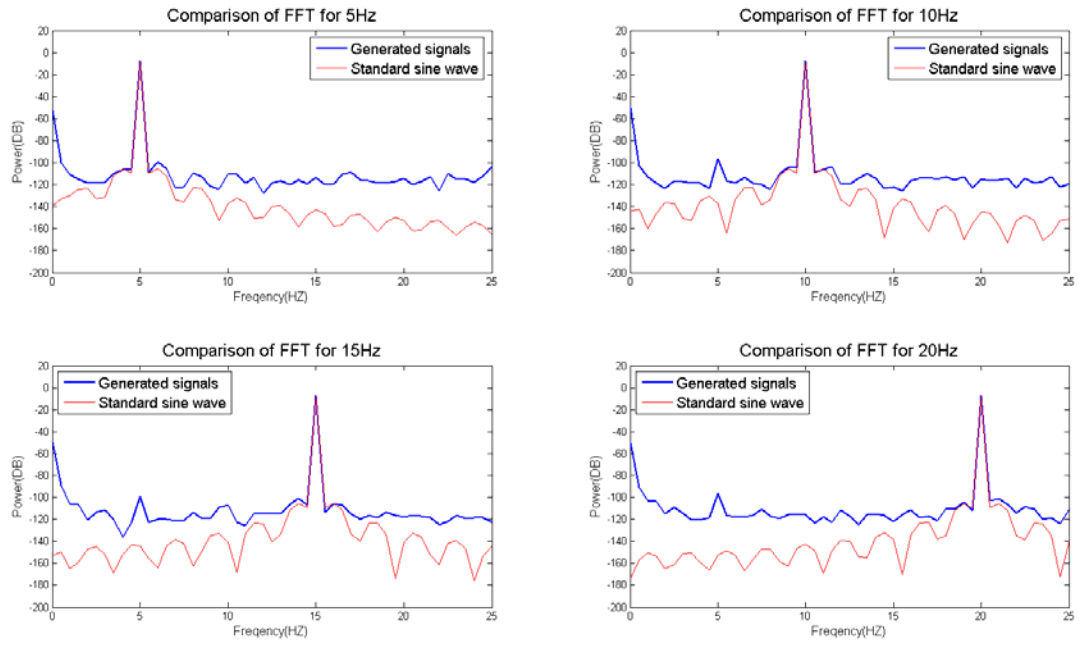


Fig. 3- 4: Results of different frequency test



3.2 Circuitry and Program test compared to reference system

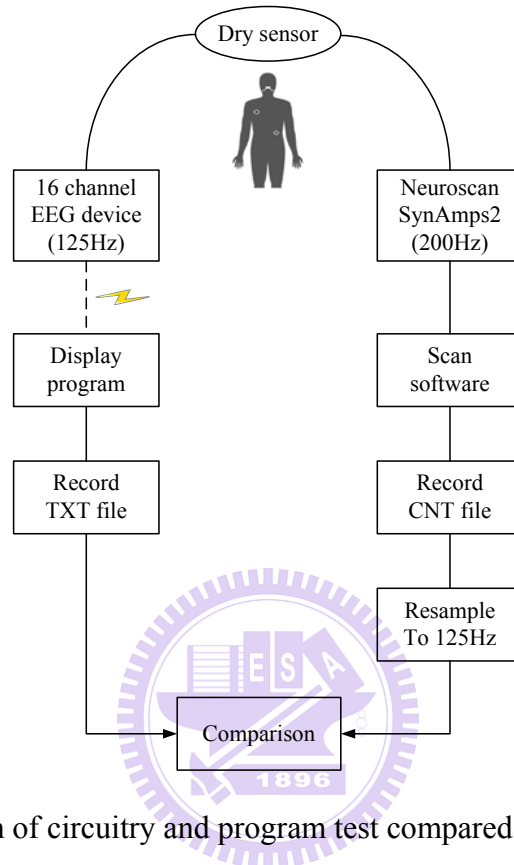


Fig. 3- 5: Diagram of circuitry and program test compared to reference system

The portable and wireless EEG acquisition circuitry and display program combine EEG preprocessing and recording data functions respectively. In advance, these could be compared with international standard EEG measurement instrument like Neuroscan system. Neuroscan system more or less includes electrode cap which need conductive gels, SynAmps2 amplifier, scan software. In this verification, we use the same sensor to make sure that the comparison can't be affect due to the difference of dry sensor and wet electrode. To choose dry sensor rather than wet electrode is in order to guarantee the performance results are not owing to wet electrode. Moreover, SynAmps2 owns itself specification of circuitry, and we can't get this detail information from Neuroscan Company. Besides, our proposed system receives data

via wireless path, but Neuroscan system receives data through wire path. Consequently the goal of verification just emerges the comparison results rather than how good performance among two systems.

Fig. 3-5 shows diagram of system comparison. Neuroscan SynAmps2 uses 200-Hz sampling rate to measure EEG activity, and our 16-channel EEG device use 125-Hz ones. The scan software interface provides menu to select suit sampling rate, so we select the most similar one- 200Hz. the file format of record data is different for two systems, but this problem could be improve in analysis stage. Before going to comparison, record data by Neuroscan system is first re-sampled to 125 Hz.

3.2.1 Participant

It is sufficient that only one subject participates the comparison test. This subject is a female. She is 24 years old and trends to have a large number of hairs.

3.2.2 Experiment Procedure and Presentation

Human brain emerges EEG activity mixing different frequencies in different pattern cognition state. Thus, we can take advantage of EEG unique characteristic to verify the system performance in different frequency band. In this experiment, we assigned the participant to behave three kinds of actions which are “Blink”, “Tooth”, and “Normal”. “Blink” action, which is referred to EOG signal, verifies the lower frequency band about 0.2 - 5 Hz. “Tooth” action, which is referred to EMG signal, verifies the higher frequency band about 10 – 25 Hz. “Normal” action verifies frequency band about 0.2 – 25 Hz. In this procedure of experiment, we required the participant to blink once per second within “Blink” command occurred, to grind the molar with uninterrupted within “Tooth” command occurred, and to do general action naturally within “Normal” command occurred. Among Normal state, EOG like eye-movement and EMG like muscle-movement at chin position are randomly

appeared to cover clear EEG signal. Thus, EOG and EMG are ordinary considered no-use activity and even interfering more important EEG feature in fact. However, system comparison in this experiment can use the characteristic of EOG and EMG to check lower and higher frequency bands respectively. Fig. 3-6 shows the space of experiment.



Fig. 3- 6: Experiment environment and setting view

Beginning of experiment, the participant sat on a chair motionlessly and was asked to keep facing on the front screen and followed occurred commands by presentation. The experiment includes four sections, each of about 10-minute duration. Each section includes thirteen trials, each of forty-five-second duration. The participant can take a rest among sections. Fig. 3-7 shows procedure of presentation in one trial.

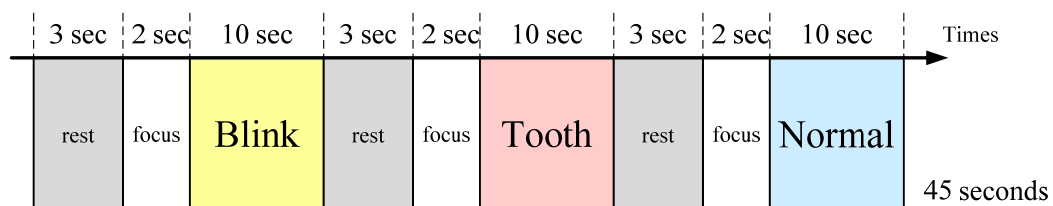


Fig. 3- 7: Experiment procedure in one trial

Referencing to 10-20 system (Guideline for Standard Electrode Position Nomenclature, 2006), we choose the edge and center positions (Fig. 3-8) to place dry sensor. The forefront side is FP1. The most left side is T3. The top side is CZ. The most right side is T4. The most behind side is OZ. In addition, the participant is also placed an electrode behind ear as reference potential and an electrode on G as ground potential. All the dry sensors are pressed by hands of the other person, because we do not find the better fixation to make the least motion artifact than manual pressing yet. The Operator has to force down the dry sensor stably to avoid the movement between sensor and skin as possible.

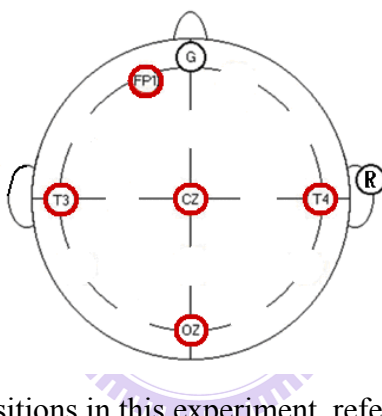


Fig. 3- 8: Sensor positions in this experiment, referring to 10-20 system

3.2.3 Method of Analysis

In time-domain analysis, we compute the correlation of 10-s signal within doing certain action in one trial. Then averaging the correlations for all trails and finding out the maximum correlation. Equally, in frequency-domain analysis, we compute the correlation of 10-s signal FFT in one trial and then find out average correlation and the maximum correlation. Finally, not only time-domain but frequency-domain get results for all sensor position, which are FP1, T3, CZ, T4 and OZ referenced to 10-20 system. In this experiment, SCAN software filtered 0~30Hz signals. Most of typical EEG activities focused on the frequency band below 25 Hz, thus we filtered and retain 0.2 –25 Hz EEG signal in off-line analysis by EEGLAB toolbox [25].

3.2.4 Experiment Results

The results as following are mainly separated three parts: (1) Blink action comparison results, (2) Tooth action comparison results, and (3) Normal action comparison results. In the following figures, “Generated signals” presented EEG data recorded by 16 channel device, and “Reference signals” presented EEG data recorded by Neuroscan system.

3.2.4.1 Blink Action Comparison Results

A. Time-Domain Correlations

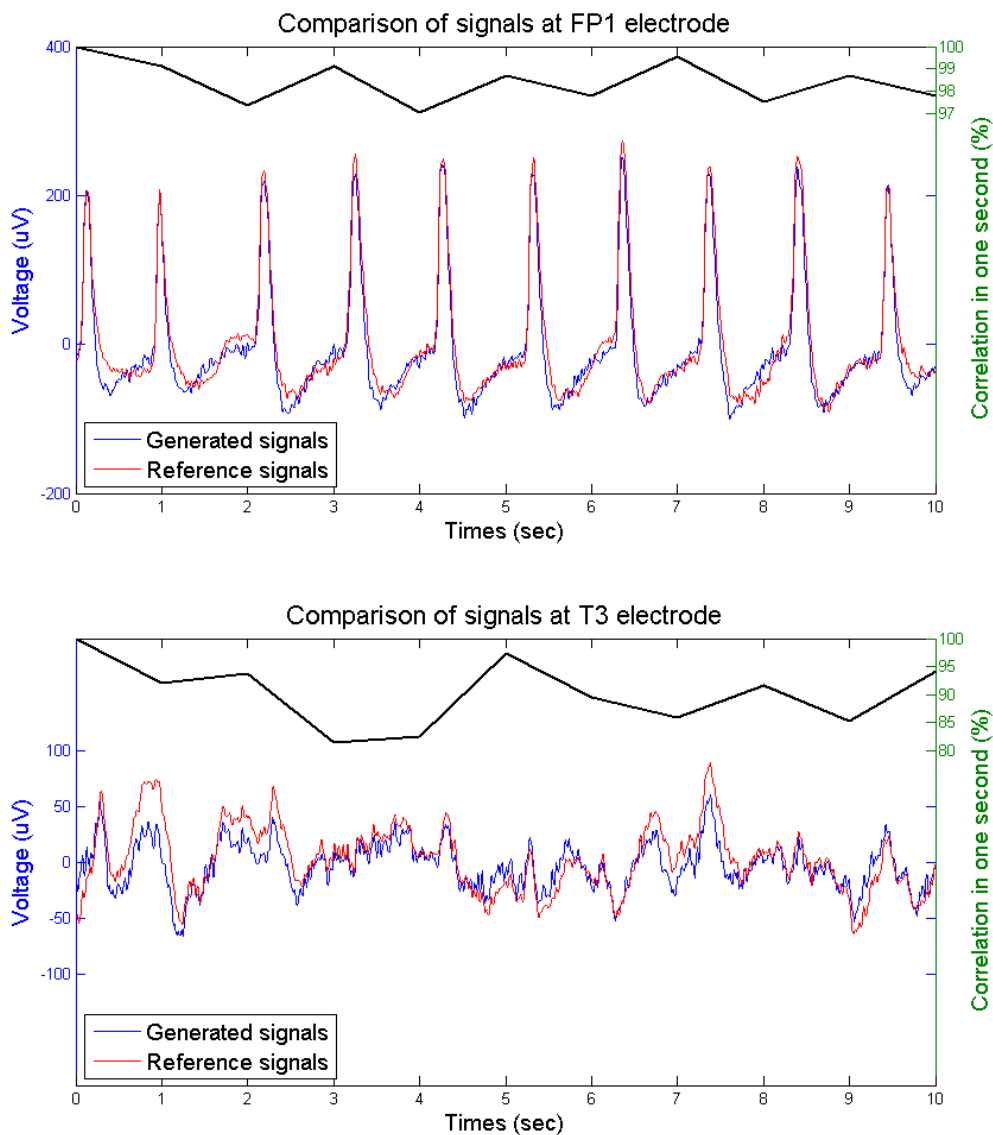


Fig. 3- 9: The best performance of time domain at FP1 (up) and T3 (down) within “Blink”

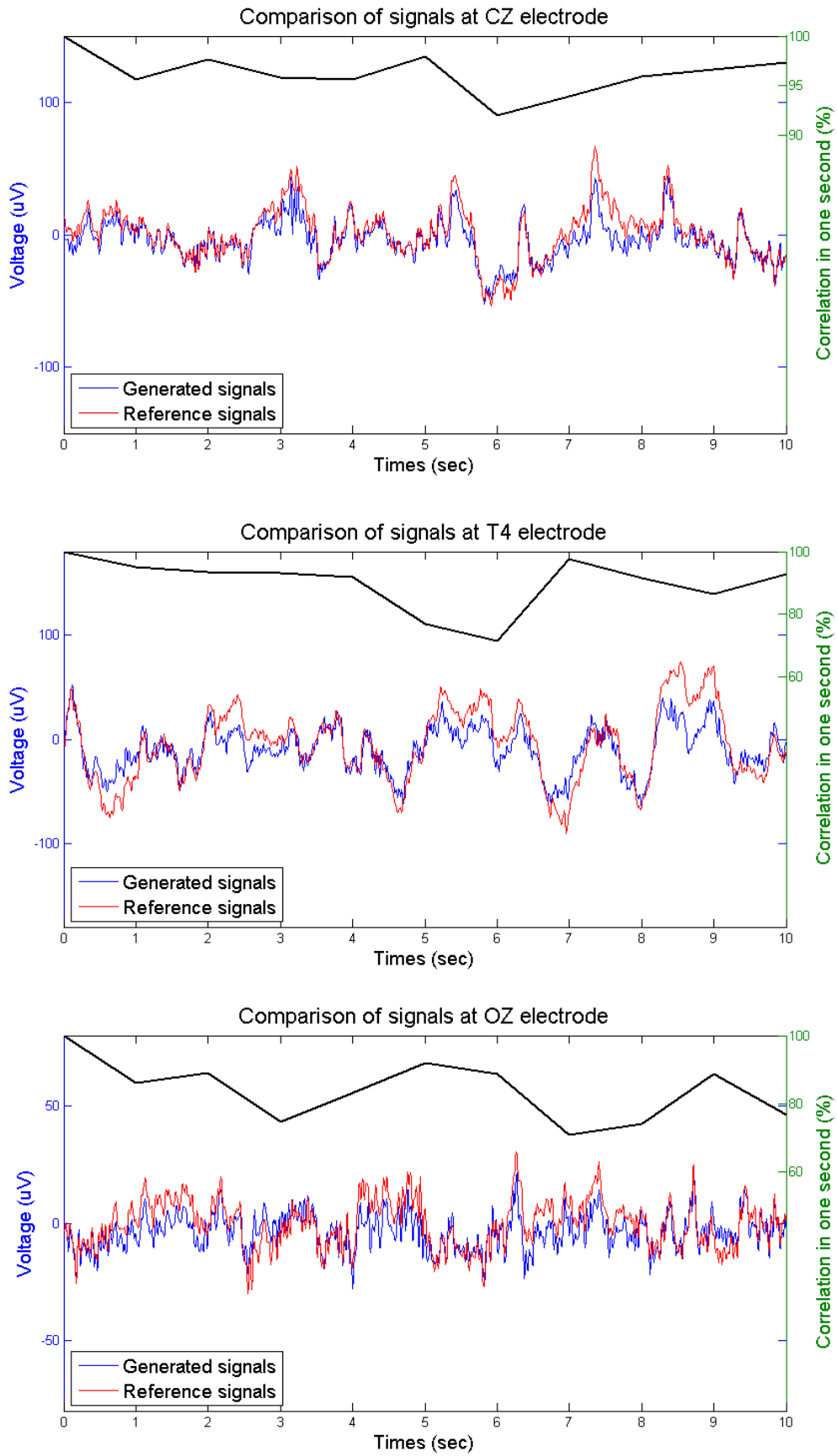


Fig. 3- 10: The best performance of time domain at CZ (up), T4 (mid), OZ (down) within “Blink”

Table 11: The maximum and average correlations of time domain at every position within “Blink”

Electrode place	10-s Max correlation (%)	10-s Average correlation (%)
FP1	98.20	97.56
T3	91.25	87.27
CZ	94.83	91.85
T4	91.46	89.09
OZ	83.72	79.03
Average	91.89	88.96

B. Frequency-Domain Correlations

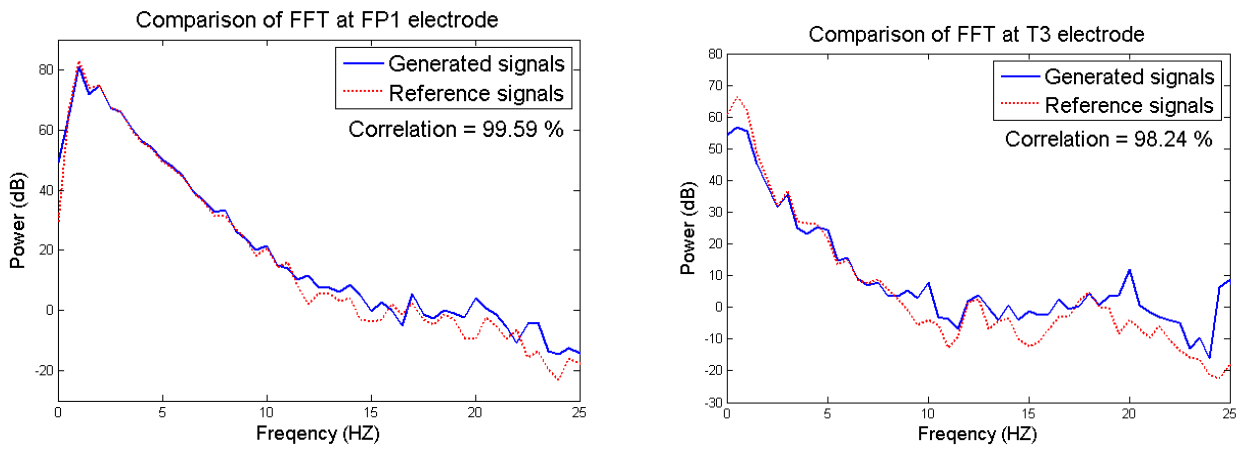


Fig. 3- 11: The best performance of frequency domain at FP1 (left), T3 (right) within “Blink”

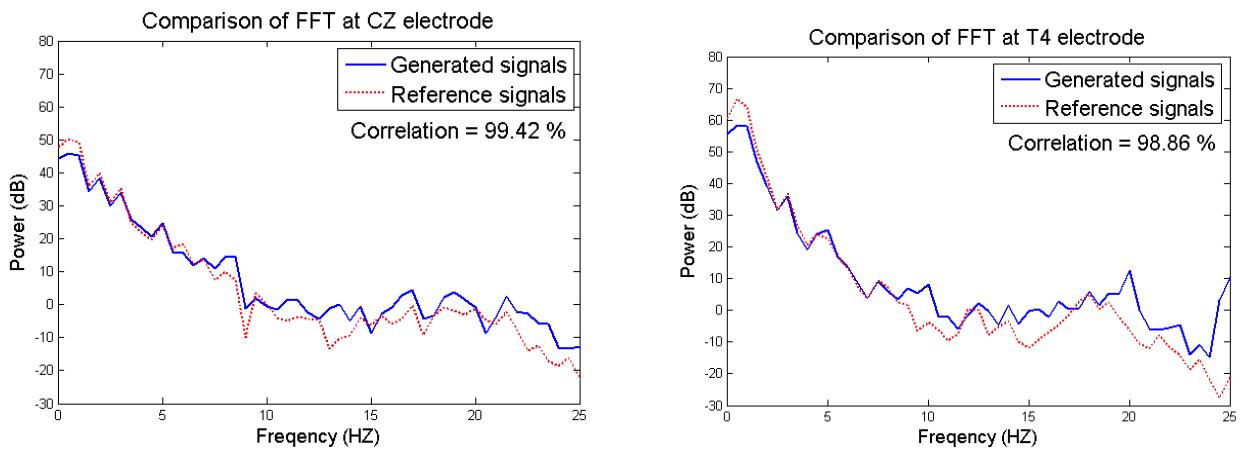


Fig. 3- 12: The best performance of frequency domain at CZ (left), T4 (right) within “Blink”

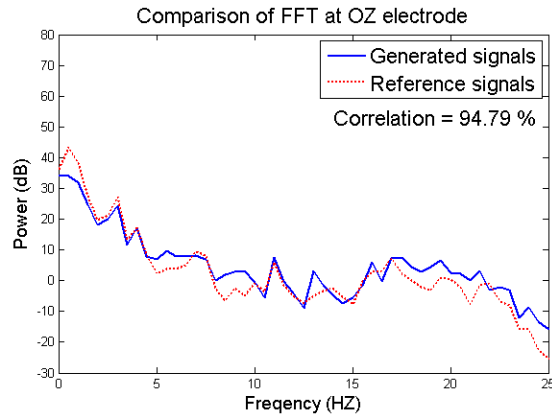


Fig. 3- 13: The best performance of frequency domain at OZ within “Blink”

Table 12: The maximum and average correlations of frequency domain at every position within “Blink”

Electrode place	10-s Max correlation (%)	10-s Average correlation (%)
FP1	99.59	99.40
T3	98.24	92.09
CZ	99.42	96.10
T4	98.86	94.56
OZ	94.79	88.20
Average	98.18	94.07

3.2.4.2 Tooth Action Comparison Results

A. Time-Domain

Correlations

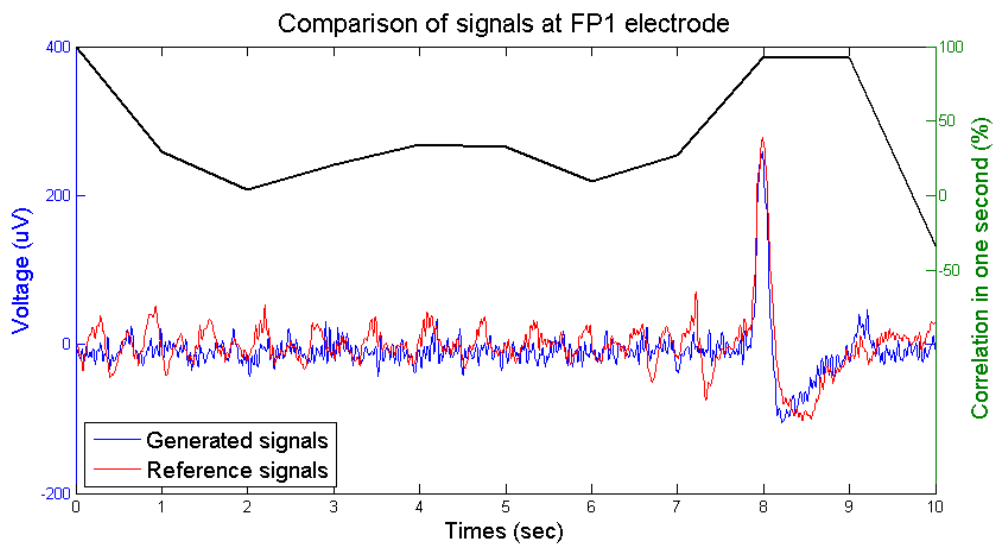


Fig. 3- 14: The best performance of time domain at FP1 within “Tooth”

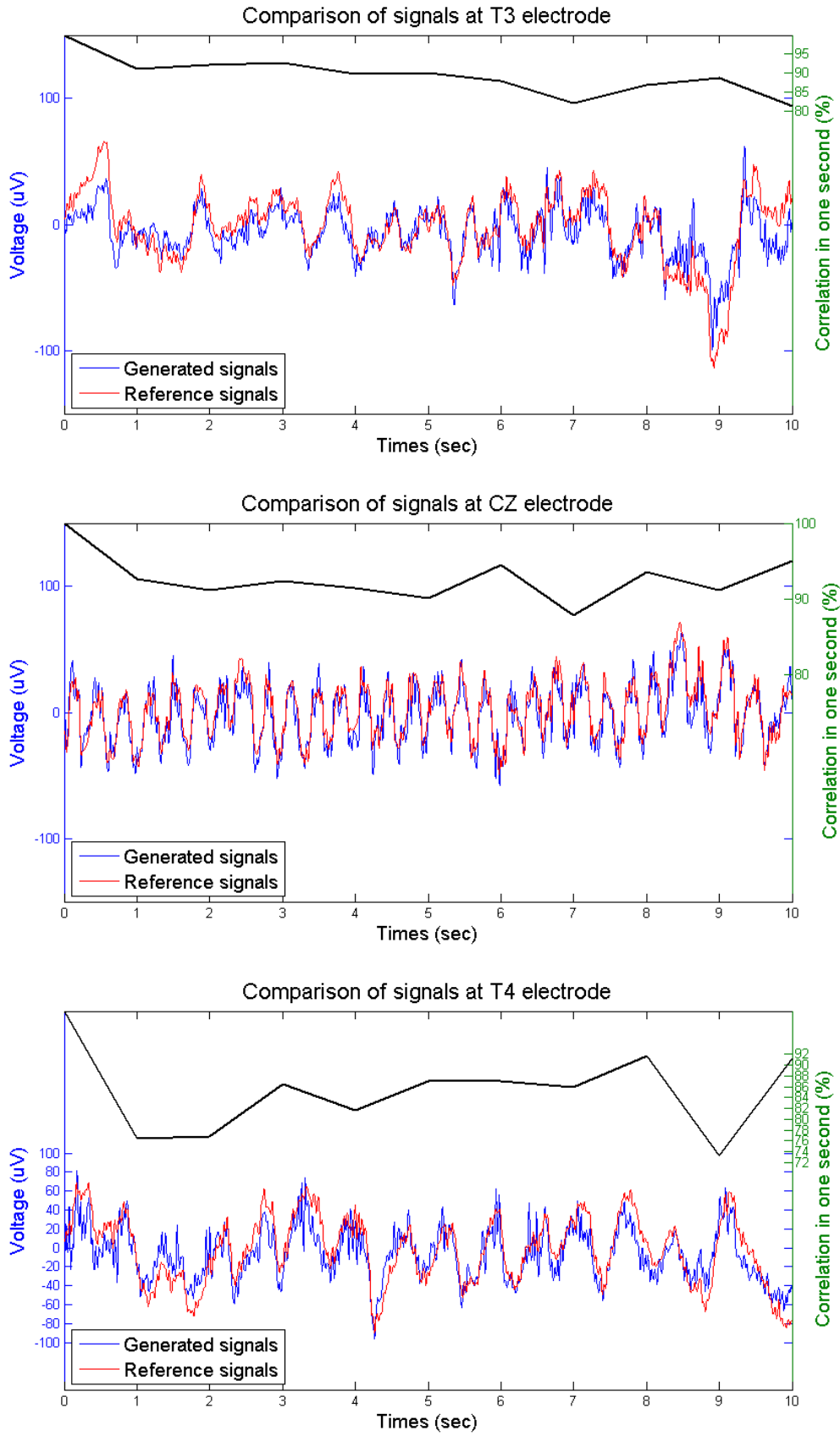


Fig. 3- 15: The best performance of time domain at T3 (up), CZ (mid), T4 (down) within “Tooth”

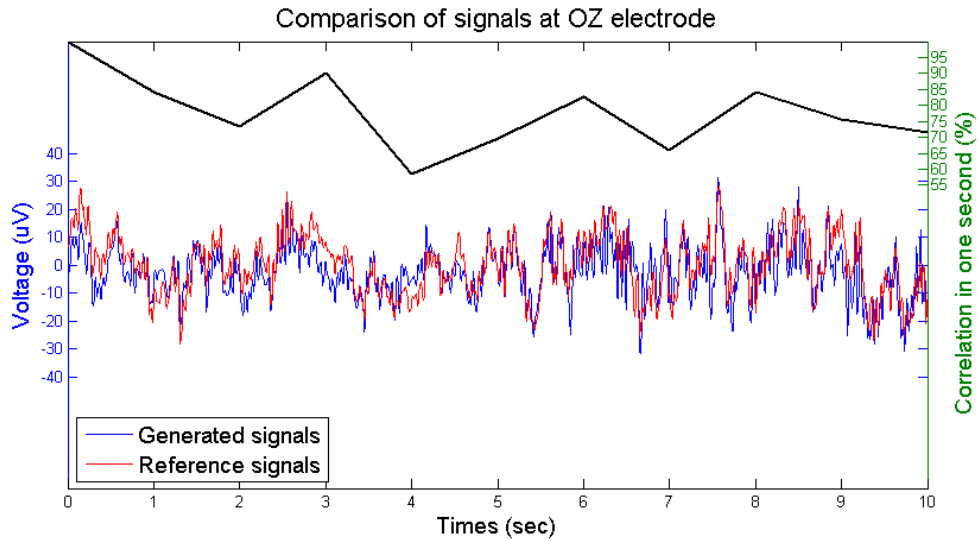


Fig. 3- 16: The best performance of time domain at OZ within “Tooth”

Table 13: The maximum and average correlations of time domain at every position within “Tooth”

Electrode place	10-s Max correlation (%)	10-s Average correlation (%)
FP1	83.34	42.69
T3	85.01	78.27
CZ	91.89	86.81
T4	85.13	82.73
OZ	77.70	69.26
Average	84.61	71.95

B. Frequency-Domain Correlations

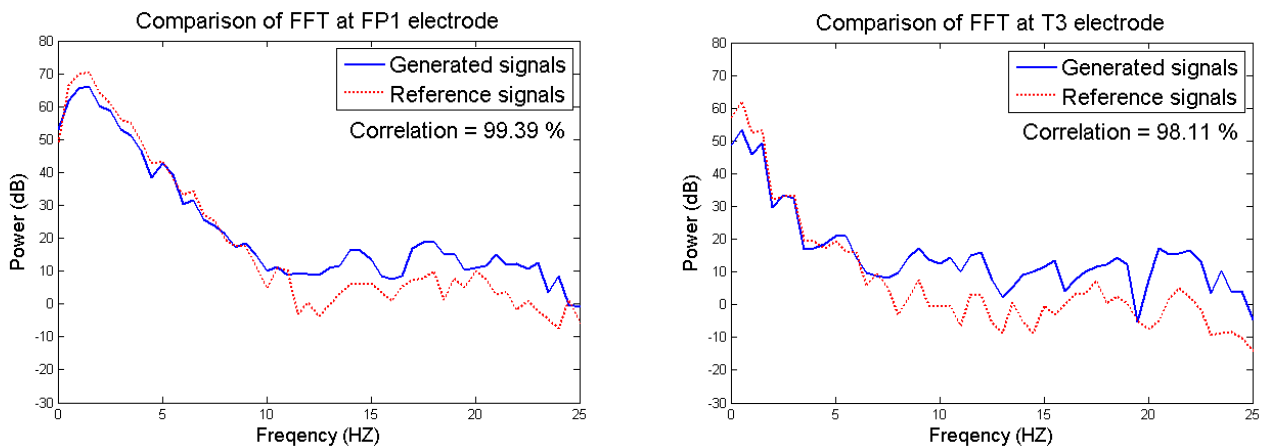


Fig. 3- 17: The best performance of frequency domain at FP1 (left), T3 (right) within “Tooth”

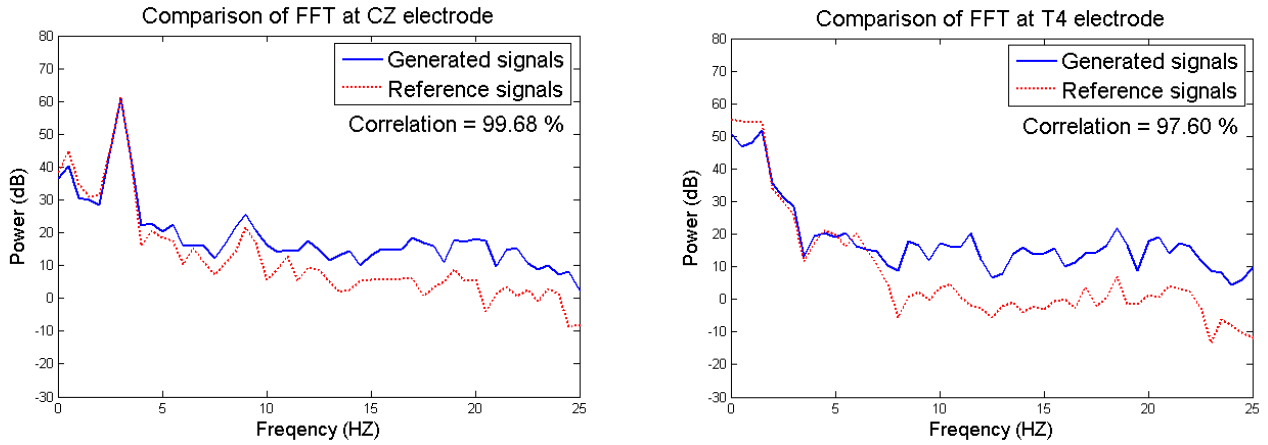


Fig. 3- 18: The best performance of frequency domain at CZ (left), T4 (right) within “Tooth”

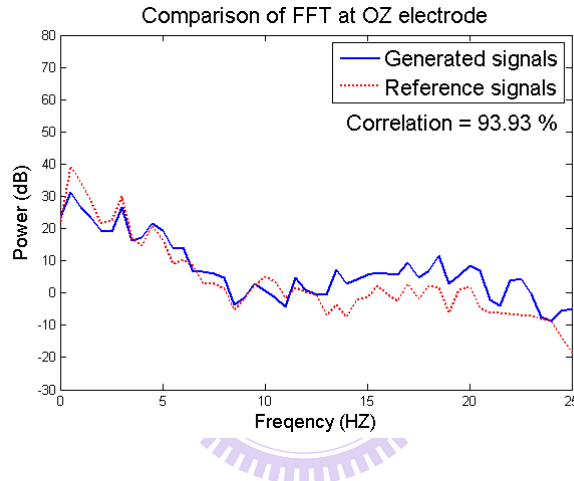


Fig. 3- 19: The best performance of frequency domain at OZ within “Tooth”

Table 14: The maximum and average correlations of frequency domain at every position within “Tooth”

Electrode place	10-s Max correlation (%)	10-s Average correlation (%)
FP1	99.39	55.32
T3	98.11	90.87
CZ	99.68	95.64
T4	97.60	87.64
OZ	93.93	82.91
Average	97.74	82.48

3.2.4.3 Normal Action Comparison Results

A. Time-Domain Correlations

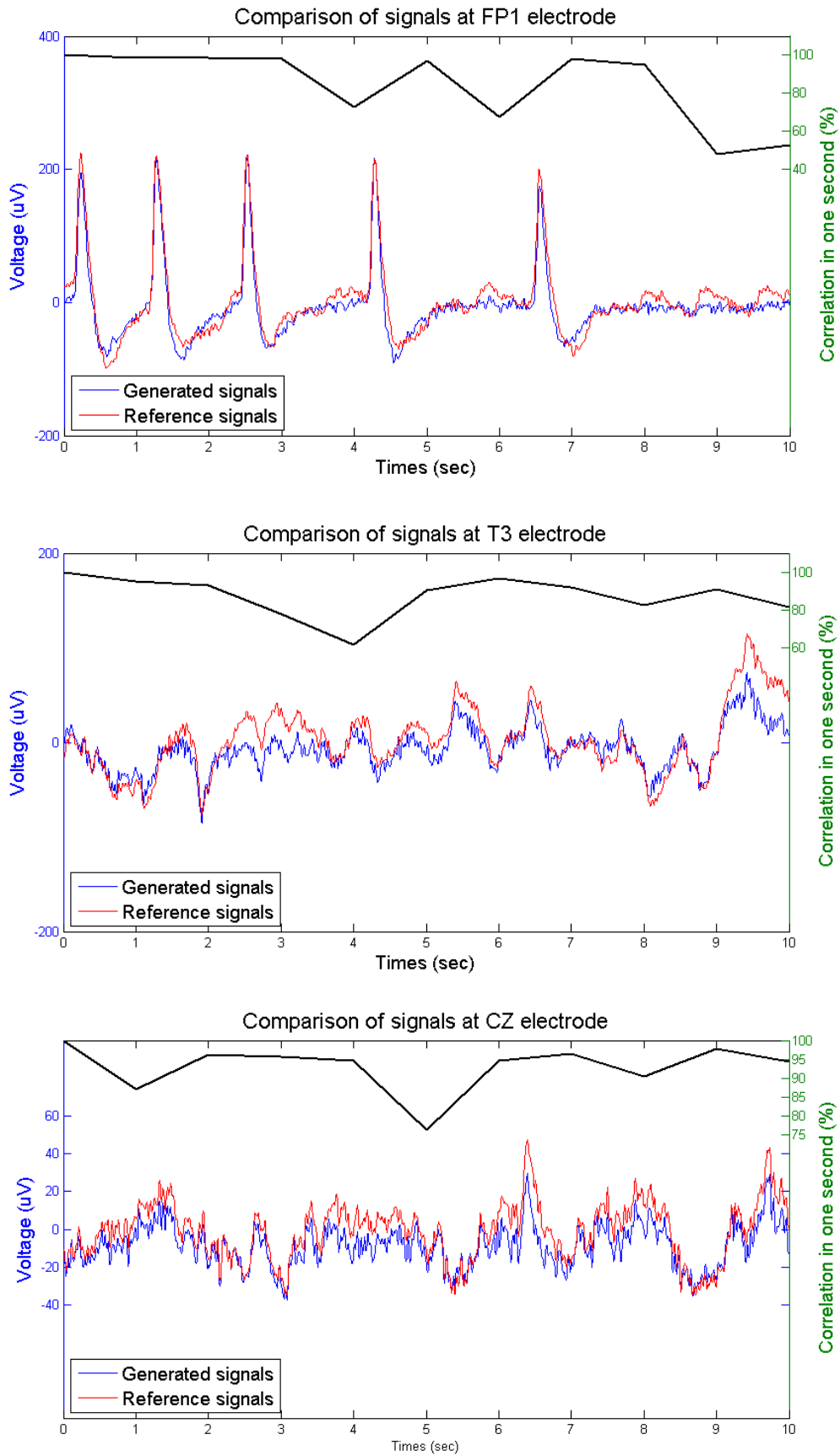


Fig. 3- 20: The best performance of frequency domain at FP1 (left), T3 (mid), CZ (down) within “Normal”

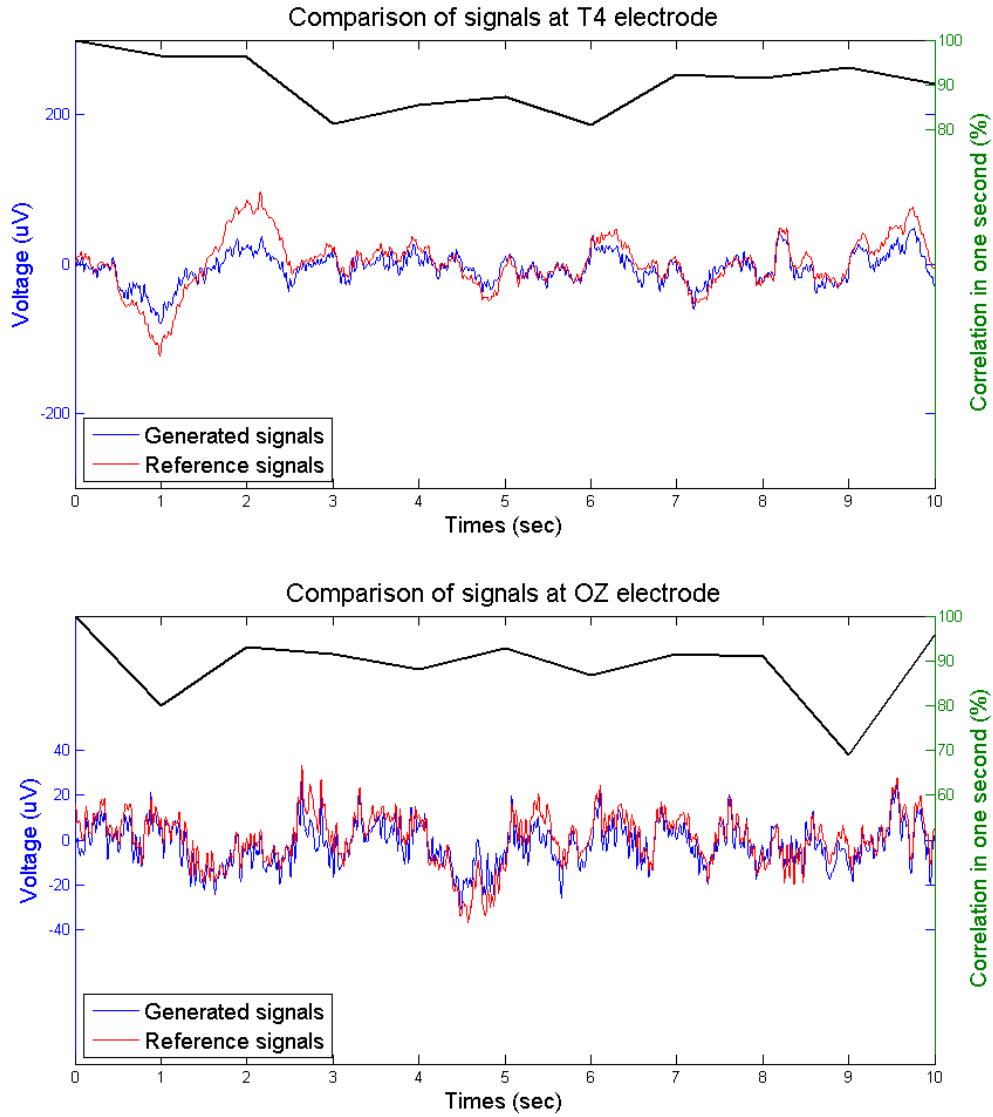


Fig. 3- 21: The best performance of time domain at T4 (up), OZ (down) within “Normal”

Table 15: The maximum and average correlations of time domain at every position within “Normal”

Electrode place	10-s Max correlation (%)	10-s Average correlation (%)
FP1	96.75	93.01
T3	90.46	86.80
CZ	94.48	91.82
T4	90.08	88.19
OZ	88.98	81.87
Average	92.15	88.34

B. Frequency-Domain Correlations

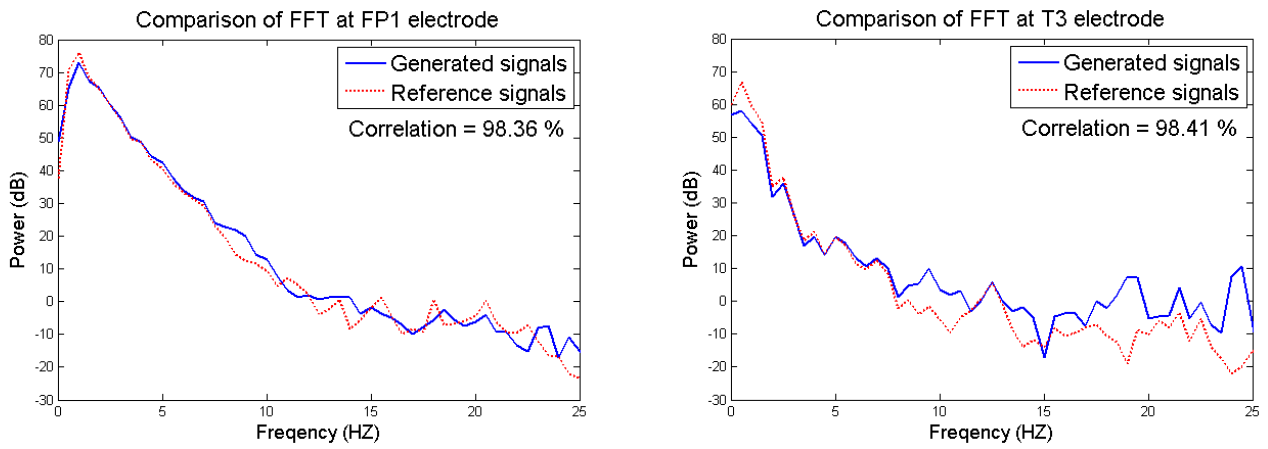


Fig. 3- 22: The best performance of frequency domain at FP1 (left) and T3 (right) within “Normal”

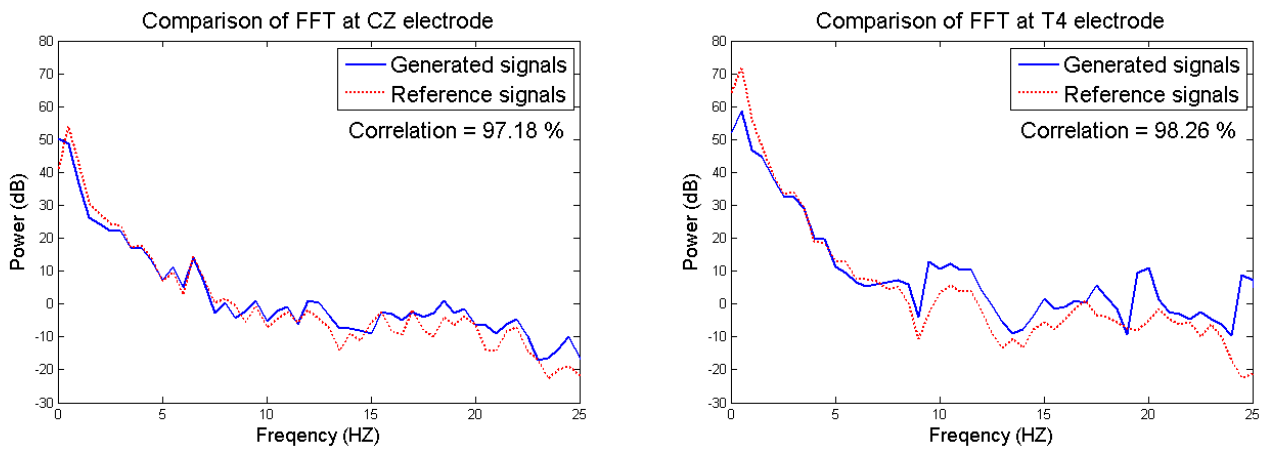


Fig. 3- 23: The best performance of frequency domain at CZ (left), T4 (right) within “Normal”

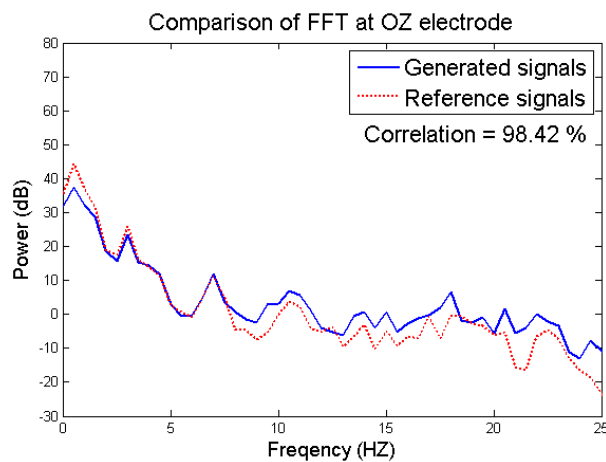


Fig. 3- 24: The best performance of frequency domain at OZ within “Normal”

Table 16: The maximum and average correlations of frequency domain at every position within “Normal”

Electrode place	10-s Max correlation (%)	10-s Average correlation (%)
FP1	98.36	96.53
T3	98.41	94.89
CZ	97.18	89.08
T4	98.26	95.44
OZ	98.42	88.69
Average	98.13	92.93

3.2.5 Discussion

A. Blink Action State

FP1 and CZ position are all found out obvious eye-movement signal, which is also called EOG. FP1 placed in forehead is generally used to recognize EOG. For time-domain results, due to a typical blink having the amplitude of 400uV, the time correlations are high in FP1. EOG signal is measured not only by FP1 but also by CZ because of signal transmitting to other position along forehead to occipital. However, the process of signal transmitting decreases the amplitude gradually. Thus, OZ almost could not measure any EOG signal. Besides, the amplitude of signal measured by OZ is very tiny about 50uV, so the average temporal correlation is the smallest one compared to other channel positions. For frequency-domain results, due to normal human brain generally having nearly 200 – 400 ms of blink duration for one blink, EOG makes high power for the frequency band around 2.5 – 5Hz. As Fig. 3-11 (left) shown, FP1 measured 50 – 70dB power for 2.5 – 5 Hz within Blink action and only measured 40 – 60 dB power within Tooth action (Fig. 3-17 (left)). In sum of the results of Blink action, we account our system can monitor good signal quality of low frequency for the whole head in time and frequency domains.

B. Tooth Action State

Five sensor positions all measured high-frequency noise, produced by muscle tension and also called EMG. For time-domain correlations, we find the signal monitored by each channel not only combined EMG but shacked by frequency around 2 – 4 Hz. we preliminary judge the result coming from the motion-artifact of dry sensor. When the participant regularly grinded the tooth, dry sensor placed on her head moved itself position regularly in the same time. Moreover, the high-frequency activity changing very fact, thus the signals in FP1 and T3 are bad average correlations even though good in frequency domain. For frequency-domain results, it is obvious to observe that the power in frequency band of 10 – 20 Hz is higher than the corresponding power for the same frequency band within Blink action stage. This results also verify our system is indeed monitoring high frequency around 10 - 25 Hz. Although the average frequency-domain correlation is not high, it is just due to different specification between our system and Neuroscan system. Because of a 0-30 Hz filtering preprocessing of SCAN acquisition software, the recorded EEG data of Neuroscan system is not sensitive for high frequency. Hence, although it is the same process for recorded data in off-line analysis, there is the different frequency response in high frequency band.

C. Normal Action State

The whole signals in Normal action state include less EOG and EMG signals and more clear EEG activity compared to Blink and Tooth action state, so that we refer the signal can be represent for normal application in dairy life and for cognitive experiments. Fig. 3-25 shows three-action correlation comparisons in time and frequency domain. The results show average time-domain correlation is 88.34% and average frequency-domain correlation is 92.93%. For time-domain correlations, Normal state is worse than Blink state owing to the higher amplitude of blinking.

Normal state is better than Tooth state as a result of the high-frequency shaking signal of muscle tension. For frequency domain, Normal state has also the medium comparison result among Blink state and Tooth result.

All in all, this circuitry and program test finally explains no matter what action occurs our system can really record EEG activity as good for standard measurement instrument like Neuroscan system.

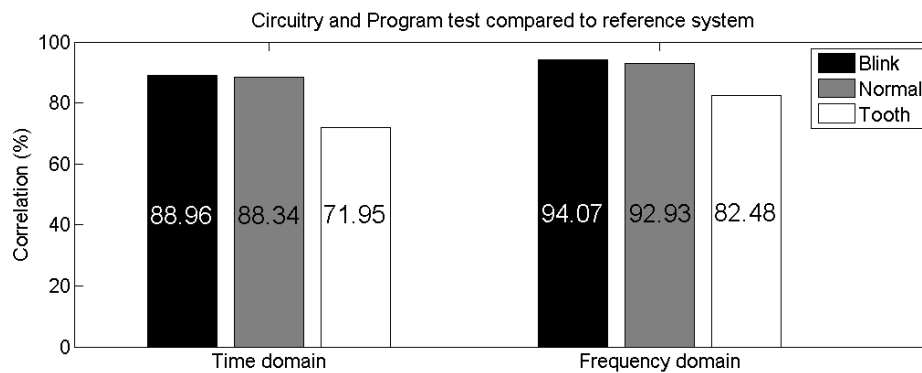
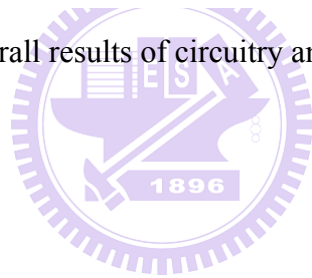


Fig. 3- 25: overall results of circuitry and program test.



3.3 Sensor Basic Test

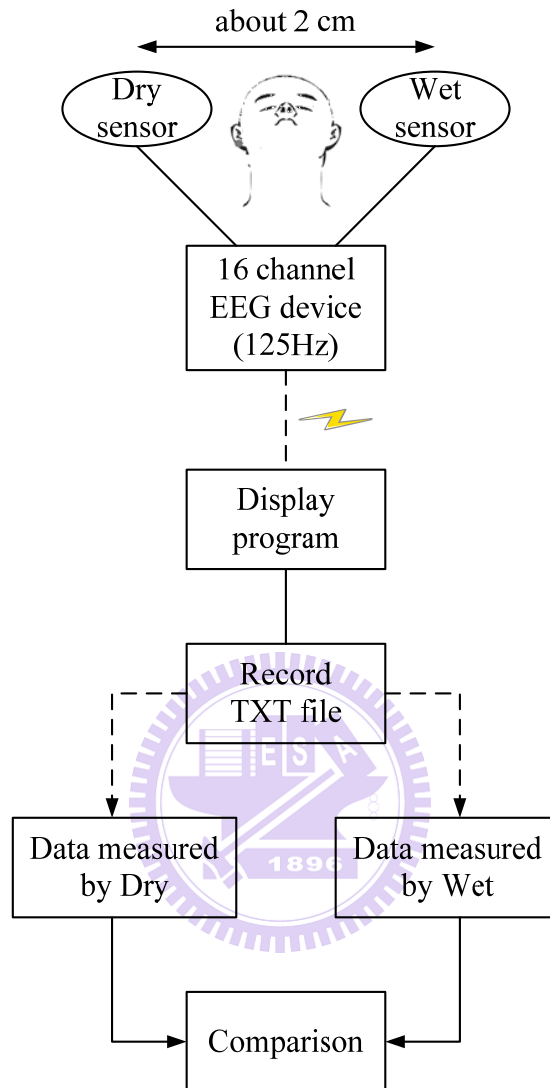


Fig. 3- 26: Diagram of sensor basic test

After the circuitry and program system comparison, we verify how good performance dry sensor has as possible as it can. Thus, we design the verification procedure as the diagram of Fig. 3-26. The participant was placed day sensor and wet sensor with about 2-cm distance. Both of sensors simultaneously monitored EEG activity, and transmitted the signal to two inputs of 16-channel mobile and wireless circuitry. The circuitry sampled signal with 125Hz of rate, and then carried it to back-end program via wireless communication interface. In analysis process, we

extracted one channel data measured by dry sensor and the other channel measured by wet sensor to compare the performance in time and frequency domain respectively.

In addition, we follow above experiment using verify the circuitry and program, and include close eye for one of actions to verify the performance of dry sensor monitoring alpha wave in this experiment. We expect to check this dry sensor whether eliminating the difference of measurement quality for many subjects or not, and furthermore, in which frequency band the measurement quality is the best and how good it is are the issues we concern.

3.3.1 Participant

Three participants are invited to go in this experiment. Two males and one female are about 20-23 years old. One of them has the thinner and general number of hairs in head, one has general number of hairs in head, and the other has the thicker and less number of hairs in head. The participants owns different characteristic of hair to each other, hence it is good for us to test the reliability of our system.

3.3.2 Experiment Procedure and Presentation

In this experiment, we assigned the participant to behave four kinds of actions which are “Blink”, “Close”, “Tooth”, and “Normal”. “Blink” action, which is inducing EOG signal, verifies the lower frequency band about 0.2 - 5 Hz. “Close” action, which is inducing alpha wave easily, verifies the medium frequency band about 8 – 13 Hz. “Tooth” action, which is referred to EMG signal, verifies the higher frequency band about 10 – 25 Hz. “Normal” action verifies frequency band about 0.2 – 60 Hz. In this procedure of experiment, we required the participant to blink once per second within occurring “Blink” command duration, to close eyes and relax within occurring “Close” command duration until the alert voice produced, to grind the molar with uninterrupted within occurring “Tooth” command duration, and to do

general action naturally within occurring “Normal” command duration. Among Normal state, EOG like eye-movement and EMG like muscle-movement at chin position are randomly appeared to cover clear EEG signal. Thus, EOG and EMG are ordinary considered no-use activity and even interfering more important EEG feature in fact. However, sensor verification in this experiment can use the characteristic of EOG and EMG to check lower and higher frequency bands respectively.

The experiment is going in general environment. Although most of cognitive experiments are executed in electromagnetic-shielded space, our system purpose to apply in daily life. Fig. 3-27 shows the space of experiment.



Fig. 3- 27: Experiment environment of sensor basic test

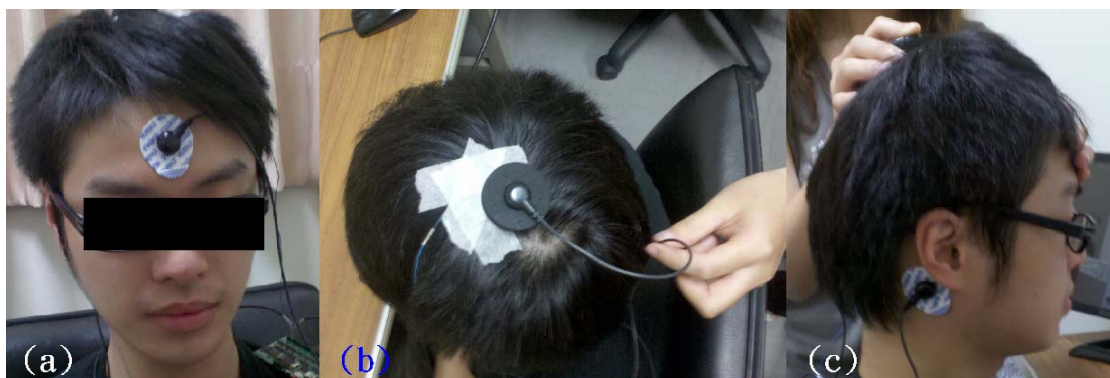


Fig. 3- 28: The view of sensor placement. (a) Ground, (b) Dry sensor and wet sensor, (c) Reference

Beginning of experiment, the participant sat on a chair motionlessly and was asked to keep facing on the front screen and followed occurred commands by presentation. The experiment includes four sections, each of about 12-minute duration. Each section includes thirteen trials, each of seventy-second duration. The participant can take a rest among sections. Fig. 3-29 shows procedure of presentation in one trial.



Fig. 3- 29: The procedure of sensor basic test in one trial

Referencing to 10-20 system (Guideline for Standard Electrode Position Nomenclature, 2006), we choose the edge and center positions (Fig. 3-28, 3-30) to place dry sensor. The forefront side is FP1. The most left side is T3. The top side is CZ. The most behind side is OZ. In addition, the participant is also placed an electrode behind ear as reference potential and an electrode on G as ground potential. All the dry sensors are pressed by hands of the other person (operator), because we do not find the better fixation to make the least motion artifact than manual pressing yet. The Operator has to force down the dry sensor stably to avoid the movement between sensor and skin as possible.

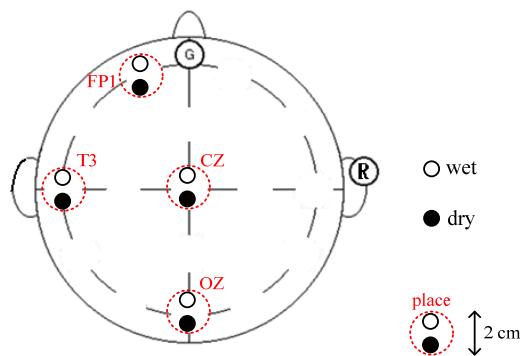


Fig. 3- 30: Positions of dry sensor and wet sensor in sensor basic test

3.3.3 Method of Analysis

The method of analysis is mainly parted two sections which are time-domain analysis and frequency-domain analysis. Before analysis beginning, we have to preprocess raw data recorded in TXT file. The preprocessing step is only one, which is rejecting no-use data. Due to dry sensor needing not conductive gels to maintain the stable impedance between sensor and skin in the brain, dry sensor has the opportunity to contact badly with the skin. As the following Fig. 3-31, we reject this data owing to voltage saturation and high impedance which is just like floating. The plunger of dry sensor is flexible in travel distance. It is possible to make capacitance effects that operator forces down the sensor in travel distance. If the sensor is not stably fixing on the skin site, there is floating data recorded by our system.

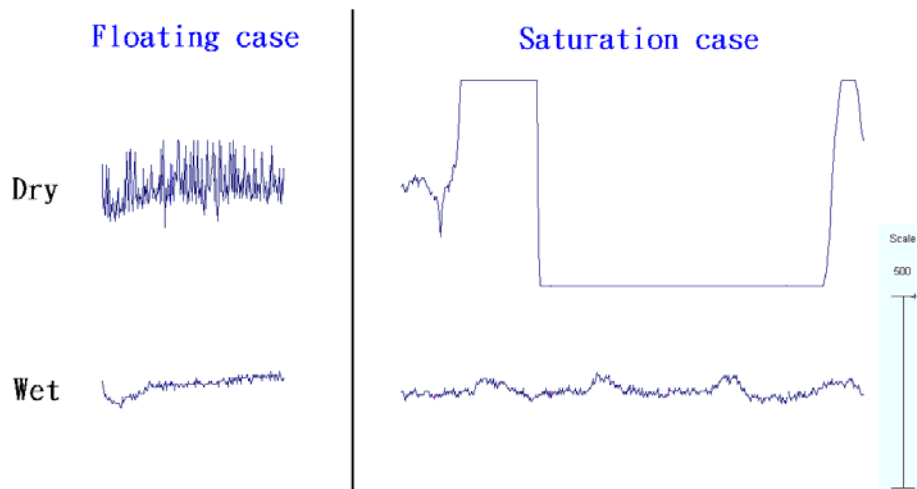


Fig. 3- 31: No-use data for floating case and saturation case

Fig. 3-32 shows the procedure diagram of analysis. First, compute all data temporal correlation for the data measured by dry and wet sensor in certain position. Next, divide the whole data to four parts toward corresponding action type. On the other word, the whole data combining four actions EEG data, and we part it to “Blink”, “Close”, “Tooth”, and “Normal” data. After time-domain analysis, in frequency domain, we analyze the FFT correlations result for each trial data. This

method finally gets eight results for each trial data induced by the same action: (1) temporal correlations for all time, (2) FFT correlation for all time, (3) 0-30-Hz FFT correlation, (4) 30-60-Hz FFT correlation, (5) FFT correlation of Delta band, and (6) FFT correlation of Theta band, (7) FFT correlation of Alpha band, and (8) FFT correlation of Beta band. Here, we just get the results of one trial. By computing all the trial data, we average the data of all the trial and get the final eight correlations for the same action.

The data got from different positions pass through average process. The record EEG data of three participants are all computed in this analysis process. In the end of analysis, the results considering different subjects and different positions are presented in the following session.

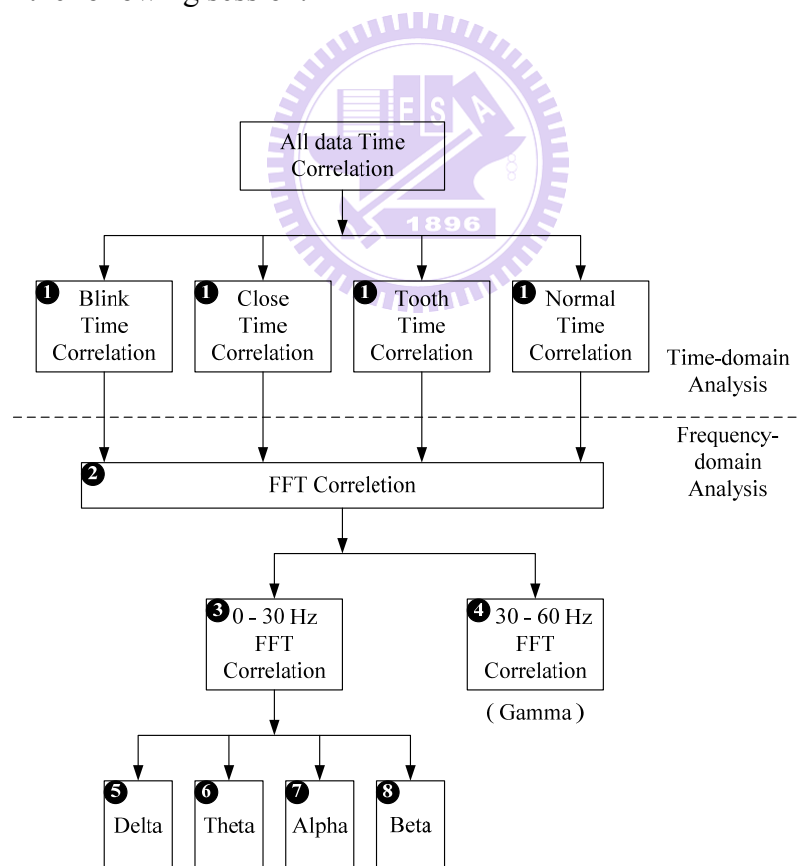


Fig. 3- 32: Diagram of analysis method in sensor basic test

3.3.4 Experiment Results

A. Results after Averaging All Subjects and All Positions

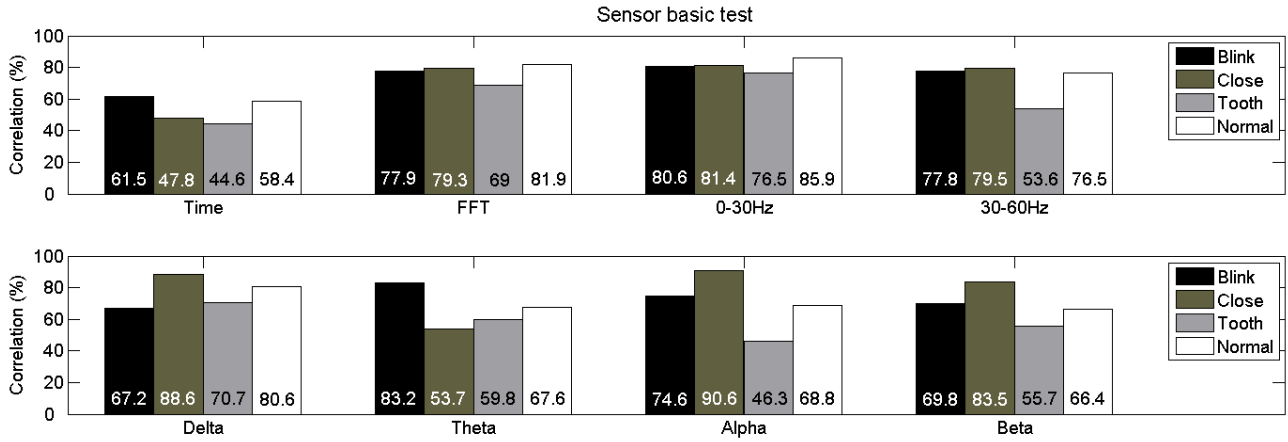


Fig. 3- 33: Overall results of sensor basic test

Table 17: Analysis results of Blink in sensor basic test

Blink	Time	FFT	0-30Hz	30-60Hz	Delta	Theta	Alpha	Beta
Subject 1	50.9	65.7	69.3	80.9	47.9	78.5	76.0	77.7
Subject 2	73.9	80.4	84.4	87.0	70.5	87.4	81.2	77.4
Subject 3	59.9	87.5	88.2	65.5	83.4	83.9	66.5	54.2
Average	61.5	77.9	80.6	77.8	67.2	83.2	74.6	69.8

Table 18: Analysis results of Close in sensor basic test

Close	Time	FFT	0-30Hz	30-60Hz	Delta	Theta	Alpha	Beta
Subject 1	46.4	69.0	74.5	77.3	86.9	53.5	91.3	90.4
Subject 2	59.2	80.7	80.8	87.7	87.1	59.0	97.6	79.6
Subject 3	37.8	88.2	90.0	73.5	91.7	48.5	82.8	80.5
Average	47.8	79.3	81.4	79.5	88.6	53.7	90.6	83.5

Table 19: Analysis results of Tooth in sensor basic test

Tooth	Time	FFT	0-30Hz	30-60Hz	Delta	Theta	Alpha	Beta
Subject 1	48.5	56.3	65.0	44.7	57.9	64.0	60.0	58.9
Subject 2	46.0	83.0	88.1	58.5	81.6	73.2	48.2	55.2
Subject 3	39.2	67.8	76.4	57.6	72.7	42.1	30.5	53.0
Average	44.6	69.0	76.5	53.6	70.7	59.8	46.3	55.7

Table 20: Analysis results of Normal in sensor basic test

Normal	Time	FFT	0-30Hz	30-60Hz	Delta	Theta	Alpha	Beta
Subject 1	54	67.7	75.3	74.6	67.5	58.9	79.5	77.7
Subject 2	68.8	87.7	91.4	89.7	88.3	74.3	56.6	62.2
Subject 3	52.4	90.3	90.9	65.0	85.9	69.8	70.4	59.2
Average	58.4	81.9	85.9	76.5	80.6	67.6	68.8	66.4

B. The Best Trial Data in Blink Action

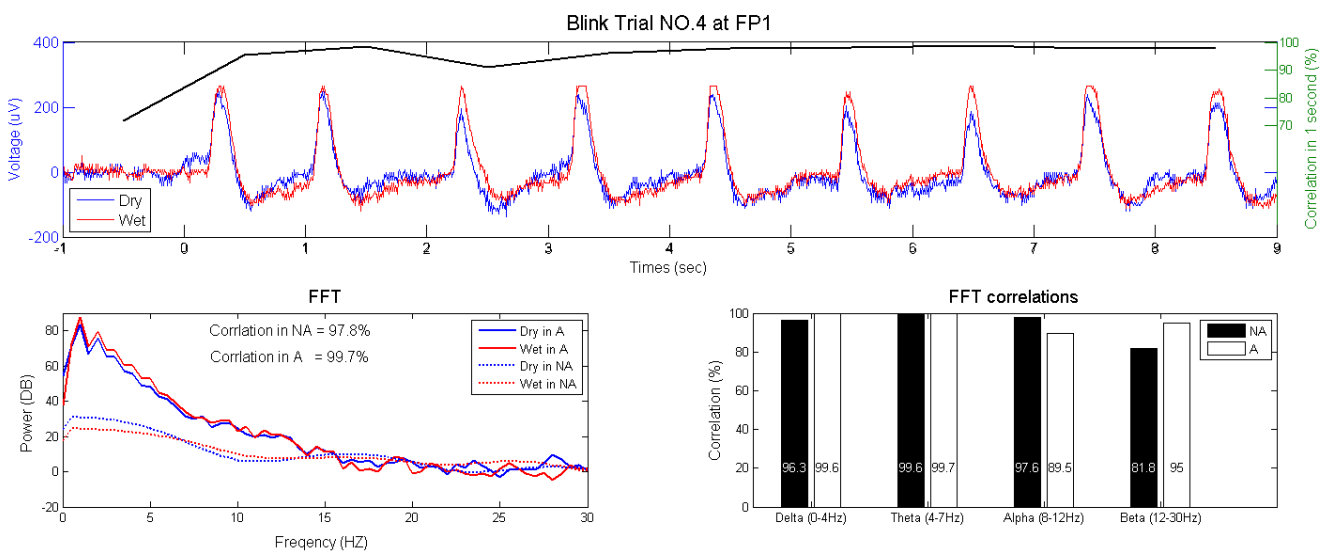


Fig. 3- 34: The best performance of Blink at FP1

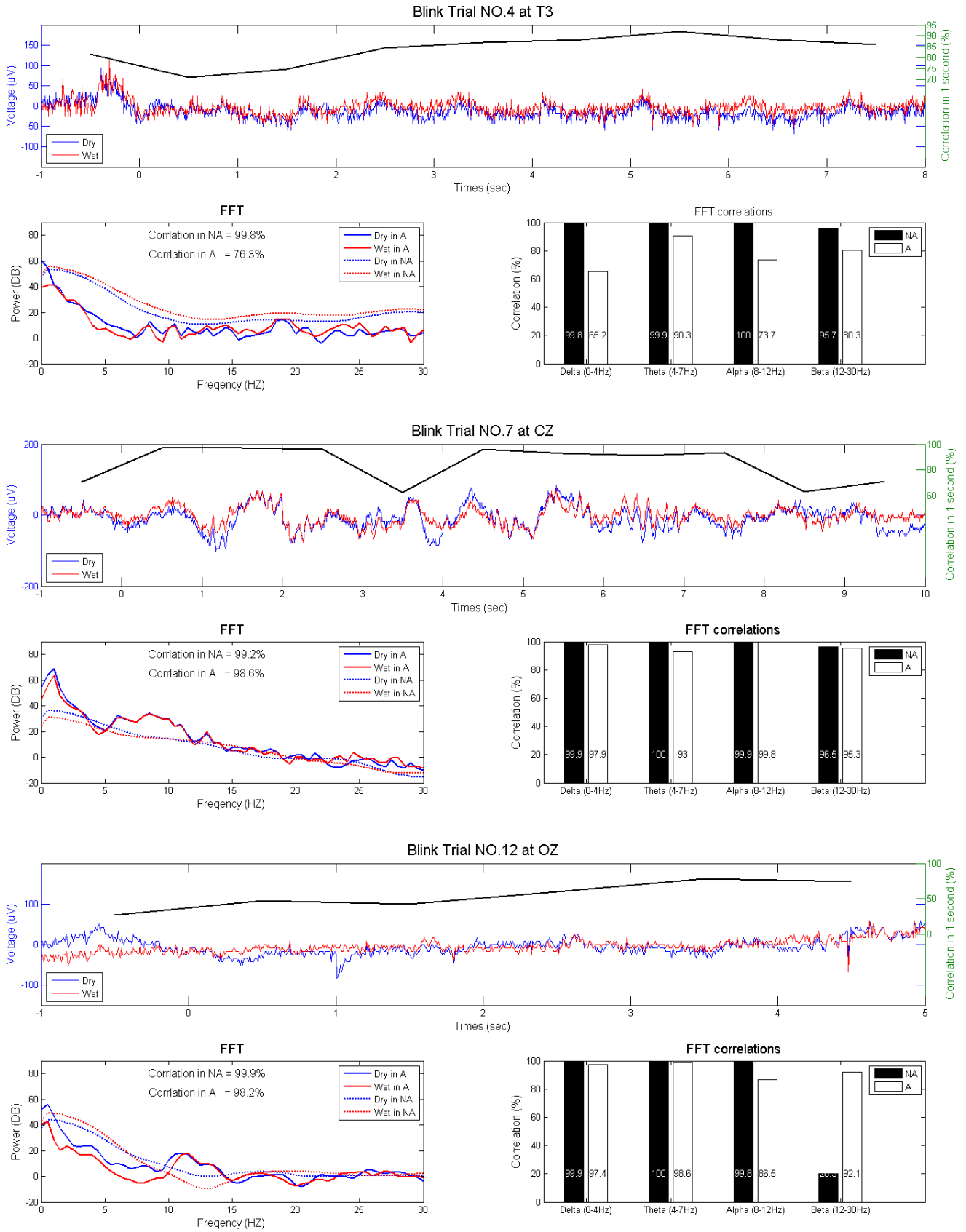


Fig. 3- 35: The best performance of Blink at T3 (up), CZ (mid), OZ (down)

C. The Best Trial Data in Close Action

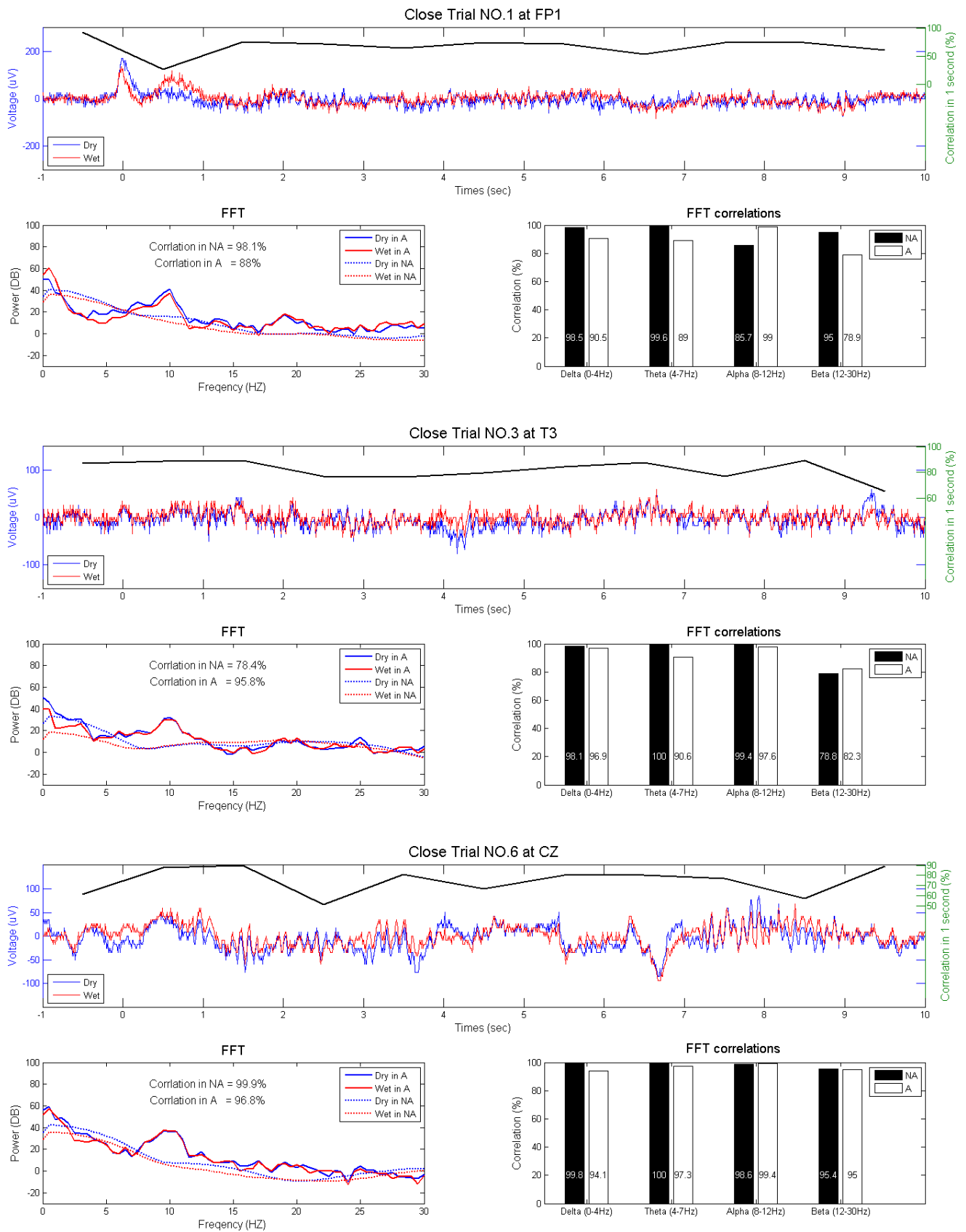


Fig. 3- 36: The best performance of Close at FP1 (up), T3 (mid), CZ (down)

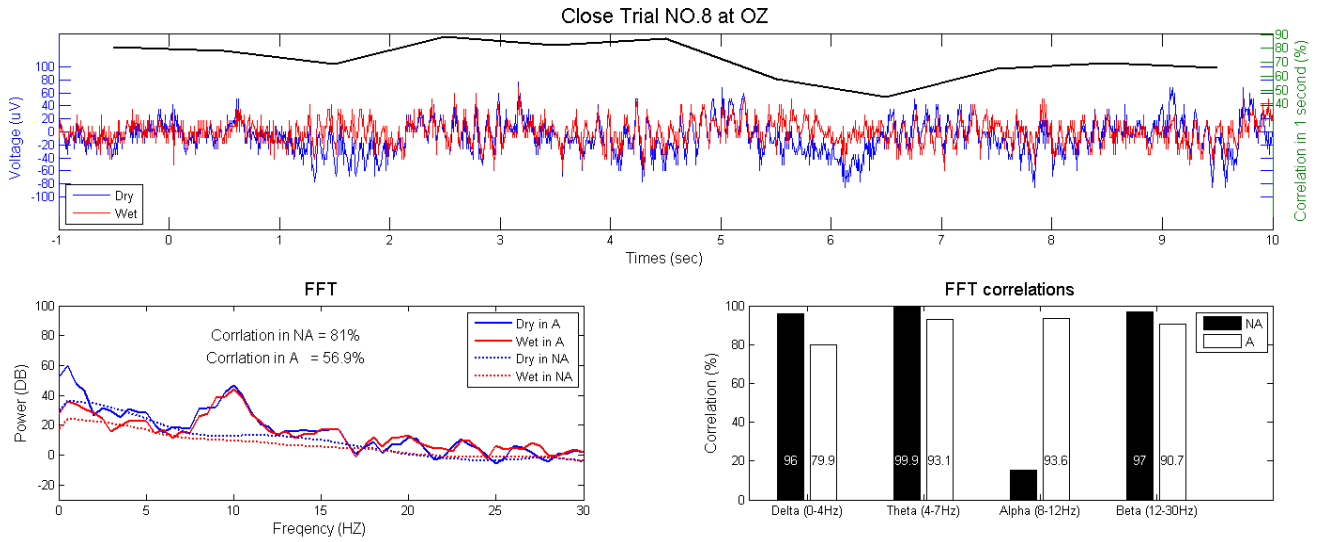


Fig. 3- 37: The best performance of Close at OZ

D. The Best Trial Data in Tooth Action

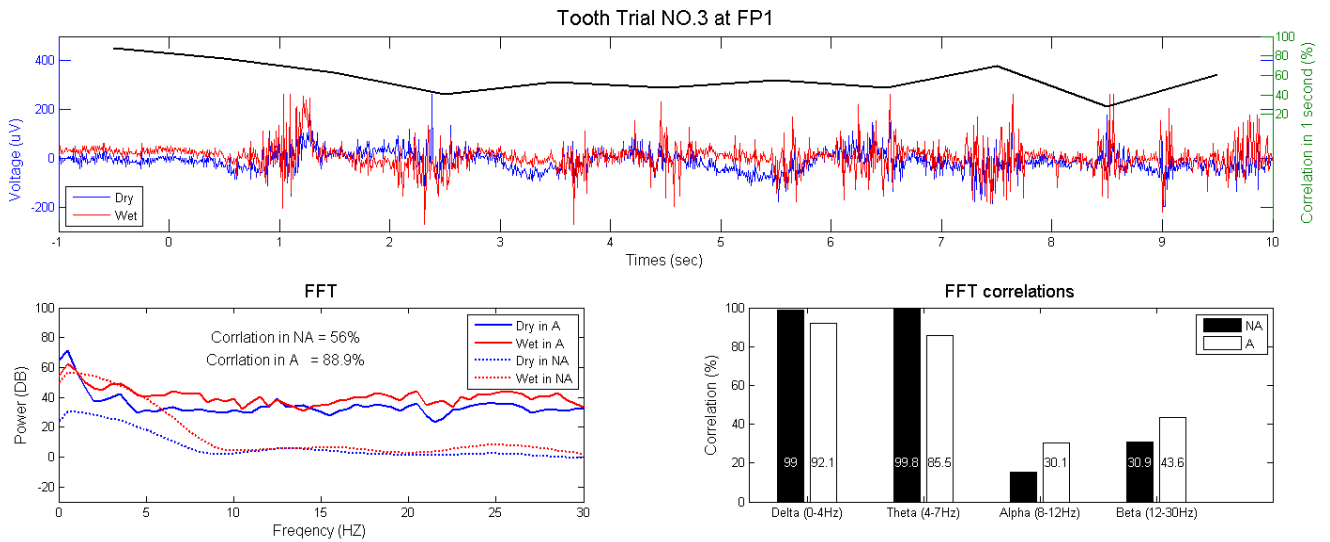


Fig. 3- 38: The best performance of Tooth at FP1

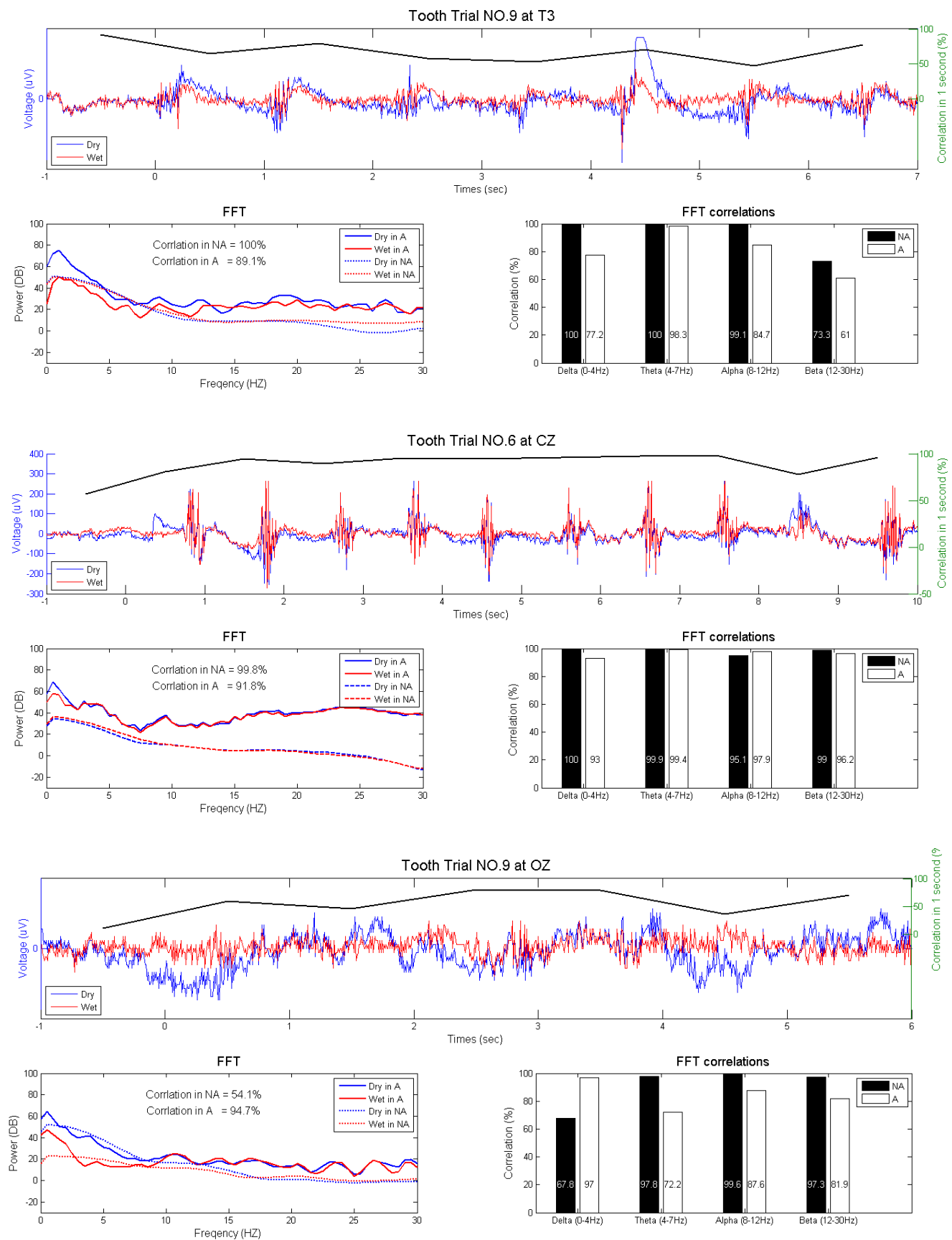


Fig. 3- 39: The best performance of Tooth at T3 (up), CZ (mid), OZ (down)

E. The Best Trial Data in Normal Action

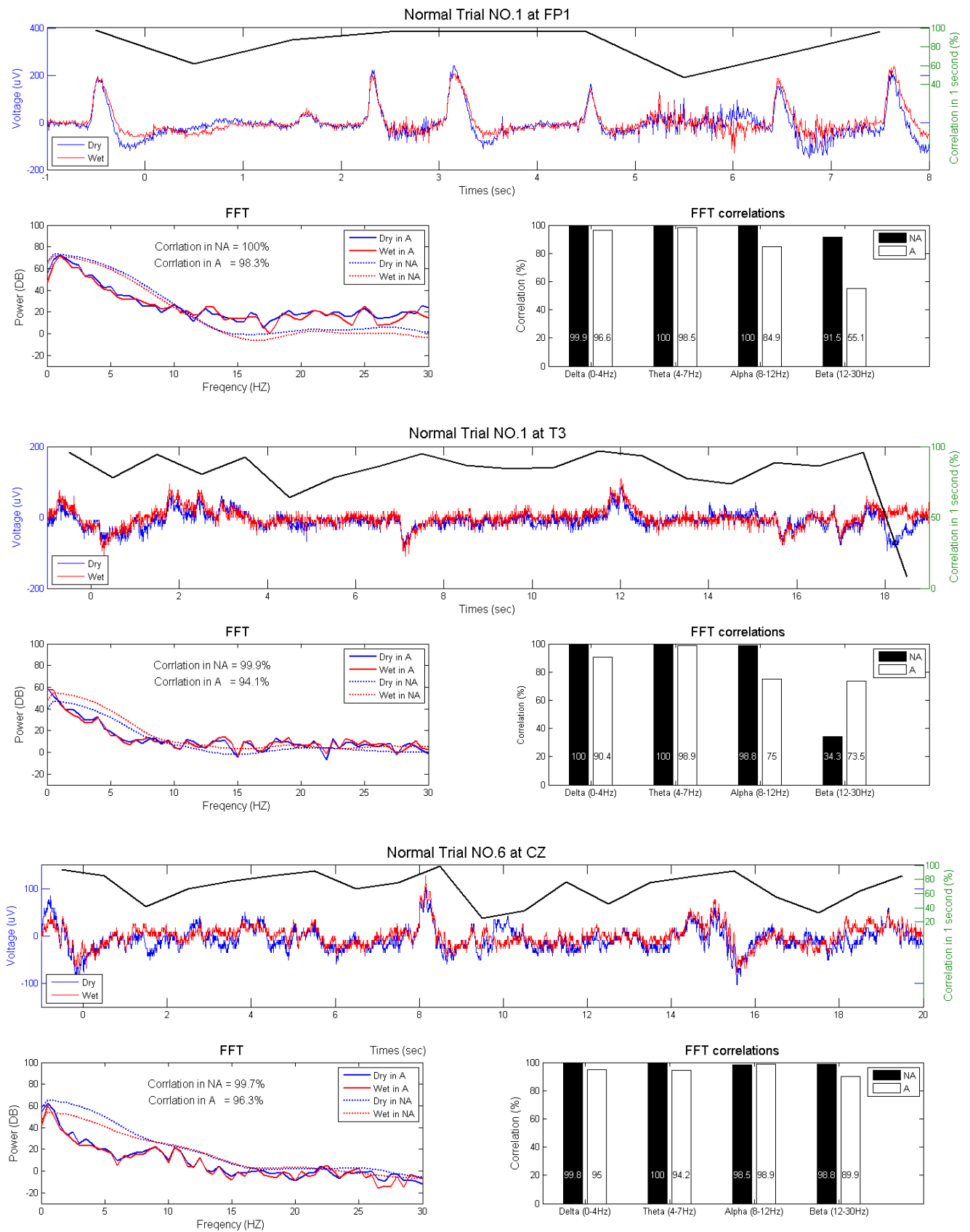


Fig. 3- 40: The best performance of Normal at FP1 (up), T3 (mid), CZ (down)

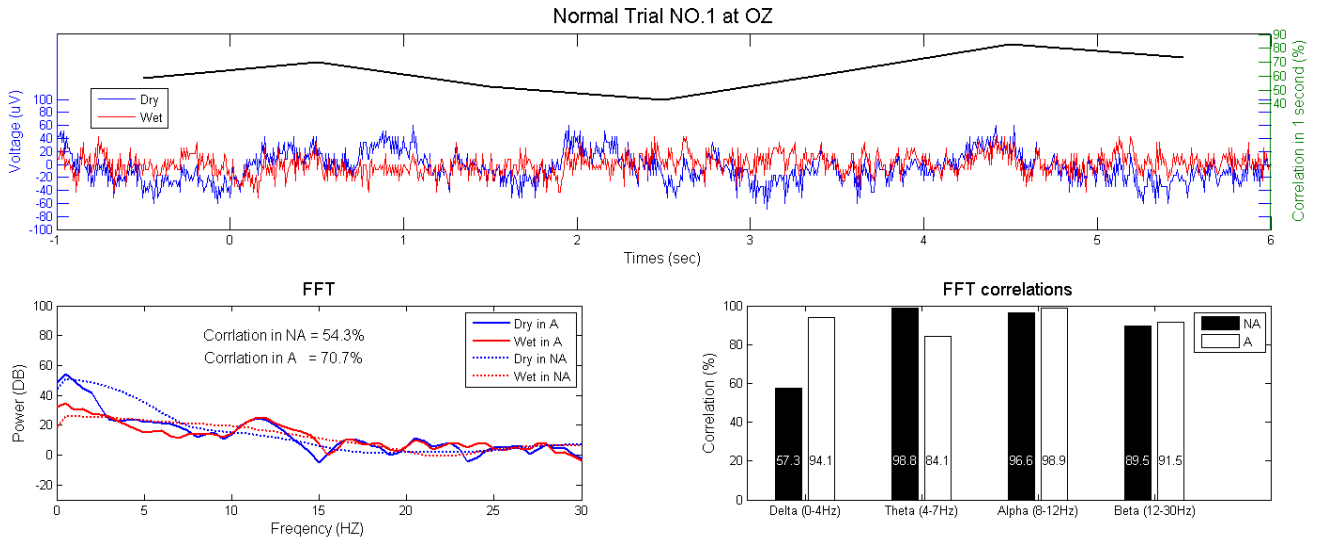


Fig. 3- 41: The best performance of Normal at OZ

F. The Worst Trial Data

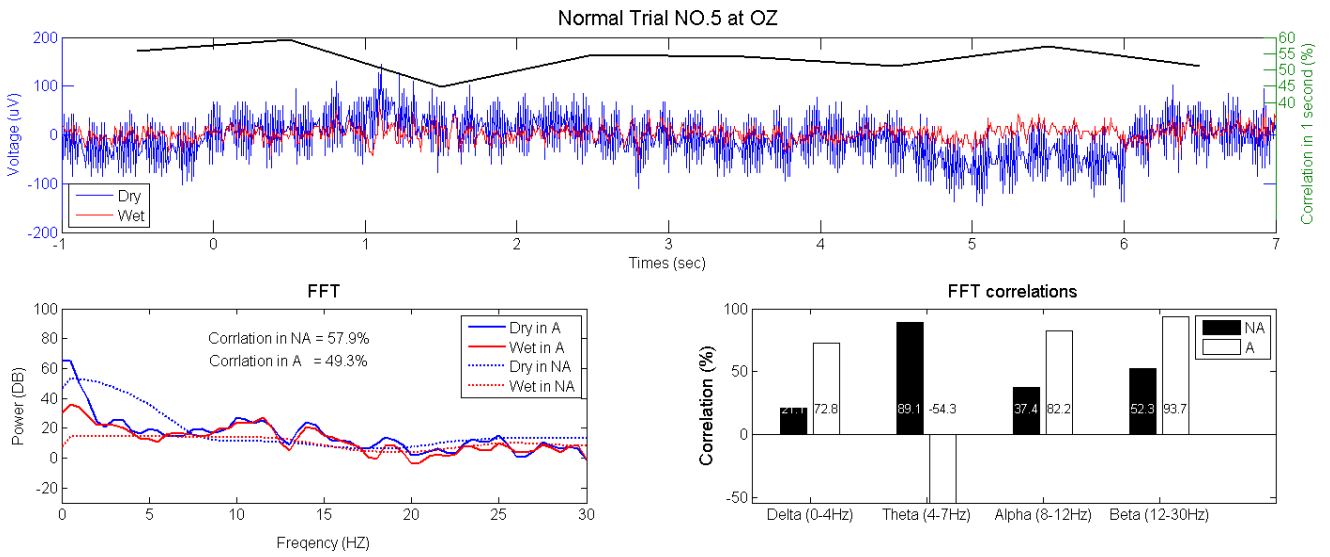


Fig. 3- 42: The worst performance during to 60-Hz Electromagnetic Interference

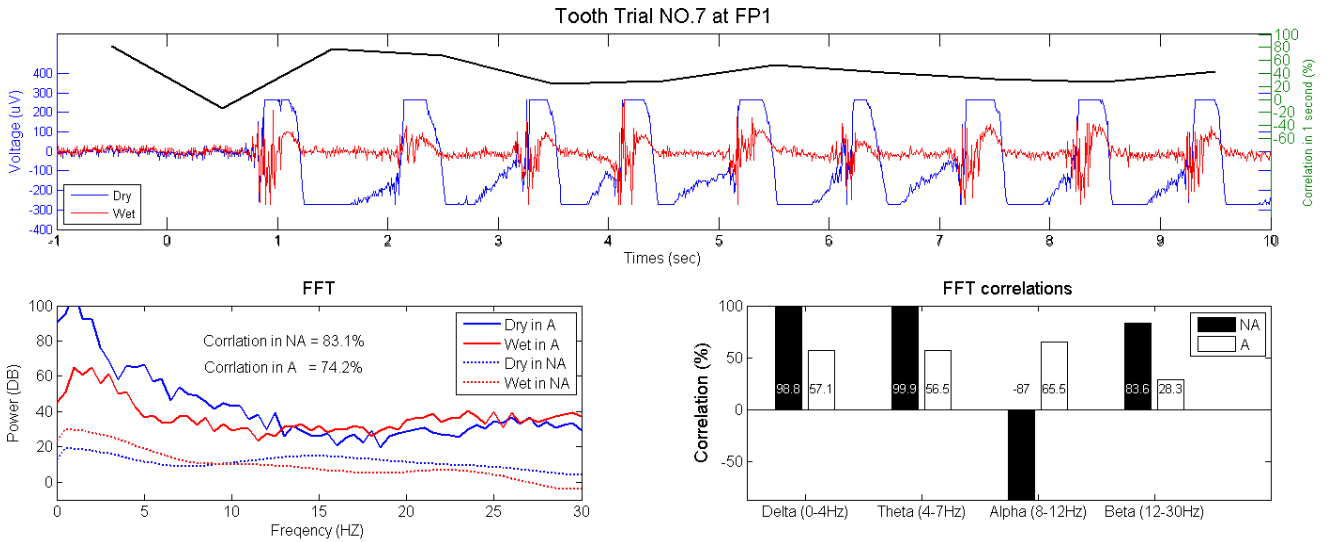


Fig. 3- 43: The worst performance during to motion artifact

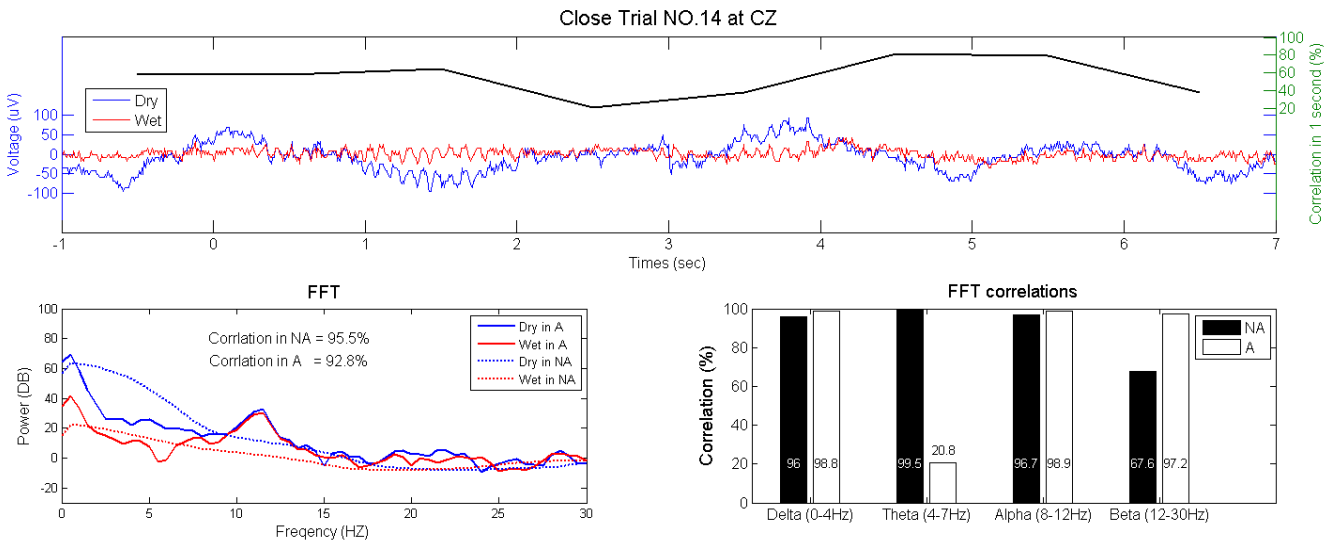


Fig. 3- 44: The worst performance during to DC shifting

3.3.5 Discussion

A. Sensor Test for All Subjects and All Positions

As Fig. 3-33 shown, the Time correlations for four actions are all less than 65%. The highest one is Blink during to the high amplitude of EOG being distributed the whole head more and less. As following we discuss results toward four actions respectively.

Blink: Time correlation is the highest one which is 61.5%, but what the reason that it can't be higher is. According to FFT correlations, we find the poor 30-60-Hz FFT correlation of 77.8%, so the whole FFT correlation is only 77.9% (because 0-30-Hz FFT correlation is 80.6%). In addition, in 0-30-Hz frequency band, we find Theta band has the best performance about 83.2%, and Delta band has the worst performance about 67.2%. In fact, Beta band has poor performance which is just a little higher than Delta band about 69.8%.

Close: Time correlation is the highest one which is 47.8%, but what the reason that it can't be higher is. According to FFT correlations, we find the poor 30-60-Hz FFT correlation of 79.5%, so the whole FFT correlation is only 79.3% (because 0-30-Hz FFT correlation is 81.4%). In addition, in 0-30-Hz frequency band, we find Alpha band has the best performance about 90.6%, and Theta band has the worst performance about 53.7%.

Tooth: Time correlation is the highest one which is 44.6%, but what the reason that it can't be higher is. According to FFT correlations, we find the poor 30-60-Hz FFT correlation of 53.6%, so the whole FFT correlation is only 69% (because 0-30-Hz FFT correlation is 76.5%). In addition, in 0-30-Hz frequency band, we find Delta band has the best performance about 70.7%, and Alpha band has the worst performance about 46.3%.

Normal: Time correlation is the highest one which is 58.4%, but what the reason that it can't be higher is. According to FFT correlations, we find the poor 30-60-Hz FFT correlation of 76.5%, so the whole FFT correlation is only 81.9% (because 0-30-Hz FFT correlation is 85.9%). In addition, in 0-30-Hz frequency band, we find Delta band has the best performance about 80.6%, and Beta band has the worst performance about 66.4%. In fact, Theta band and Alpha band also have poor performance which is just a little higher than Beta band about 67.6% and 68.8%

respectively.

In conclusion, during to there are different frequency bands with the best and the worst performances toward four kinds of actions, we demonstrate that dry sensor can not measure the best or the worst performance in certain frequency band. In fact, the best and worst results are caused by the behaved action more. From Table 17 to Table 20, we recognize the best performance in “Blink” is owing to three subjects consistently presenting the best, and the worst one in “Blink” is owing to two subjects consistently presenting the worse; the best performance in “Close” is owing to two subjects consistently presenting the best, and the worst one in “Close” is owing to three subjects consistently presenting the worse; the best performance in “Tooth” is owing to two subjects consistently presenting the best, and the worst one in “Tooth” is owing to two subjects consistently presenting the worse. However, there is not any consistent performance in “Normal”. Thus, we know that the best and the worst performances of comparing between dry sensor and wet sensor in different behaviors are as a result of many subjects rather than single subject.

B. The Similarities between Dry Sensor and Wet Sensor

As Fig. 3-34 to Fig. 3-41 shown, we verify dry sensor measuring the same EEG feature with wet sensor.

Blink: In Time domain, dry sensor monitor EOG signal at FP1 position as wet sensor. Moreover, there are a little attenuated EOG at not only T3 position but CZ position. Because of CZ being behind the head, there is almost no EOG signal measured at CZ position. In frequency domain, the signal of low frequency is more obviously occurred in activity stage (A) than non-activity stage (NA).

Close: In time domain, there is existing alpha wave in every position. In frequency domain, the power of Alpha band is enhanced in activity stage, and the highest power which is over 40dB occurred in CZ position.

Tooth: In time domain, EMG high-frequency signal distribute FP1, T3 and CZ positions. In frequency domain, there is large power enhanced within the frequency band over 10Hz.

Normal: In frequency band, the power distribution in non-activity stage is pretty similar to in activity stage because of the participant assigned to behave nature action (the same as in “baseline” stage) in “Normal”.

C. The Differences between Dry Sensor and Wet Sensor

Although dry sensor presents the same measured EEG patterns as wet sensor, the drawback of dry sensor is still existent to make the poor performance compared to wet sensor. We sort out three conditions of bad measurement quality:

(1) 60-Hz Electromagnetic Interference

Fig. 3-42 displays that dry sensor measures more 60-Hz noise from natural environment. It may mean dry sensor is more sensitive than wet sensor. The ability of resisting high-frequency noise for Dry sensor is worse than wet sensor.

(2) Motion artifact

Fig. 3-43 shows when the participant grinding the teeth, dry sensor moves a little offset related original skin site, which is referred to motion artifact. Hence, the mechanism for fixation is relatively important toward dry sensor.

(3) DC shifting during to unequal force pressed

Dry sensor is forced down by hands of operator, so there is inevitable that a little manually shaking happened within the process of experiment. Thus, the record data combines a little manual negligence such as DC shifting (Fig. 3-44).

3.4 Sensor Test in Oddball Task

In this session, we illustrate our procedure of oddball task, the participants, and experiment results. By last experiment, we get some sensor performance information, but the performance of Event-Related Potential (ERP) seems more important. Owing to ERP being a very tiny EEG activity, it needs to average more trials not only for reducing noise but for enlarging event-related potential. For the purpose of verifying whether our system can monitor tiny signal even ERP or not, we follow the same system verification procedure diagram as Fig. 3-40 and re-design an Oddball experiment. Finally, in analysis process, we compare the performance between dry sensor and wet sensor.

3.4.1 Participant

There are ten participants with 6 males and 4 females (19 – 23 ages). Most of them are normal number of hairs, two people are fewer number of hairs, and three people are larger number of hairs.

3.4.2 Experiment Procedure and Presentation

The oddball task combines normal stimulus and target stimulus. The participant was asked to click button when target stimulus occurred. The target only presented in 75-ms duration, and the following 1925-ms duration is for waiting next stimulus. Due to past researcher indicating that the ratio of normal stimulus to target stimulus is 8 to 2. We designed the target to be randomly occurred, total number of times is 5-time less than non-target (normal) stimulus in oddball task. When one session of experiment beginning, the screen presents a letter first and show “Please put down the button for non-X” to tell the participant what normal letter “X” is in this session. The normal letter, which is possible to be A, B, C, D or E, is random produced by presentation program in each session (Fig. 3-45).

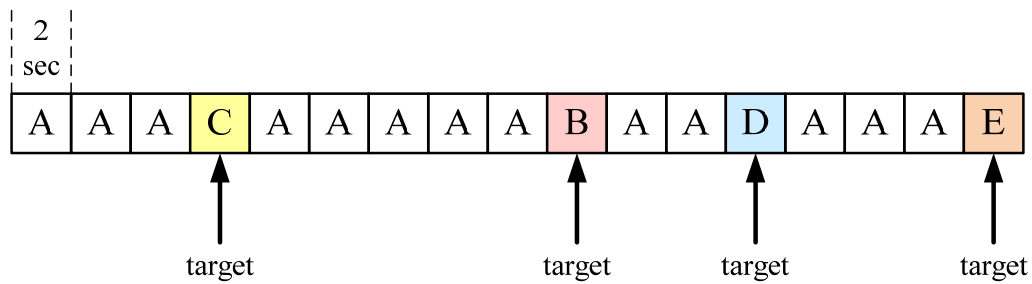


Fig. 3- 45: Procedure of oddball experiment

Beginning of experiment, the participant sat on a chair motionlessly and was asked to keep facing on the front screen and followed occurred commands by presentation. The experiment includes four sections, each of about 10-minute duration. Each section includes 300 trials, each of 2-second duration. Among one session, there are 240 trials with normal stimulus and 60 trials with target stimulus. The participant can take a rest among sections. This experiment may be executed for one hour. Fig. shows procedure of presentation in 18 trials with random-stimulus.

Referencing to 10-20 system (Guideline for Standard Electrode Position Nomenclature, 2006), we choose CZ position (Fig. 3-46) to place dry sensor. All the dry sensors are pressed by hands of the other person. All channels are linked to 16-channel EEG device, and the program record EEG data.

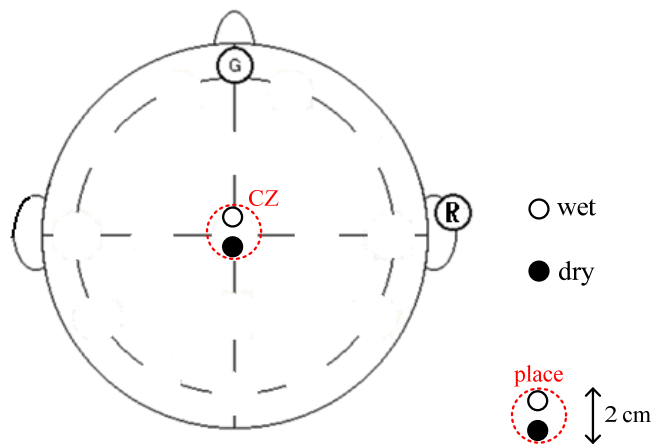


Fig. 3- 46: Positions of dry sensor and wet sensor in oddball task

3.4.3 Method of Analysis

As following steps describe the method of analyzing ERP in oddball task using EEGLAB toolbox [25]:

(1) Low-pass filter: Dry sensor record the frequency combined 0.2 – 125 Hz signals. Only P300 is the EEG data of interest. To filter high-frequency signal is good for us to view the pattern of P300. Hence, first step is to filter for remaining low 0.2 – 30 Hz EEG signal.

(2) Separate the epoch for data of the same event: To separate “Normal epoch” for normal stimulus event and “Oddball epoch” for target stimulus event, both of them are remained interval of [-0.5 1.5], in which [-0.5 0] is baseline, is one step of ERP preprocessing.

(3) Reject no-use data: According to last experiment of sensor basic test, we get the information about the measuring effects of dry sensor like DC-shifting, floating, and voltage saturation. They are all no-use data for computing ERP, so we reject them early. Fig. 3-47 shows what kind of data we reject. In most researches, EOG is also rejected, but it is difficult to reject EOG here during to only monitoring CZ position in which EOG is difficultly distinguished within EEG data.

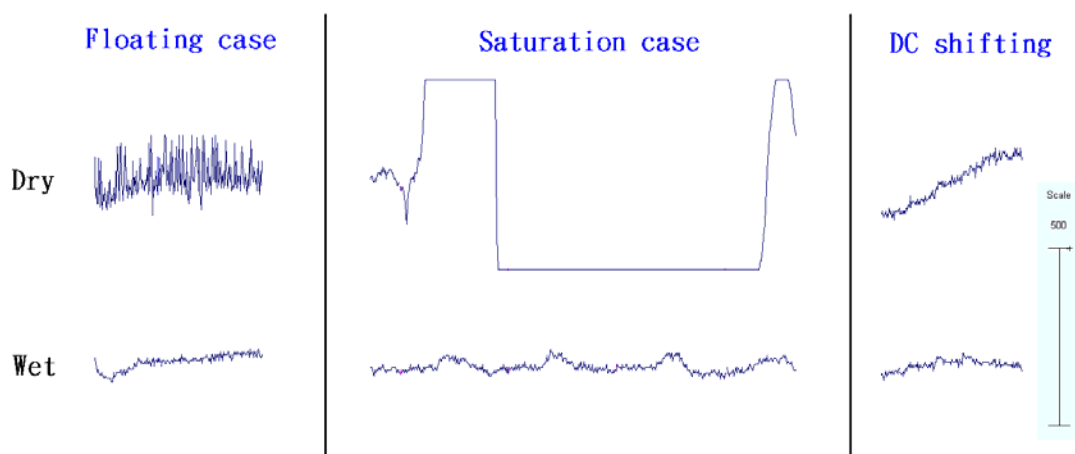


Fig. 3- 47: No-use data for floating case, saturation case, and DC shifting

(4) Compute ERP: EEG data, which is separated to the same interval related event, pass through averaged more and more trial data not only to enhance event-related potential but to decrease the influence of noise. In this step, “Normal epoch” and “Oddball epoch” respectively average all trial data. Thus, the averaged data are corresponding Normal ERP and Oddball ERP.

3.4.4 Experiment Results

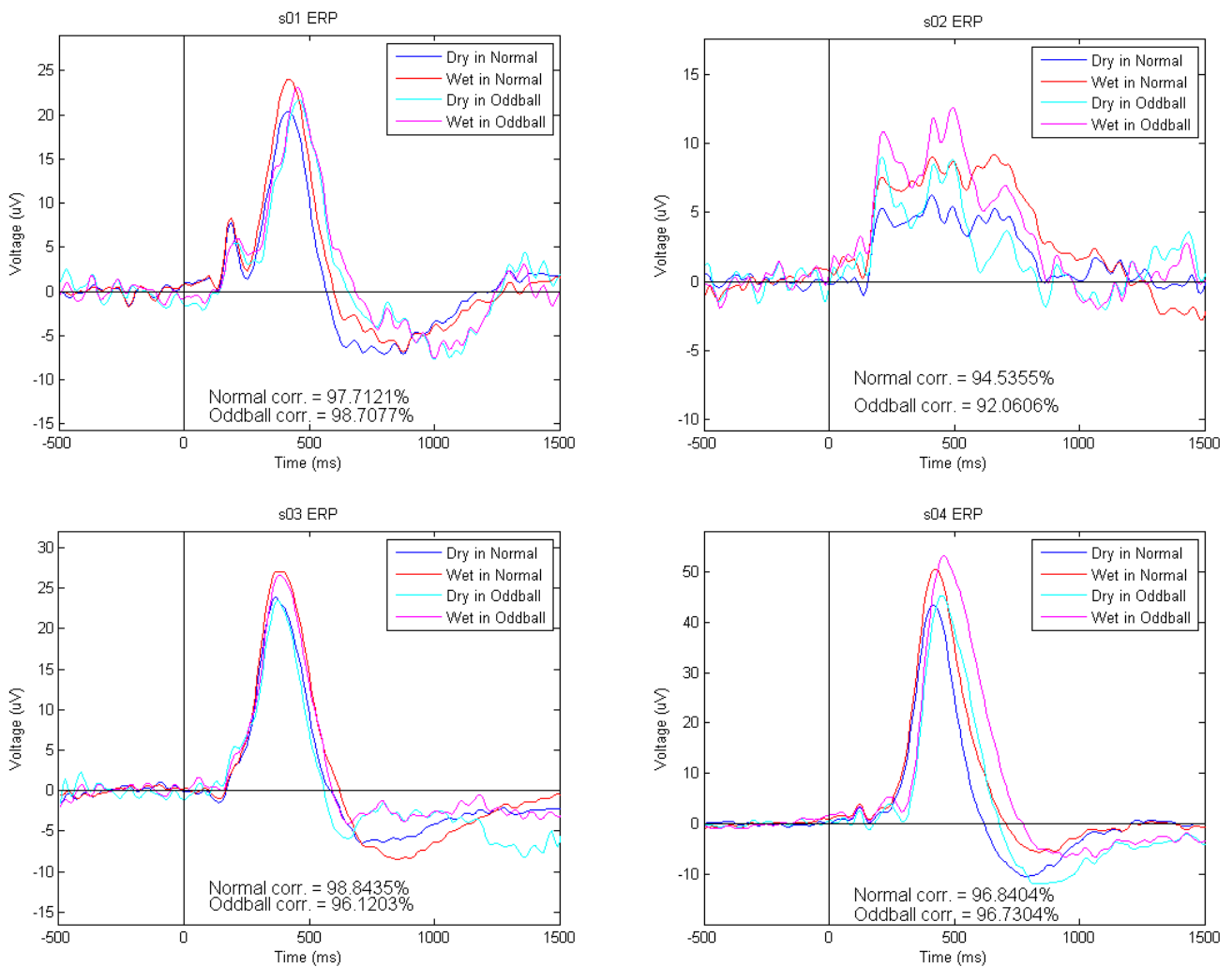


Fig. 3- 48: ERP of s01 (left-up), s02 (right-up), s03 (left-down), s04 (right-down) in oddball task

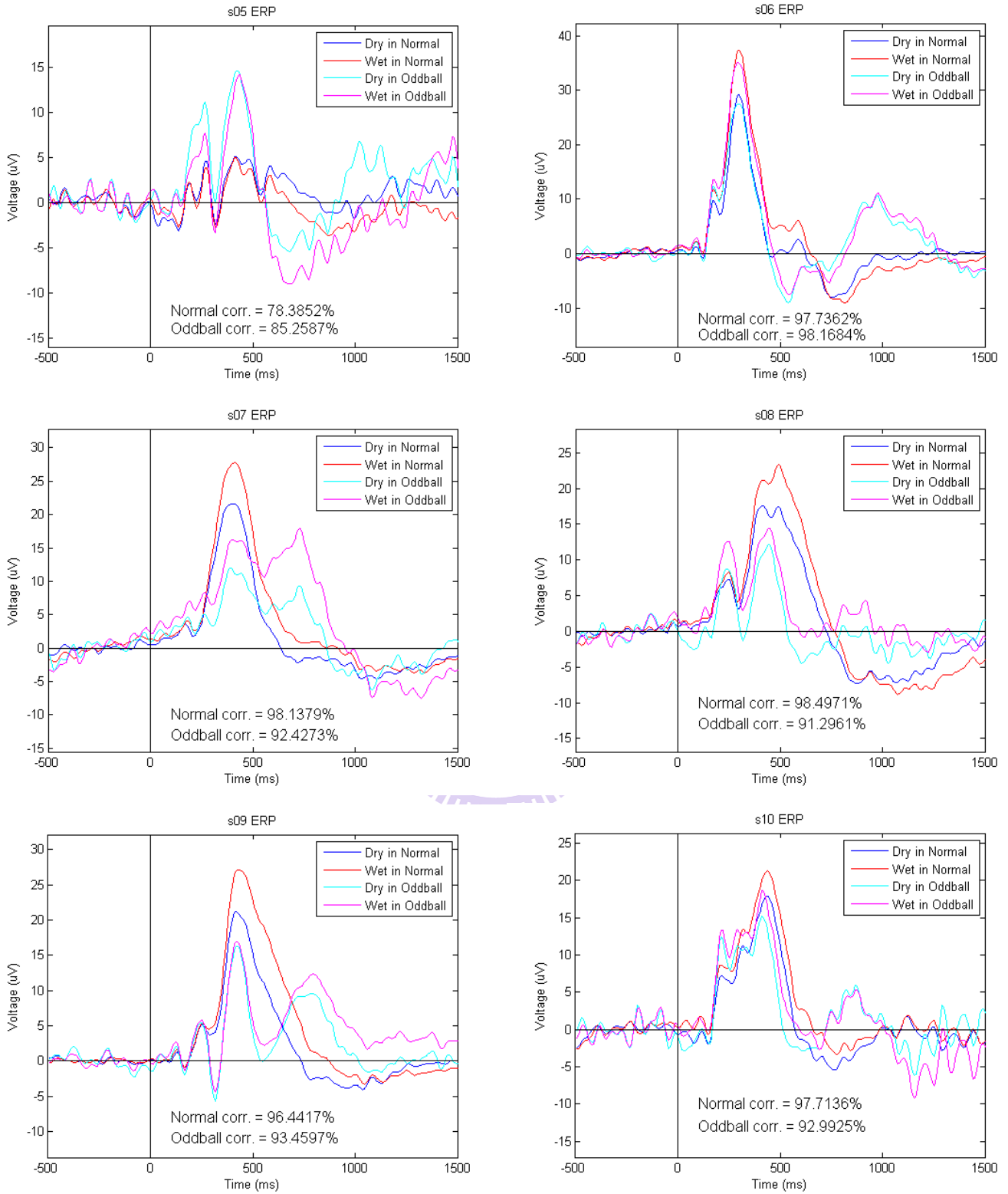


Fig. 3- 49: ERP of s05 (left-up), s06 (right-up), s07 (left-mid), s08 (right-mid), s09 (left-down), s10 (right-down) in oddball task

3.4.5 Discussion

A. P300 of Single Stimulus

This experiment presents a stimulus per 2 seconds, each of in about 75-ms duration. No matter using dry sensor or wet electrode, there is measured P300 by our multi-channels mobile and wireless system. From Fig. 3-48 to Fig. 3-49, the figures show event-related potential of single stimulus for all participants. In baseline interval, there is no potential occurred. After stimulus, which may be normal stimulus or target stimulus, triggered, ERP simultaneously occurs in 300ms – 500ms. Hence, we get a result of ten participants all inducing P300 by single stimulus. On the other words, all ten participants own the same P300 tendency for single stimulus on CZ position.

B. P300 of Oddball Task

In this discussion about P300 through Oddball task, we have to respectively discuss “Normal” and “Oddball” state for ten participants initially. It is noteworthy that the ERP pattern in this experiment is a little different from standard ERP pattern possibly owing to EOG signal being not rejected.

Subject 1 (s01): Dry sensor measured the larger amplitude of P300 in “Oddball” than “Normal”, and we can recognize that P300 in “Oddball” is a little later than in “Normal” (the P300 latency in “Oddball” is higher than in “Normal”). However, wet sensor measured the higher latency in “Oddball” and the very similar amplitude in “Oddball” and “Normal”.

Subject 2 (s02): Dry and wet sensors both measured the higher amplitude of P300 in “Oddball”.

Subject 3 (s03): No matter the amplitude or the latency of P300, dry sensor measured almost the same ERP in “Oddball” and “Normal”. And wet sensor is the same as dry sensor.

Subject 4 (s04): Dry sensor and wet sensor both measured the higher amplitude and the higher latency of P300 in “Oddball”.

Subject 5 (s05): Dry sensor and wet sensor both measured the obviously higher amplitude of P300 but the latency is not changed in “Oddball”.

Subject 6 (s06): Dry sensor and wet sensor both measured the obviously higher amplitude in 900ms after stimulus occurred in “Oddball”.

Subject 7 (s07): Dry sensor and wet sensor both measured the higher latency of P300 in “Oddball”. Although the lower amplitude occurred in 300ms, there is the obviously higher amplitude occurring in 700 ms in “Oddball”.

Subject 8 (s08): There isn't any feature to be found in “Oddball” not only by dry sensor but also by wet sensor.

Subject 9 (s09): In “Oddball”, although dry sensor and wet sensor both measured the lower amplitude in 300ms, they both measured the obvious higher amplitude in 900ms.

Subject 10 (s10): dry sensor and wet sensor both measured the higher amplitude in 900ms in “Oddball”. The amplitude of ERP in 300ms in “Oddball” is the same as in “Normal”.

In sum of the above discussion, we get three points of conclusions. One is that s03 and s09 could not present the prospective Oddball feature of P300 through this oddball task, because they may not feel obvious different for target stimulus although they indeed click the button toward target stimulus. The second point is that s06, s09, and s10 behaved the higher amplitude of ERP in 900ms and s07 behaved it in 700ms are possibly owing to the higher latency of P300. The third point is that for eight participants, we can recognize the obvious difference between “Normal” and “Oddball”. Four of eight participants behaved the standard pattern of P300 in Oddball task. Hence, we demonstrate our proposed system really measure very tiny EEG

activity even ERP.

C. Comparison between Dry and Wet Sensor

By averaging the results of ten participants, average correlations between dry sensor and wet sensor in “Normal” and “Oddball” are respectively shown in Fig. 3-50. As a result of measured data of one participant (s05) being worse (Fig. 3-51), the average correlation is also decreasing. The average correlation for s05 in “Normal” is 78.4%, and the average correlation for s05 in “Oddball” is 85.3%. According to Fig. 3-49 (left-up), we can find that ERP is obviously shacking and not smooth because of remaining less trial data in reject no-use data process. ERP needs more and more trial data to decrease the influence of uniform noise. Thus, ERP of s05 is look like shaking more obvious than ERPs measured from other subjects. Nevertheless, there is no doubt that the sensor comparison result is great.

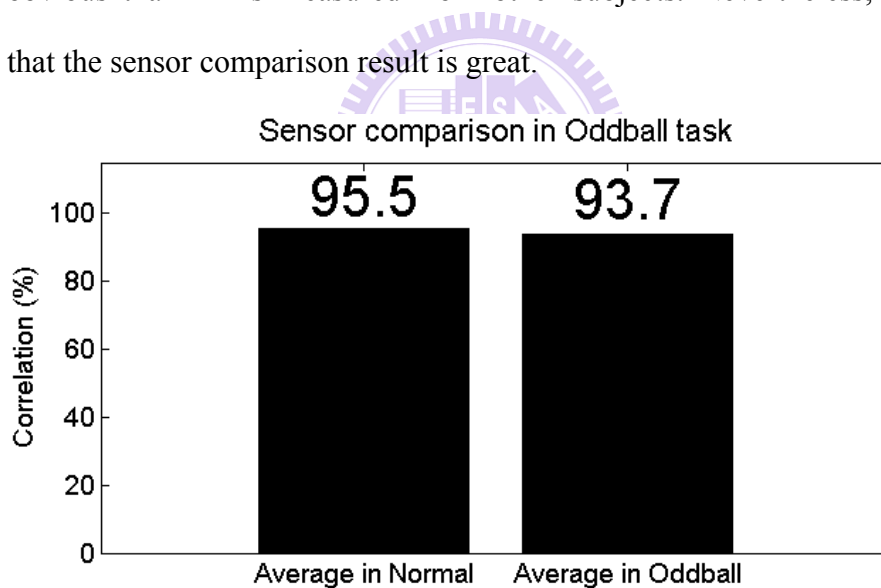


Fig. 3- 50: Sensor overall comparison in oddball task

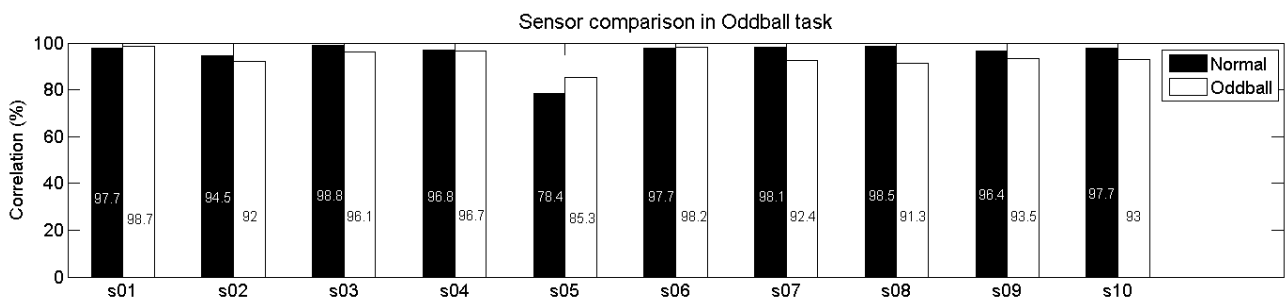


Fig. 3- 51: Sensor comparisons for all subjects in oddball task

Chapter 4 Conclusions and Future Works

4.1 Conclusions

In this study, we expect to establish a miniature multi-channels mobile and wireless EEG system for wide-use applications. The system combines three parts: (1) dry sensor, (2) multi-channels mobile and wireless EEG acquisition circuitry, and (3) EEG display program. We indeed implement this device with 50mm x 60mm large and 16 channels included. It's weight of less than 50g to be conveniently carried in daily life. Dry sensor which needs not conductive gels is flexible in a travel distance to make users feel comfortable. Furthermore, this dry sensor can measure EEG activity for long-time monitoring. Our 16-channel EEG device including dry sensor even can be continuously used almost 10 hours by a loaded battery with 3.7V. the wireless circuitry transmits EEG data to the back-end display and record program. Finally, the program creates a TXT file to save record data for off-line analysis.

In system verification, we use three experiments to verify the segmental performance of system. The results demonstrate the performance of our circuitry and program is 88.34% temporally correlate and 92.93% frequency-domain correlate to standard measurement instrument like Neuroscan system in Normal action state. The dry sensor can monitor the similar EEG feature like wet sensor. Dry sensor applied in multi-channels device can also detect very tiny EEG signal even ERP in Oddball task with 93-95% correlated to wet sensor. In conclusion, our proposed system is exactly reliable and convenient to apply in medical, cognitive, and diary-use area.

4.2 Future Works

Dry sensor which has the drawback of motion artifact in our system is sensitive for shaking. The future work may design a new mechanism (Fig. 4-2) to fix 16 channel sensors in one. The mechanism would be best for flexibly adjusting by users for difference size of head. And once finishing adjustment, the mechanism isn't easy to sway all sensors for avoiding a little movement between sensor and skin. If the mechanism achieved, the experiments can also repeat testing the performance of system combining the new mechanism for verification. As the following Fig. 4-1 shown, the position on which sensors placed are suggested by referencing to 10-20 system (Guideline for Standard Electrode Position Nomenclature, 2006).

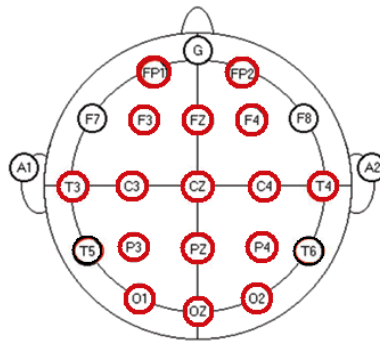


Fig. 4- 1: The 16-channel electrode positions



Fig. 4- 2: The mechanism example

References

- [1] Towle VL, Bolaños J, Suarez D, Tan K, Grzeszczuk R, Levin DN, Cakmur R, Frank SA, Spire JP. (1993), "The spatial location of EEG electrodes: locating the best-fitting sphere relative to cortical anatomy," *Electroencephalogr Clin Neurophysiol* 86 (1): 1–6. doi:10.1016/0013-4694(93)90061-Y. PMID 7678386.
- [2] "Guideline seven: a proposal for standard montages to be used in clinical EEG, American Electroencephalographic Society," *Journal of Clinical Neurophysiology* 11 (1): 30–6. 1994.PMID 8195424.
- [3] Niedermeyer E. and da Silva F.L. (2004), *Electroencephalography: Basic Principles, Clinical Applications, and Related Fields*, Lippincot Williams & Wilkins. ISBN 0781751268.
- [4] H. Aurlien, I.O. Gjerde, J. H. Aarseth, B. Karlsen, H. Skeidsvoll, N. E. Gilhus (March 2004), "EEG background activity described by a large computerized database," *Clinical Neurophysiology* 115 (3): 665–673. doi:10.1016/j.clinph.2003.10.019. PMID 15036063.
- [5] Electroencephalography, from wikipedia, the free encyclopedia, [Online]. Available: <http://en.wikipedia.org/wiki/Electroencephalography>
- [6] Neuroscan systems, [Online]. Available: <http://www.neuroscan.com/systems.cfm>
- [7] Starlab, [Online]. Available: <http://starlab.es>
- [8] Biosignal, from wikipedia, the free encyclopedia, [Online]. Available: <http://en.wikipedia.org/wiki/Biosignal>
- [9] Wiley John, "Medical instrumentation application and design 3rd", " John G. Webster, 1998.
- [10] Electrooculography, from wikipedia, the free encyclopedia, [Online]. Available: <http://en.wikipedia.org/wiki/Electrooculography>
- [11] Electromyography, from wikipedia, the free encyclopedia, [Online]. Available: <http://en.wikipedia.org/wiki/Electromyography>
- [12] T. Johnson, T. Scott. , "Sleep apnea, the phantom of the night", 2003

- [13] Lun-De Liao, I-Jan Wang, Sheng-Fu Chen, Jyh-Yeong Chang and Chin-Teng Lin, "Design, Fabrication and Experimental Validation of a Novel Dry Contact Sensor for Measuring Electroencephalography Signals without Skin Preparation," 11, 5819-5834, *Sensors*, 2011.
- [14] Texas Instrument. [Online]. Available:
<http://focus.ti.com/lit/ug/slau049f/slau049f.pdf>
- [15] Chia- Hsin Chung, "The Development of Wireless Polysomnography System for Sleep Monitoring At Home" , 國立交通大學, 碩士論文。
- [16] 賴家達, "無線嵌入式生醫平台" , 國立交通大學, 碩士論文, 民國九十七年。
- [17] Polich, J., & Criado, J. R. (2006), "Neuropsychology and neuropharmacology of P3a and P3b", *Int J Psychophysiol*, 60(2), 172-185.
- [18] Linden, D. E. J. (2005), "The P300: Where in the Brain Is It Produced and What Does It Tell Us? ", *The Neuroscientist*, 11(6), 563-576.
- [19] Conroy, M. A., & Polich, J. (2007), "Normative Variation of P3a and P3b from a Large Sample: Gender, Topography, and Response Time", *Journal of Psychophysiology*, 21(1), 22-32.
- [20] Polich, J. (2007), "Updating P300: an integrative theory of P3a and P3b", *Clin Neurophysiol*, 118(10), 2128-2148.
- [21] Comerchero, M. D., & Polich, J. (1999), "P3a and P3b from typical auditory and visual stimuli", *Clin Neurophysiol*, 110(1), 24-30.
- [22] Comerchero, M. D., & Polich, J. (1998), "P3a, perceptual distinctiveness, and stimulus modality," *Brain Res Cogn Brain Res*, 7(1), 41-48.
- [23] Hagen, G. F., Gatherwright, J. R., Lopez, B. A., & Polich, J. (2006), "P3a from visual stimuli: task difficulty effects," *Int J Psychophysiol*, 59(1), 8-14.
- [24] Event-related potential, from wikipedia, the free encyclopedia, [Online]. Available: http://en.wikipedia.org/wiki/Event-related_potential
- [25] EEGLAB toolbox. [Online]. Available : [http:// http://sccn.ucsd.edu/eeglab/](http://sccn.ucsd.edu/eeglab/)